DEVELOPMENT OF AN ENERGY SYSTEM FOR A MOZAMBIQUE RURAL VILLAGE WITHOUT ELECTRIC GRID ACCESS

Ricardo de Castro Amorim

FEUP
Universidade do Porto
Faculdade de Engenharia

DEMEGI

Integrated Master in Mechanical Engineering – Thermal Energy

MIEM

Porto, 2010

Abstract

United Nations (UN) in 2000 created the Millennium Development Goals (MGD) with the objective to reduce extreme poverty, reducing child mortality rates, fighting disease epidemics and developing a global partnership for development. *Engenharia para o Desenvolvimento e Assistência Humanitária (EpDAH)* is a non profitable and nongovernmental association which has *Autarkheia* project, like other projects, that is based in the UN MDG. *Autarkheia* project has the objective to identify critical factors and project engineer solutions to minimize or eliminate these factors. The *Autarkheia* project is based in the multiplication and replication of similar projects to other villages and enabling them to take responsibility from their own development, minimizing extreme poverty and contributing access to education, health services and decent living conditions. The village name is *Malonguete* and belongs to *Chicuacuala* district, Gaza province of Mozambique. Using renewable energy technology it is possible to provide villagers an energy system capable to produce water the entire year for the population and capacitating the future village health center with a vaccine refrigerator that operates with 2 to 8ºC temperature range for vaccine conservation.

To satisfy the water needs for 400 villagers, and based in a consumption profile for each villager that is constant over the year the best studied system is a 320 W_p photovoltaic array with a Grundfos SQFlex 2.5-2 helical rotor submersible pump. For the future health center it was studied the water/lithium bromide absorption cycle and it was selected two refrigerators with different vaccine volume capacity.

Resumo

As Nações Unidas no ano 2000 criaram os Objectivos de Desenvolvimento do Milénio (ODM) com o objectivo de reduzir a pobreza extrema, reduzir a mortalidade infantil, combater epidemias e desenvolver uma parceria global para o desenvolvimento. Engenharia para o Desenvolvimento e Assistência Humanitária (EpDAH) é uma organização não governamental sem fins lucrativos. O projecto Autarkheia, como outros projectos da associação, é baseado nos ODM. Além do objectivo de desenvolver soluções de engenharia que sejam capazes de suprimir as necessidades dos habitantes de uma aldeia também é necessário que esses projectos sejam replicados e multiplicados por outras aldeias responsabilizando os habitantes pelo seu próprio desenvolvimento. Assim o projecto contribui para o desenvolvimento, reduzindo a pobreza extrema e contribuindo para um melhor acesso à educação, serviços de saúde e condições de vida dignas. O nome da aldeia é *Malonguete* e situa-se na província de Gaza, distrito de *Chiqualaquala* em Moçambique. Recorrendo a fontes de energia renovável é possível capacitar a aldeia com um sistema de água que garanta o abastecimento de água a 400 habitantes e também capacitar o futuro centro de saúde de um refrigerador com a capacidade de conservar vacinas que opera entre 2 e 8ºC.

Para satisfazer as necessidades de água a 400 habitantes e considerando que o consumo se mantêm constante o melhor sistema estudado é um gerador fotovoltaico com 320 W_p e uma bomba Grundfos SQFlex *helical rotor* 2.5-2. Foi estudado o ciclo frigorifico de absorção brometo de lítio/água e seleccionou se dois refrigeradores com capacidades diferentes em termos de volume para conservar vacinas.

Preface

I'm volunteer since November of 2009 in the association *Engenharia para o Desenvolvimento e Assistência Humanitária* (EPDAH). This dissertation was realized in collaboration with EpDAH that has the mission to promote the human development through a professional volunteer activity in the engineer domain. This dissertation is integrated in the Autarkheia project that has the objective to identify critical factors and project engineer solutions to minimize or eliminate these factors. The Autarkheia project is based in the multiplication and replication of similar projects to other villages and enabling them to take responsibility from their own development, minimizing extreme poverty and contributing to access to education, health services and decent living conditions.

I want to show here my gratitude for the people that contributed for my experience in Mozambique and helped me directly or indirectly realizing this dissertation

Anabela Seabra

António Amorim

Beatriz Barros

Professor Clito Afonso

Ernestina Amorim

Tiago Granja

Content

Figures content list

Table content list

Nomenclature

	Description	Units		Description	Units
AM	Air Mass		$\dot{Q}$	Heat rate	[W]
BHP	Break Horse Power	[W]	$\dot{Q}_{rad}$	Radiation heat transfer	[W]
$CCT_{I;sc}$	Short Circuit temperature coefficient	[1/ºC]	$\dot{Q_a}$	Absorber Heat Rate	[W]
$CCT_{V;oc}$	Open Circuit temperature coefficient	[1/ºC]	$\dot{Q_c}$	Condenser Heat Rate	[W]
c_p	Specific heat at constant pressure for vaccine	[J/kgK]	$\dot{Q_e}$	Evaporator Heat Rate	[W]
C_Q	Pump Flow coefficient		$\dot{Q_g}$	Generator Heat Rate	[W]
C_Q	Pump Power coefficient		Refri. Time	Refrigeration time	[s]
D	Pump diameter	[m]	RPS	Shaft speed	[RPS]
$EX\varepsilon$	Solution heat exchanger efficiency		RR	Roughness Ratio	
F	Darcy friction factor		r_s	Series resistance	[Ω]
F	Solution Circulating Ratio		$r_{s;ref}$	Reference series resistance	[Ω]
g	Gravitation Acceleration	[m^2/s]	r_{sh}	Shunt Resistance	[Ω]
G	Radiation incident on a horizontal surface	[W/m^2]	r_t	Hourly and daily total radiation on a horizontal surface ratio	
G_{sc}	Solar constant	[W/m^2]	T	Absolute Temperature	[K]
$G_{b,T}$	Beam radiation	[W/m^2]	T_{air}	Ambient air temperature	[ºC]
$G_{T;ref}$	Reference Radiation	[W/m^2]	T_{cel}	Cell temperature	[ºC]
H_{est}	Static Head	[m]	$T_{cel;ref}$	Cell Reference Temperature	[ºC]
H_f	Friction head	[m]	T_{cell}	Cell temperature	[ºC]
$\overline{H}$	Monthly average radiation on a horizontal surface	[MJ/m^2]	TDH	Total Dynamic Head	[m]
$\overline{H_d}$	Monthly average diffuse radiation on a hor. surface	[MJ/m^2]	T_{ext}	Outside air temperature	[ºC]

$\overline{H_T}$	Monthly average radiation in a tilted surface	[MJ/m^2]	Ur	Global heat transfer coefficient	[W/ºC]
I_0	Extraterrestrial hourly radiation on a horizontal surface	[MJ/m^2]	V	Velocity	[m/s]
I_0	Dark Saturation Current	[A]	v	Specific volume	[m^3/kg]
$I_{0;ref}$	Reference dark current	[A]	V_e	Voltage	[V]
I_b	Beam radiation	[MJ/m^2]	VI	Pump energy consumption	[MJ]
I_d	Diffuse radiation	[MJ/m^2]	V_m	Tank water volume in instant m	[m^3]
I_e	current	[A]	V_{m-1}	Tank water volume in instant m-1	[m^3]
I_L	Light Current	[A]	$\bar{\dot{V}}$	Consumption flow	[m^3/day]
$I_{L;ref}$	Reference Light current	[A]	$\overline{\dot{V}_m}$	Mean daily flow in instant m	[m^3/day]
I_{mp}	Maximum Power Current	[A]	$\bar{V}_{annua}$	Annual Volume	[m^3]
$I_{mp\ single}$	Maximum Power Current of a single panel	[A]	$\dot{V}_{m-1}$	Mean daily flow in instant m-1	[m^3/day]
I_{sc}	Short Circuit Current	[A]	V_{OC}	Open Circuit Voltage	[V]
$I_{SC\ single}$	Short Circuit Current of a single panel	[A]	$V_{OC\ single}$	Open Circuit Voltage of a single panel	[V]
I_T	Radiation incident on a tilted surface	[W/m^2]	W	Refrigerator width	[m]
$\overline{I_T}$	Monthly average hourly radiation	[MJ/m^2]	WHP	Water Horse Power	[W]
K	Boltzmann's Constant	[J/K]	$\dot{W}$	Compressor or pump power	[W]
$\overline{K_T}$	Average clearness index		X	Mass Fraction	
K_T	Daily clearness index		Z	Height	[m]
k_T	Hourly clearness index			**Greek**	
L	Refrigerator length	[m]	ρ_g	Ground Reflectance	
M	Vaccine mass	[kg]	μ	Dynamic viscosity	[Pa.s]

m	Air mass				
$\dot{m}$	Mass flow	[kg/s]	$\mu_{I;SC}$	Short Circuit temperature coefficient	[A/ºC]
n	Average day of the year	[day]	$\mu_{V;OC}$	Open Circuit temperature coefficient	[V/ºC]
n_{month}	Number of days in month	[day]	β	Tilted angle	[º]
NOCT	Normal Operating Cell Temperature	[ºC]	δ	Declination	[º]
$nr_{cel;s}$	Number of cells connected in series		E	Surface Roughness	[m]
$nr_{pv\ parallel}$	Number of PV panels connected in paraller		Θ	Angle of incidence	[º]
$nr_{pv\ serie}$	Number of PV panels connected in series		Θ_z	Zenith angle	[º]
N_s	Specific speed		ρ	Specific mass	[kg/m^3]
Nu	Nusselt number		□	Surface azimuth angle	[º]
P	pressure	[Pa]	Φ	Latitude	[º]
P_{mp}	Maximum Power Point	[W]	η_{pump}	Pump efficiency	
PV_{eff}	Photovoltaic panels efficiency		η	Efficiency	
PV_{power}	Photovoltaic panels power	[W]	ω	Hour angle	[º]
Q	Flow	[m^3/s]	ω_s	Sunset hour angle	[º]
q	Specific heat	[J/kg]			
q_e	Electron Charge	[C]			

1. Introduction

Collaborating with EpDAH that operates in Mozambique this project tries to apply engineering knowledge with the objective to contribute to a better life for the population of a rural village in Mozambique.

This project tries to give people enough water for consumption and possible to agriculture. Developing the agriculture creates more food and develops the village. With money coming to the village, villagers can buy other things that they need, for example, seeds, animals, upgrade the water system. With water and a developed agriculture there is enough food for everyone and with potable water disease decreases and people have a better quality of life.

Not only water contributes to a better quality life for the villagers. Give villagers health care is very important and the association is considering building a health center. Some drugs and vaccines need to be conserved at low temperatures (2ºC to 8ºC) and they are stored in refrigerators.

The project, direct or indirectly, approach the following themes in the *Autarkheia* project:

- Energy
- Water
- Agriculture
- Health
- Economic activities

1.1 ONU Millennium Development Goals (MDG)

The millennium Development Goals are eight international development goals with 21 targets and a series of measurable indicators for each target [38]. This project intervenes in Goal 6: Combat HIV/AIDS, malaria and other diseases and in Goal 7: Ensure environmental sustainability in the following targets:

- **Target 6C:** Have halted by 2015 and begun to reverse the incidence of malaria and other major diseases
- **Target 7C:** Halve, by 2015, the proportion of people without sustainable access to safe drinking water and basic sanitation

1.2 About Malonguete village

Malonguete village distance 80 km from the district capital city *Chicualacuala* (Figure 2) located in Gaza province (Figure 1). There is only one road and is very precarious. Normally in rainy days is almost impossible to circulate due to bad road state and surface rivers. So is difficult to transport merchandise, people and animals. There for *Malonguete* is 3 or 4 hours away from the district capital.

The people that live in the village are very poor and live from the local undeveloped agriculture. There is an agriculture association since 2003. Since then they only afforded 3 cows. Their objective is to have one cow for each associate. There are about 400 villagers in

the village. It is very important to develop the village and create job opportunities so young people don't immigrate to other countries like South Africa.

The agriculture is for family sustain and depends on annual rainfall. Without enough water it's not possible to have a developed agriculture. There is a river which crosses the village named *"Chefu"* (born in Zimbabwe). People build their houses along the river to have water near them (maximum distance is 1 km). Some families go to the river every day and others only once per weak because they have animals and wains to transport high volumes of water. Only a few mouths of the year the river is at the surface (2 or 3 mouths). In the other mouths they have to dig to have access to water. The water is for consumption because they don't have the habit to irrigate the crops. The animals they have are not for consumption. Animals are used as a bank account. For example, when someone gets ill they sell an animal to have money for the treatment. The nearest health center distance 12 km from the village and there is only transport two times a week (Wednesday and Friday). Usually people use bikes or their own feet.

The village have a well that needs maintenance. Today nobody uses that well. It was built in 2007 and belongs to the villagers. Villagers said that this well, since it was built, never run dry. They stop using the well because the wood seal that closes the tank from atmosphere was taken by the river.

Figure 1 – Mozambique map with province capitals

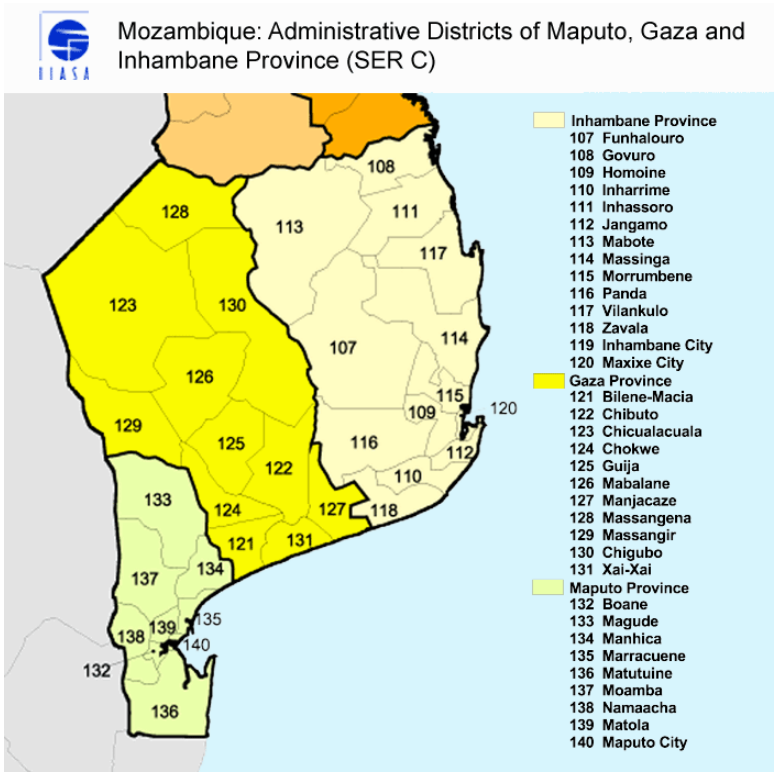

Figure 2 – Inhambane, Gaza and Maputo provinces. Chicualacuala district is the number 123

1.3 ***Systems used in developing countries to satisfy the water needs***

Actually there are two mature water systems that are widely applied in developing countries with villages without grid power. The most reliable (and expensive) is the solar water pumps system. Experience of operating PV pumps has shown that due to their simplicity, high reliability and the stand-alone operation these systems are appropriate for remote rural areas [I. Odeh et. al, 2005]. On the other hand it is used diesel powered pumps. Diesel pumps are characterized by a lower first cost but a very high running and maintenance costs. Solar is the opposite. Solar pumps sometimes run for years without anyone touching them [Self, 2008].

Sometimes it's not the cost of diesel maintenance that cares but the time to repair the malfunction. In a village were crops depend on water one or four weeks without water could mean the crops end. So it is important to achieve a compromise between first cost, running cost and reliability. Another problem for diesel pumps is the escalating fuel prices and fuel shortages [Self, 2008].

Diesel pumps required sometimes skilled labour hand. Solar powered pumps normally are simpler systems and require unskilled labour to keep them running. The most frequency maintenance in solar systems is cleaning the dust from PV array every 2-4 weeks [Self, 2008].

In some cases it is almost impossible to have a solar powered pump. But this is the case were fuel is very cheap and the system power is very high. I. Odeh et. al (2005) showed that PV water pumping systems have shown better economic viability than diesel water pumping

systems for equivalent hydraulic energy capacities of up to 8000 m4/day, 4100 m4/day and 2600 m4/day depending on the interest rate. Hydraulic energy is defined by equation 1.

$$Hydraulic\ energy = H.\dot{Q} \qquad \textbf{Eq. 1}$$

Wind powered pumps have shown a reliable potential in some remote areas [Vick, 1996]. A mechanical wind pump, like the name suggests, transforms wind energy in mechanical energy. Electric-wind water pump produces electric energy from wind energy. The mechanical wind powered pump was applied many years ago. Today is more frequent to use electric-wind or solar water pumps. Both needs some local studies to predict the energy output from the system. If the collected data over a year isn't accurate the wind-electric system could be a failure because the power output varies with the cubic of wind velocity. In this area (Chicualacuala) is very difficult to obtain technical data. They only register the precipitation in the district capital. Depending on wind and radiation conditions at the local the wind-electric generator could produce much more energy if the local has high mean wind speeds. Like in the diesel systems is hard to tell witch system is better to apply because there is no data about weather conditions (wind and radiation on site).

Considering the solar radiation data in the *Maniquenique* station, the only system that can satisfy the village needs of water, in a simple and reliable way is the solar powered pumps. There is another possibility: a hybrid system that operates most of the time using solar energy and in case of failure the backup system activates (Diesel or Otto cycle). Failure here means system malfunction or insufficient energy production (several rainy days). The backup system could be a gasoline or diesel engine.

1.4 ***Vaccine refrigerators used in developing countries***

Refrigeration systems are divided in three categories: 1) electric operated; 2) thermal operated; 3) hybrid systems [Afonso, 2007]. Electric grid access is limited outside the country coastal cities and the alternatives normally are vapour compression cycle powered with photovoltaic technology or thermal operated with and absorption cycle by burning gas as a heat source or other heat source.

Photovoltaic refrigerators are powered by sun and at night or when the sun irradiation is low the refrigerator is running due to the application of deep cycle batteries that stores electric energy. As an electric energy source it could be used a diesel generator our wind but for the reasons pointed above they are not commonly used.

Thermal operated refrigerators use a heat source to produce a cold effect and this is achieved using an absorption cycle. Common refrigerators use an ammonia/water or water/lithium bromide fluids (refrigeration fluid/absorber) and as a heat source. These refrigerators are interesting because they have no moving parts and use gas or propane as their primary source of energy. Also these refrigerators could use a thermal solar collector to power the generator.

To select the right category several parameters should be analysed, for example:

- Initial system cost
- Maintenance and operation cost
- Fuel transport and shortages
- System reliability

1.5 ***Projects realized over the world – water systems***

Solar Energy For Africa Ltd (SEFA Ltd) is a private company specialized in photovoltaic business with projects particularly in Uganda and in the East African region in general. From the list of their projects two of them are very similar to the project realized in this dissertation:

- Solar water pumping system at Moroto Municipality - A Grundfos SP 3A 10/140 volts is powered by 32 photovoltaic panels each one with a 50 watt peak that pumps 50 cubic meters per day of water at a head of 60 meters that is stored in a tank.
- Solar water pumping system at Usuk Health center – Funded by the NGO of Soroti Catholic Diocese Development Organization (SOCADIDO) SEFA installed a SQFlex 2.5-2 system powered by 14 photovoltaic panels each one with 50 watt peak pumping 15 cubic meters of water per day at a head of 40 meters from the borehold to the tank.

NAPS System group is located in Finland and since 1981 delivered solar electric systems to more than 50 countries all over the world, one of them is the water supply in Yemen. The system was designed for a high mountain application in the west coastal area of Yemen and is powered by 24 photovoltaic panels producing 1200 peak watts to pump 8000 to 9000 liters per day (very high heads).

1.6 ***Sustainable development***

Sustainable development has three pillars: 1) economic; 2) social; 3) environmental. Diesel motors pollute air by emitting CO2 and other polluting gases. However, it is in the economic side. Solar powered water pumps are in the environmental side and runs away from the economical side. Both of them have positive and negative impacts in society. The ideal energy production technology is the balance between economy, society and environment.

Figure 3 – Sustainable development diagram

2. Solar powered water pump systems

The simplest Solar Water Pump (SWP) consist in a PV array, power controller, a water pump operated by a DC brushless motor and a storage tank (direct-coupled system – see figure 4 and Figure 5). There is another system that needs a DC/AC inverter if the electric motor uses AC current. The system gets more expensive with the addition of batteries (battery-coupled system) and possible less reliable. If the system is not carefully dimensioned the overall system efficiency is reduced with batteries because batteries dictate the operating voltage and not the PV panels [Buschermohle,]. This reduced efficiency could be minimized if a proper controller is selected to boost the battery voltage supply to the water pump. Using batteries increase initial, operating and maintenance costs. In this particular case there is no need to install batteries because solar energy is stored in water tanks in the form of potential energy. Figure 4 exemplifies a direct couple system with a storage tank.

Another problem of battery-coupled system is the battery life time. With high temperatures the battery life time becomes smaller resulting in a more frequency battery replacement. Another issue is an ambient problem. What services Mozambique provide to recycle old batteries replacing the old ones with new batteries? Normally batteries sold are car battery and they are not suited to PV systems. In rural areas batteries should be avoided if possible. Batteries could be used if it is need to store electric energy and use the electric energy when the generator can't produce energy providing the system autonomy for several days depending on consumption. Batteries probably are the weakest element in a PV system and needs control system to avoid overcharging and over discharging. Huacuz, Jorge M. concluded that human interaction with batteries and batteries control has a big impact in batteries life time.

2.1 ***Solar water pumps***

Solar water pumps are designed to use solar power efficiently. Electric motors that are coupled to the pump could use AC or DC current. Solar arrays produce DC current and to transform in AC current it is necessary to install additional equipment to transform DC to AC current (DC/AC inverter). Using this equipment generally reduces system efficiency but induction motors are reliable and maintenance free operation and less expensive. DC motors, except brushless motors, need frequent maintenance because of the sliding brush contacts. Brushless motors are available for applications that require low power which are suitable to solar water systems. The only problem of using brushless motors is there high cost. Nowadays some manufactures produce submersible pumps with brushless motors.

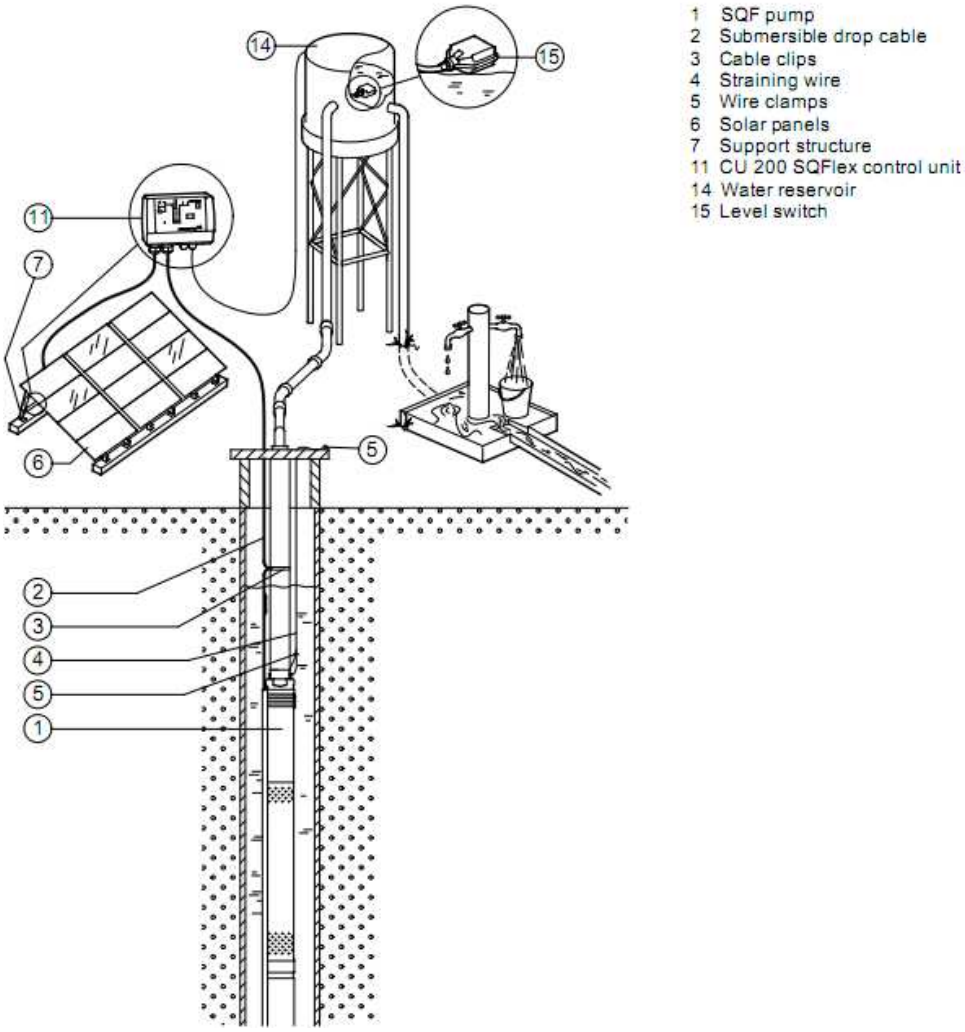

Figure 4 – Solar system components [Source: Grundfos SQFlex catalogue]

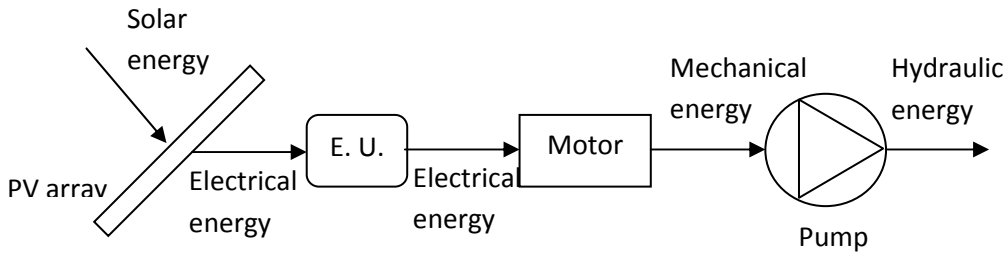

Figure 5 – Solar powered water pump system components – direct system

2.2 About water pumps

A pump is used to move liquid through a piping system and to raise the pressure liquid. The pump should add enough energy to the liquid to raise the liquid from one to a higher elevation (static head) and overcome the frictional losses. There are two other reasons, but not applied in this particularly system. The first is to move liquid to a higher pressure (pressurised vessel). The other is the liquid velocity because not all of the velocity energy is converted to potential

or pressure energy. The last one should take importance in calculations when the pressure is measured in a point where velocity isn't zero.

Pumps transform mechanical energy (torque, horsepower) to raise liquids pressure. To do this transformation there are two principals which results in different types of pumps. Positive displacement pumps increases liquid energy periodically by applying force to one or more moveable volumes. A three screw PDP is shown in Figure 6. Listed below are some positive displacement pump types:

- Reciprocating
    1. Piston or plunger
    2. Diaphragm
- Rotary
    1. Single rotor
        I. Sliding vane
        I. Flexible tube or lining
        II. Screw
        III. Peristaltic
    2. Multiple rotors
        I. Gear
        II. Lobe
        III. Screw
        IV. Circumferential piston

Dynamic pumps increase liquid velocity by means of fast moving blades or vanes and when the velocity is reduced the liquid pressure increase by exiting into a diffuser section. Water enters the impeller at the center and flows radially outward and is discharged from the circumference into the case. In the impeller the fluid gains velocity and pressure at the same time. The doughnut-shaped diffuser section of the casing decelerates the flow and further increases the pressure. See Figure 6 to better understand. The diffuser may be vaneless as in Figure 6 or fitted with fixed vanes to help guide the flow toward the exit. There is no closed volume and the liquid energy is continuously increased. The discharge is smooth and has less vibration problems than PD pumps requiring minor foundations. Listed below are some kinetic type pumps:

- Centrifugal
    1. Radial exit flow
    2. Axial flow
    3. Mixed flow (between radial and axial)
- Special designs

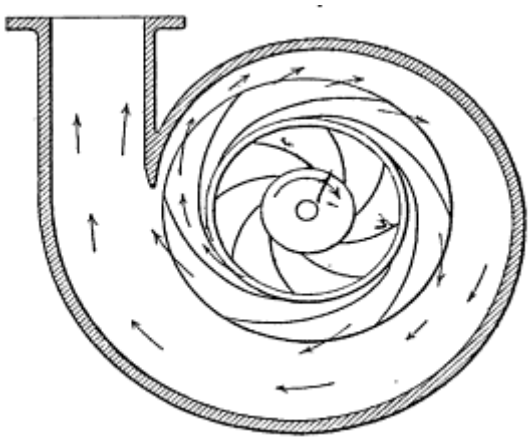

Figure 6 – Radial centrifugal pump – volute case

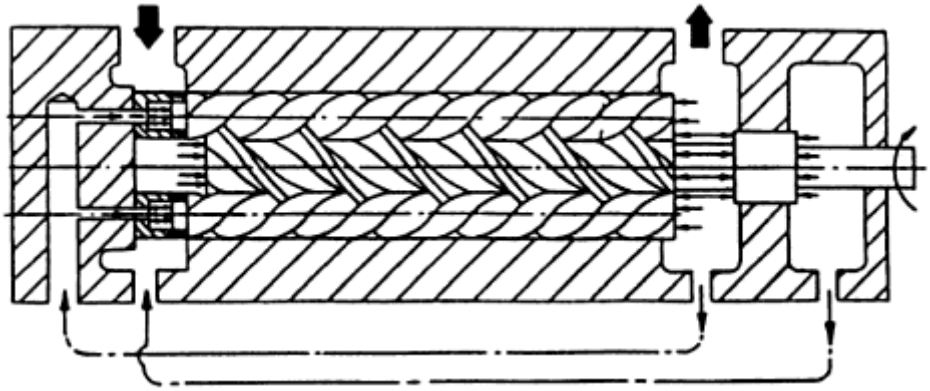

Figure 7 – Three screw positive displacement pump

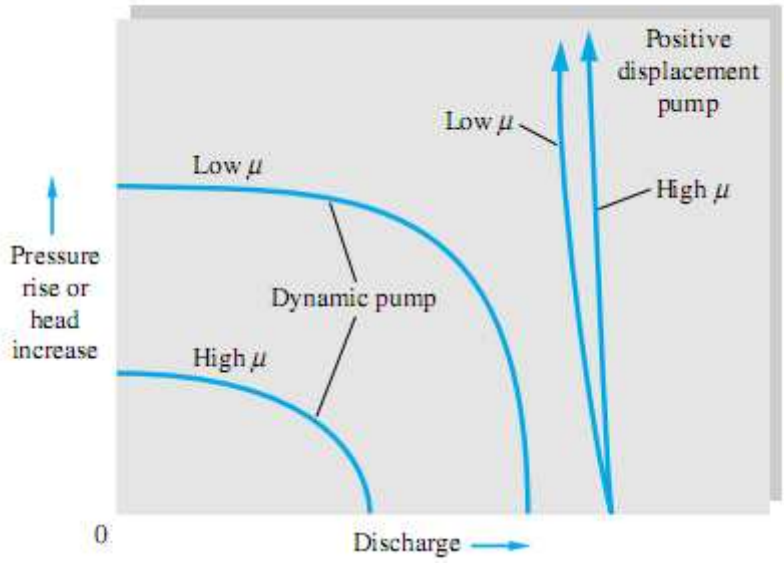

Figure 8 – Head versus flow rate curves at constant speed for typical dynamic and positive-displacement pumps [Source: White]

For this project the working fluid is water and only the first two items in the following list are important. The difference between the two pump types behaviour to the dynamic viscosity is shown in Figure 8. To select a PD pump instead of a centrifugal pump type the following applications key criteria must be met:

- High pressure
- Low flow
- High viscosity
- High efficiency
- Low velocity
- Low shear
- Self priming

The first two items in the list should be considered in more attention. It is also possible to find a centrifugal pump that produces very high pressures. And smaller centrifugal pumps are able to deliver small amounts of water. If the application needs very high pressure and demands a low flow then only the PD pumps can satisfy both conditions. Other listed items are important if the fluid wasn't water.

2.3 Basic output parameters

Assuming steady flow, neglecting viscous work, heat transfer and incompressible flow the pump head is equal to:

$$H = \left(\frac{P}{\rho \cdot g} - \frac{V^2}{2 \cdot g} - z\right)_2 - \left(\frac{P}{\rho \cdot g} - \frac{V^2}{2 \cdot g} - z\right)_1 \quad \textbf{Eq. 2}$$

The velocity in the inlet and exit are almost the same and the difference between z_2 and z_1 is minimum and the net head is approximately equal to:

$$\Delta H \approx \frac{\Delta P}{\rho \cdot g} \quad \textbf{Eq. 3}$$

Water horse power (WHP) or hydraulic power is the power delivered by the pump to the fluid for a given specific gravity, flow and head.

$$WHP = \rho \cdot g \cdot Q \cdot H \quad \textbf{Eq. 4}$$

The power required to power the pump is called break horsepower (BHP) and is equal to the torque (T) developed by the motor and the shaft angular velocity (ω).

$$BHP = \omega \cdot T \quad \textbf{Eq. 5}$$

Pump effectiveness is defined by the ratio between the hydraulic power and the break horsepower delivered by the motor.

$$\eta = \frac{WHP}{BHP} \quad \textbf{Eq. 6}$$

$$\eta_{motor} = \frac{BHP}{Electric\ power\ input} \quad \textbf{Eq. 7}$$

$$\eta_{sub\_pump} = \frac{WHP}{Electric\ power\ input} \quad \textbf{Eq. 8}$$

Submersible pumps manufactures assemble the pump and the motor in the same case that is sealed to avoid water inlet to electronic components. The electric power input required by the motor and the water horse power produced by the pump are normal data displayed in their catalogues.

2.4 ***Dimensionless pump performance***

The output variables head and break horsepower should be dependent upon discharge (Q), rotational shaft speed and impeller diameter. Other possible parameters are the fluid viscosity μ, density ρ and surface roughness ε.

$$\frac{g \cdot H}{RPS^2 \cdot D^2} = \mathrm{g_1}\left(\frac{\mathrm{Q}}{\mathrm{RPS} \cdot \mathrm{D}^3}, \frac{\rho \mathrm{n} \mathrm{D}^2}{\mu}, \frac{\epsilon}{\mathrm{D}}\right) \quad \textbf{Eq. 9}$$

$$\frac{BHP}{\rho \cdot RPS^3 \cdot D^5} = \mathrm{g_2}\left(\frac{\mathrm{Q}}{\mathrm{RPS} \cdot \mathrm{D}^3}, \frac{\rho \mathrm{n} \mathrm{D}^2}{\mu}, \frac{\epsilon}{\mathrm{D}}\right) \quad \textbf{Eq. 10}$$

The quantities $\rho \mathrm{n} \mathrm{D}^2/\mu$ and ϵ/D are the Reynolds number and roughness ratio (RR), respectively. The pump dimensionless parameters, capacity, head and power coefficient, respectively, are equal to:

$$C_Q = \frac{\mathrm{Q}}{\mathrm{RPS} \cdot \mathrm{D}^2} \quad \textbf{Eq. 11}$$

$$C_H = \frac{\mathrm{g} \cdot \mathrm{H}}{\mathrm{RPS}^2 \cdot \mathrm{D}^2} \quad \textbf{Eq. 12}$$

$$C_P = \frac{\mathrm{BHP}}{\rho \cdot \mathrm{RPS}^3 \cdot \mathrm{D}^5} \quad \textbf{Eq. 13}$$

The pump efficiency is already dimensionless and is related to the other three dimensionless parameters:

$$\eta = \frac{C_Q \cdot C_H}{C_P} \quad \textbf{Eq. 14}$$

2.5 ***The specific speed definition: Mixed and Axial Flow pumps***

Specific speed is a dimensional number that it is used to select the best size and shape (centrifugal, mixed or axial) for the pump. To calculate N_s it is necessary to know the head and discharge at BEP (best efficiency point) and pump (or motor) speed.

$$N_s = \frac{{C_Q}^{1/2}}{{C_H}^{3/4}} = \frac{\mathrm{RPS} \cdot {\mathrm{Q_{BEP}}}^{1/2}}{(\mathrm{g} \cdot \mathrm{H_{BEP}})^{3/4}} \quad \textbf{Eq. 15}$$

N_s is only applied to BEP. The specific speed is directly related to the most efficient pump design. Low N_s means low flow and high head hence a centrifugal pump and large N_s means and axial pump. The centrifugal pump is best for N_s between 10 and 20, the mixed flow pump for N_s between 80 and 200 and the axial pump for N_s above 200 as illustrated in Figure 9.

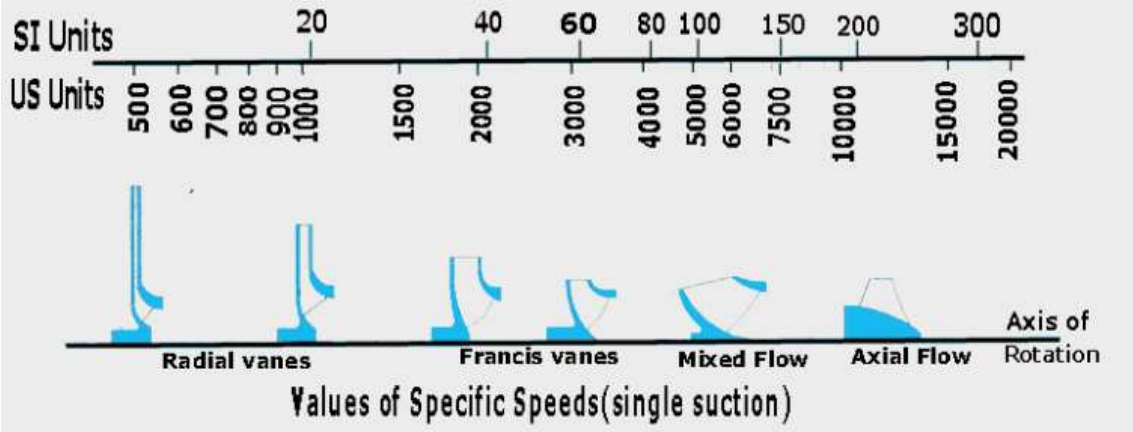

Figure 9 – Vane design of dynamic pumps as a function of specific speed [Source: White]

2.6 ***Pump capacity and TDH***

Pump capacity is the design flow rate that the pump must deliver. Usually the capacity is easy to find because the pump works in a circuit that demands a flow rate like an industrial pipe line which is not this case. Solar pumps capacity varies with the power that is delivered to the motor, the total dynamic head (TDH), impeller size and pump speed.

Total dynamic head (TDH) is calculated by the sum of 4 components:

- Static head
- Friction head
- Pressure head
- Velocity head

Static head is the total elevation change which the liquid must undergo. In this case static head is the vertical distance between the free surface of the well and water tank as illustrated in Figure 10. Friction head is the head necessary to overcome friction losses due to piping, valves and fittings for the system in which the pump operates. Using smaller cross section increases operation costs and decreases initial costs. Smaller piping system components raise friction head loss. In this case the considered initial costs are the sum of PV array, controller and pump cost. Photovoltaic technology is very expensive so it as a high weight in the initial costs. Another important issue is that smaller cross section suction lines might cause the pump to cavitate due to the increased friction line in the pump inlet pipes. If the selected pump is submersible cavitation problems shouldn't exist.

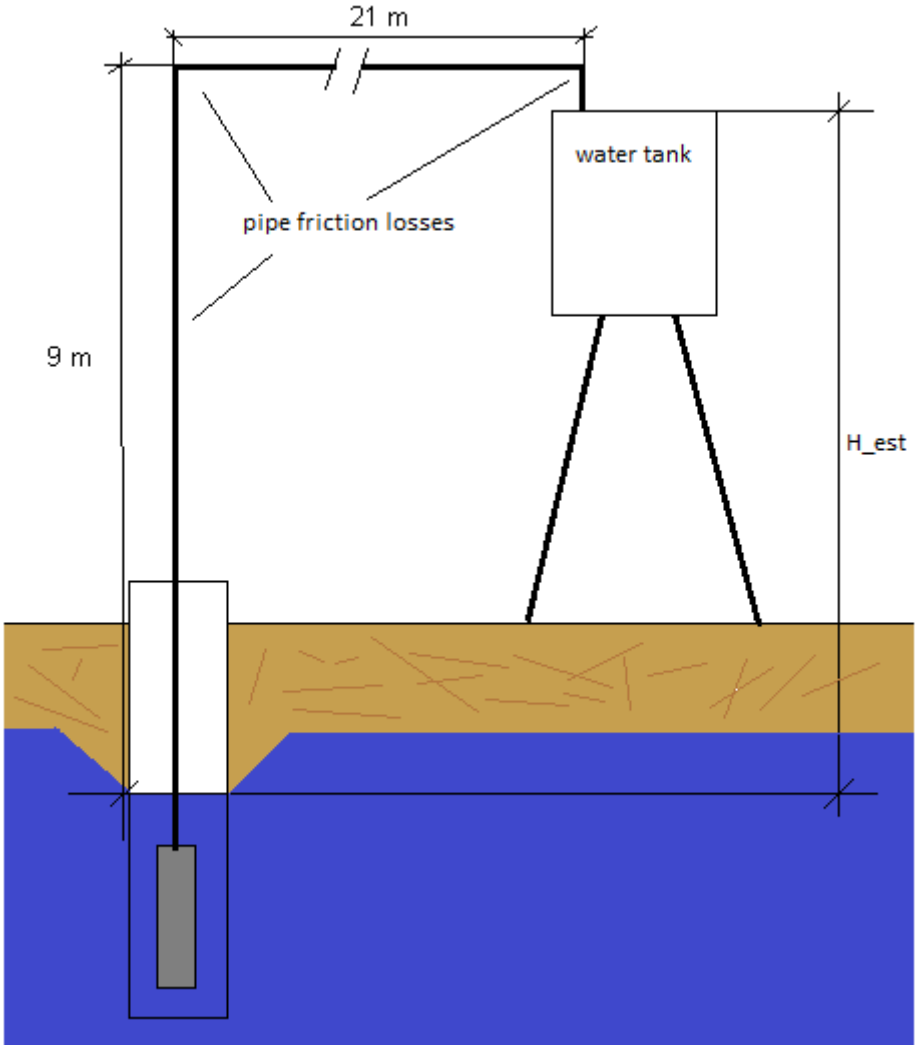

Figure 10 - Static head and pipe friction head

Pressure head and velocity head are important in some systems. In this project it is considered that the well and water tank are at the same pressure (atmospheric pressure). Velocity head is important if the head is measured in points were velocity is not zero. This is because not all of the velocity energy is converted to potential or pressure energy. TDH is calculated by equations 14 to 17.

$$TDH = H_{est} + H_f \quad \textbf{Eq. 16}$$

$$H_f = H_{f\,(pipe)} + H_{f\,(valve/fitting)} \quad \textbf{Eq. 17}$$

$$H_{f\,(pipe)} = f \cdot \frac{L}{D} \cdot \frac{V^2}{2g} \quad \textbf{Eq. 18}$$

$$H_{f\,(valve/fitting)} = K \cdot \frac{V^2}{2g} \quad \textbf{Eq. 19}$$

$$\frac{1}{f^{1/2}} = -2{,}0 \cdot \left(\frac{\varepsilon/D}{3{,}7} + \frac{2{,}51}{Re_d \cdot f^{1/2}}\right) \quad \textbf{Eq. 20}$$

The program selected to solve the equations (EES) has built in functions that are suited to be solved using computer calculations. The Darcy friction factor "f" is calculated using the Churchill correlation (Eq. 21). The function input variables are the Reynolds number (Eq. 22) and relative roughness (Eq. 23). The Churchill relation provides a smooth transition between laminar and turbulent flow regimes as shown in Figure 11. This eliminates the use of a function that determines if the flow is laminar or turbulent and the use of two equations for each fluid regime.

The value in Figure 11 for relative roughness was calculated for $D=1^{1/2}$ (38,1 mm) and ε = 0,0015mm (plastic pipe roughness) [White, 2003].

$$f = 8 \cdot \left[\left(\frac{8}{Re} \right)^{12} + \left(\left[2{,}457 \cdot \ln \left(\frac{1}{\left[\frac{7}{Re} \right]^{0{,}9} + 0{,}27 \cdot rough} \right) \right]^{16} + \left[\frac{37530}{Re} \right]^{16} \right)^{-1{,}5} \right]^{\left[\frac{1}{12} \right]} \quad \textbf{Eq. 21}$$

$$Re_d = \frac{\rho \cdot V \cdot D}{\mu} \quad \textbf{Eq. 22}$$

$$RR = \frac{\varepsilon}{D} \quad \textbf{Eq. 23}$$

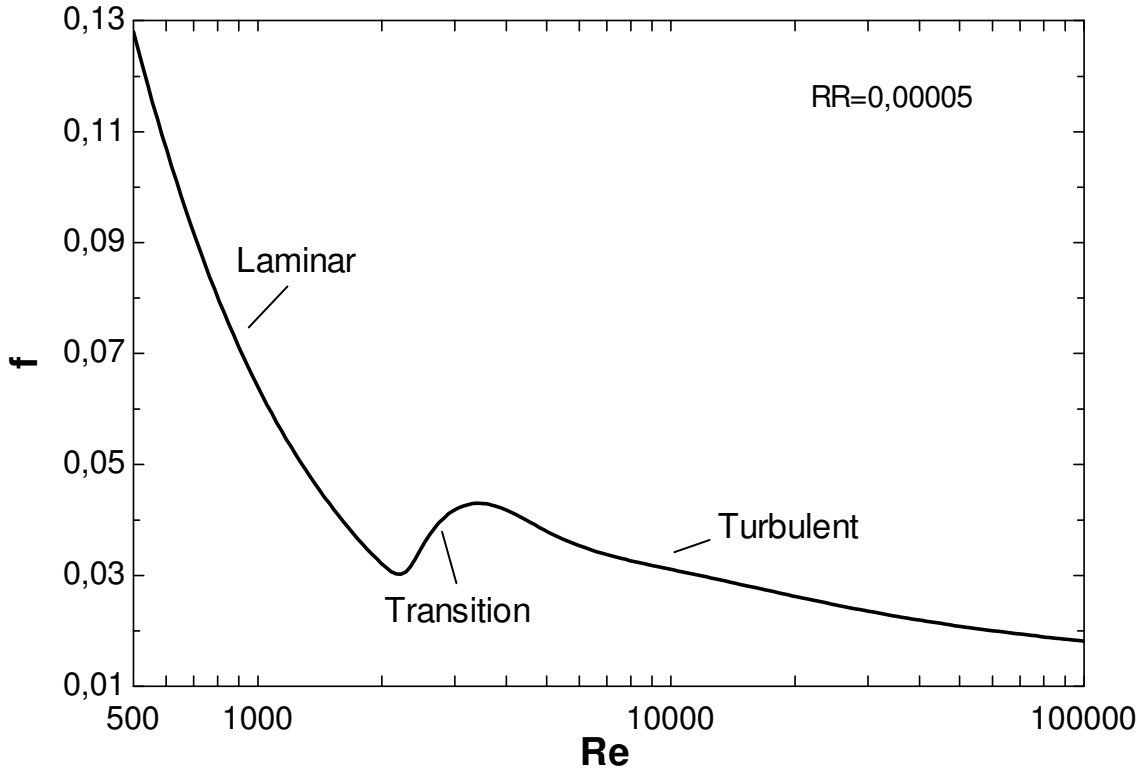

Figure 11 – Darcy friction factor as a function of Reynolds and relative roughness (RR) drawn using Eq. 21

H_f also depends from local losses, i.e., valves, fittings, sudden expansion or contraction, bends, inlets and outlets. These losses are measured experimentally and correlated with flow parameters. The loss coefficient K is given by Eq. 24.

$$K = \frac{\Delta P}{\frac{1}{2}\rho V^2} \qquad \text{Eq. 24}$$

The value K can be obtained from manufactures catalogues or consulting tables in the bibliography. These additional losses are also called *minor losses* [White, 2003]. There is an error associated by not taking into account these minor losses. It is difficult to know all the local losses, but as exampled in Table 1 it is considered that the total loss coefficient K is equal to 4. The considered pipe length is 30 meters as shown in figure 10.

Table 1 – Loss coefficient for several system components

Description	K
Pump entrance	0,5
90º regular elbow (screwed)	2x1,25
Tank discharge	1

Figure 12 illustrate the error by neglecting minor losses as function of flow rate, static head and pipe diameter. Since $H_{f\ (valve/fitting)}$ depends on the square of velocity increasing pipe diameter reduces substantially the error. Selecting pipe fixing between screwed (higher K) and flanged (lower K) influences the error by a factor of 2 as shown in Figure 13 and 14.

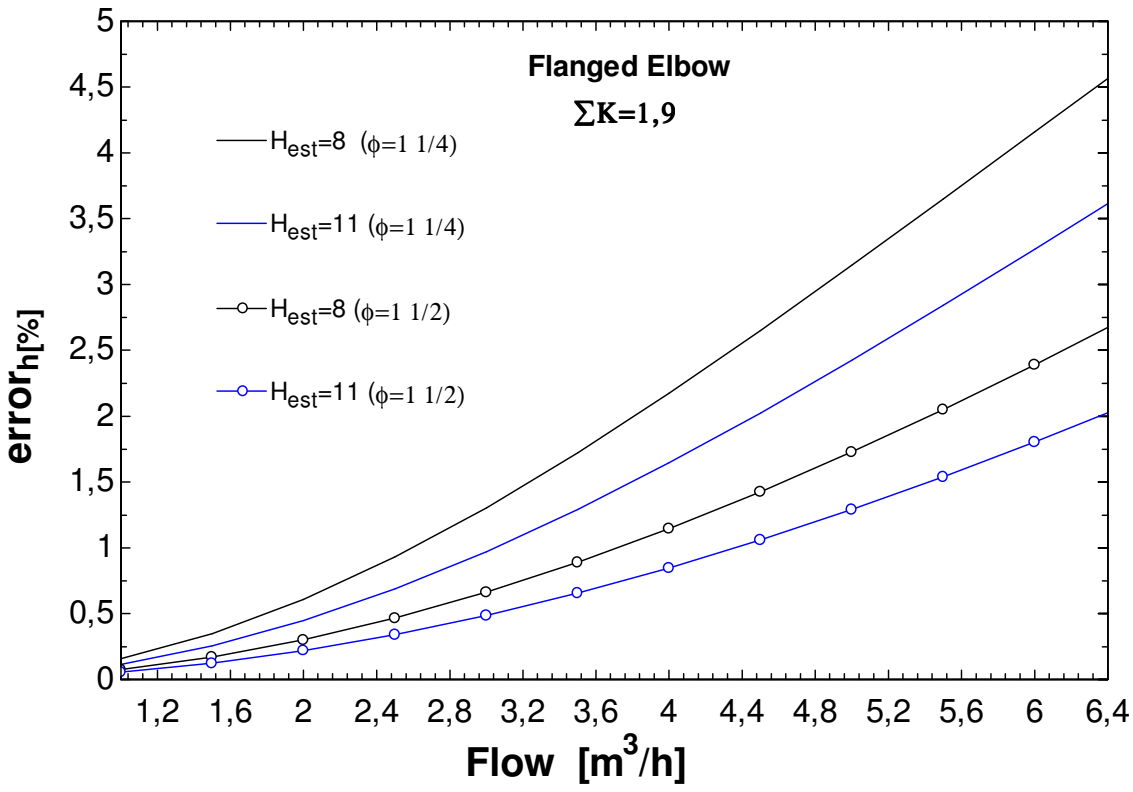

Figure 12 – H_f error by neglecting minor losses as function of Flow, Static head (H_est) and pipe diameter for K=1,9

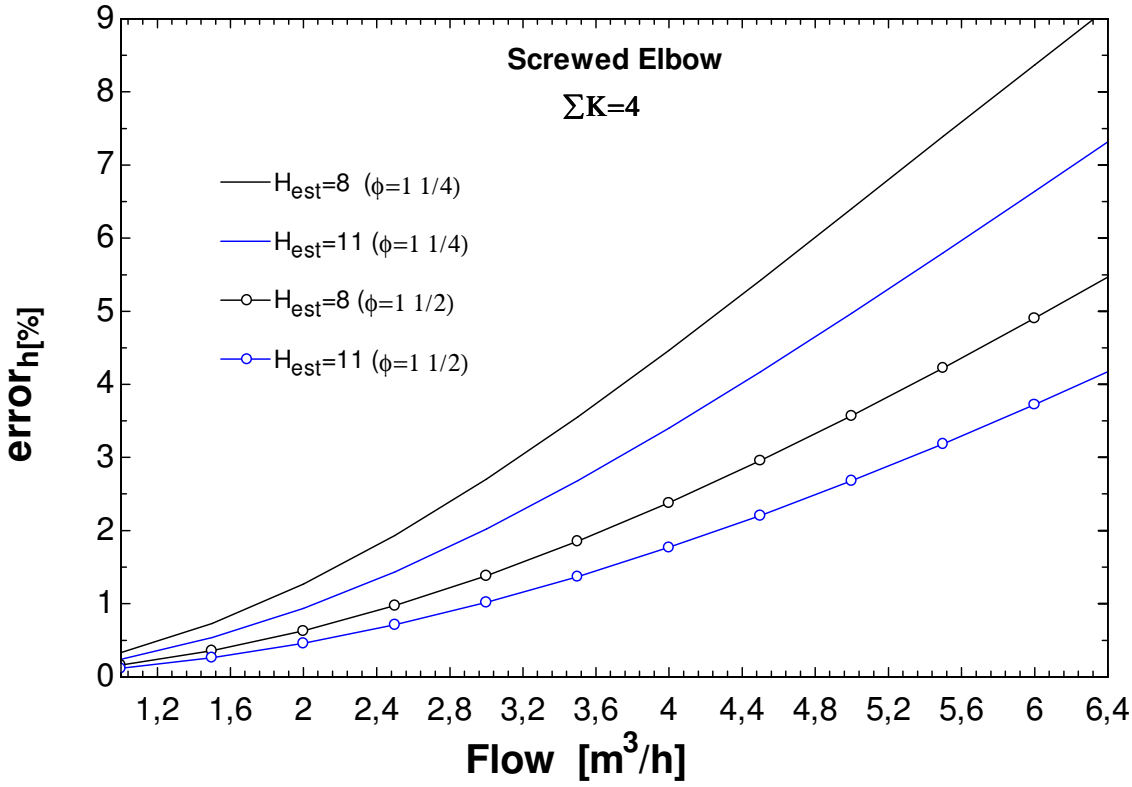

Figure 13 - H_f error by neglecting minor losses as function of Flow, Static head (H_est) and pipe diameter for K=4

The error considering ΣK=1,9 or ΣK=4 compared to the TDH considering ΣK=0 is calculated by equation 25.

$$error_h = \frac{TDH - TDH_{k=0}}{TDH} \qquad \textbf{Eq. 25}$$

In Figure 14 the H_f error, by neglecting the minor losses, as minimum impact in the annual water volume predicted, for the SQF 2.5-2 system, and varies linearly with the array area. Otherwise indicated the loss coefficient will have the value of 4. It's hard to predict all the minor losses due to a several reasons (from the most to the less influent):

- Connection type – flanged or screwed
- Tube roughness can vary from 0.0015 to 0.007 mm (ε/D ratio)
- Elbow radius or R/D ratio

The annual predicted volume of water error is defined as

$$error_h = \frac{\bar{V}_{annual} - \bar{V}_{annual;k=0}}{\bar{V}_{annual}} \qquad \textbf{Eq. 26}$$

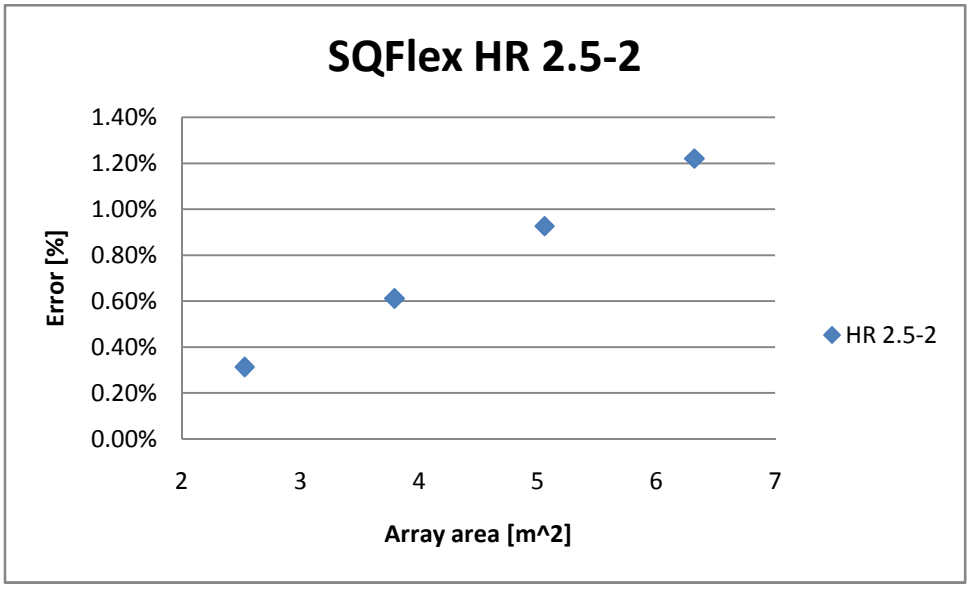

Figure 14 – Error in the annual predicted volume as a function of array area for the SQFlex HR 2.5-2 pump and K=4 and 30 meters of pipe length

2.7 System head curve

System head curve is designed to understand how head varies with the flow. After the designed system curve it is important to select a pump that operates most of the time at or near best efficiency point (BEP). To know where the pump operates it is necessary to have technical data about the selected pump to design the pump H-Q curve. The interception between these two curves is the pump operating point.

The distance between the two curves drawn in Figure 15 is the static head which varies in time. Without technical data it's hard to predict the river level within a year. It is known that the rainy season happens between October and January. In the well the highest level will probably be in December and January. Table 2 lists the considered static head for each month of the year to simulate the static head variations in a year.

Table 2 – Static head considered for the 12 months of a year

Month	Static head H_{est} [m]	Month	Static head H_{est} [m]
January	7	July	10
February	7	August	11
March	9	September	11
April	9	October	10
May	9	November	8
June	10	December	7

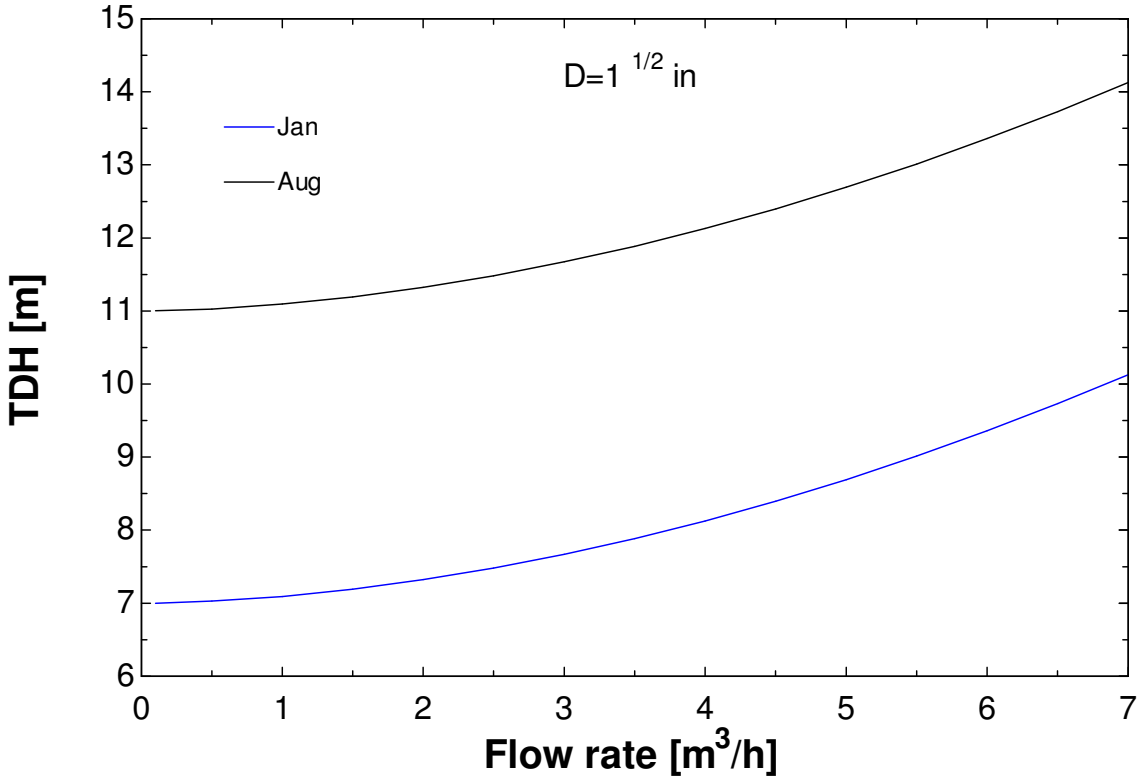

Figure 15 – System head-flow rate curve for 2 months of the year for D=38,1mm

The system head flow is drawn by varying the flow rate and from equations 16 to 20 the TDH is calculated and plot against the flow rate. The curve slope depends from flow rate, pipe diameter and *minor losses*.

2.8 ***Pump H-Q curve***

The flow delivered by the pump varies with the head. The lower the head the higher is the flow delivered by the pump. Pump horse power and efficiency varies with the flow rate as shown in Figure 16. The pump should operate at BEP (best efficiency point) but due to high static head variations over a year, as listed in Table 2, is hard to satisfy this condition. In Figure 16 the pump operation point is near the best efficiency point (BEP) for the August month (H_{est}=11m). For the other months the pump operation point is away from the BEP. The variations of efficiency during the year are less than 5% from the BEP. As proved here the pump must work within a range of flow rate.

Solar energy in a tilted surface varies with time and the power delivered by the generator to power the pump varies with time too. For a system, with a specific static head, there is only one H-Q curve but for the pump there is one for each shaft rotation speed (RPM). This means that solar pumps operate with a large spectrum of RPM and usually from 500 to 3600 RPM.

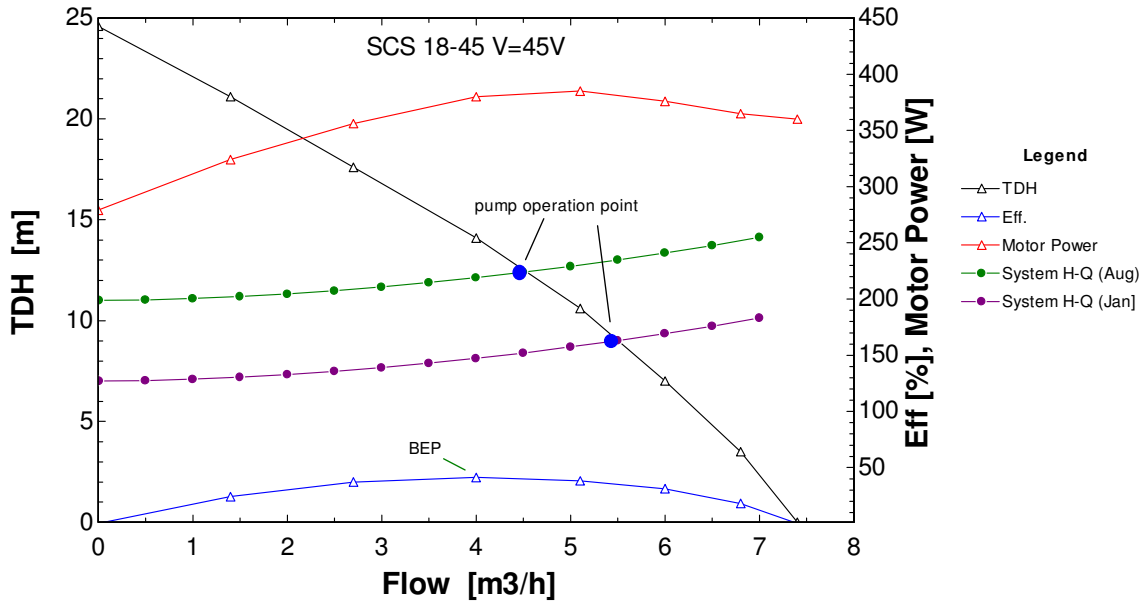

Figure 16 – Sunpump SCS 18-45 TDH, pump efficiency and motor power as a function of flow rate and system head for the1st and 8th month of the year (pipe diameter D=1 ½ in and motor voltage=45V)

2.9 Selecting a pump type and solar water pumps manufactures

It is important to select a type of pump. To do this it could be used the key applications criteria as shown before and the difference between the different type pumps. For example, centrifugal pumps are used in applications with low head and high demand flow. PD (positive displacement) pumps are used in applications with high heads and low flow demand. Generally PD pumps are more efficiency but centrifugal pumps possibly have lower maintenance expense. In low power consumption systems the energy that is economized often is not sufficient to overcome the maintenance expense. In remote areas maintenance must be kept as lower as possible due to lack of spare parts and specialized labour hand. Manufactures solutions converged to some types of pumps and this is a sign of the technology maturity.

Solar water pump manufactures display data about their pumps in different ways. Lorrentz and Sunpumps display their data as H-Q curve as illustrated in Figure 16 and datasheets. Grundfos display their data only in the form of graphics similar to Figure 17. With Figure 17 it is not possible to draw the system head curve and know the pump operation point. It is not possible to draw pump H-Q curve, from the Grundfos curves, because power varies with discharge as shown in Figure 16. The Grundfos curves were designed to simply read the flow as a function of motor power and TDH for a given pump.

As said before the power delivered to the pump varies with time because the generator is powered by solar energy. To exemplify and using Figure 17 if TDH is equal to 15 meters and the power delivered to the motor is equal to 200 W the pump will discharge approximately 1 m^3/h.

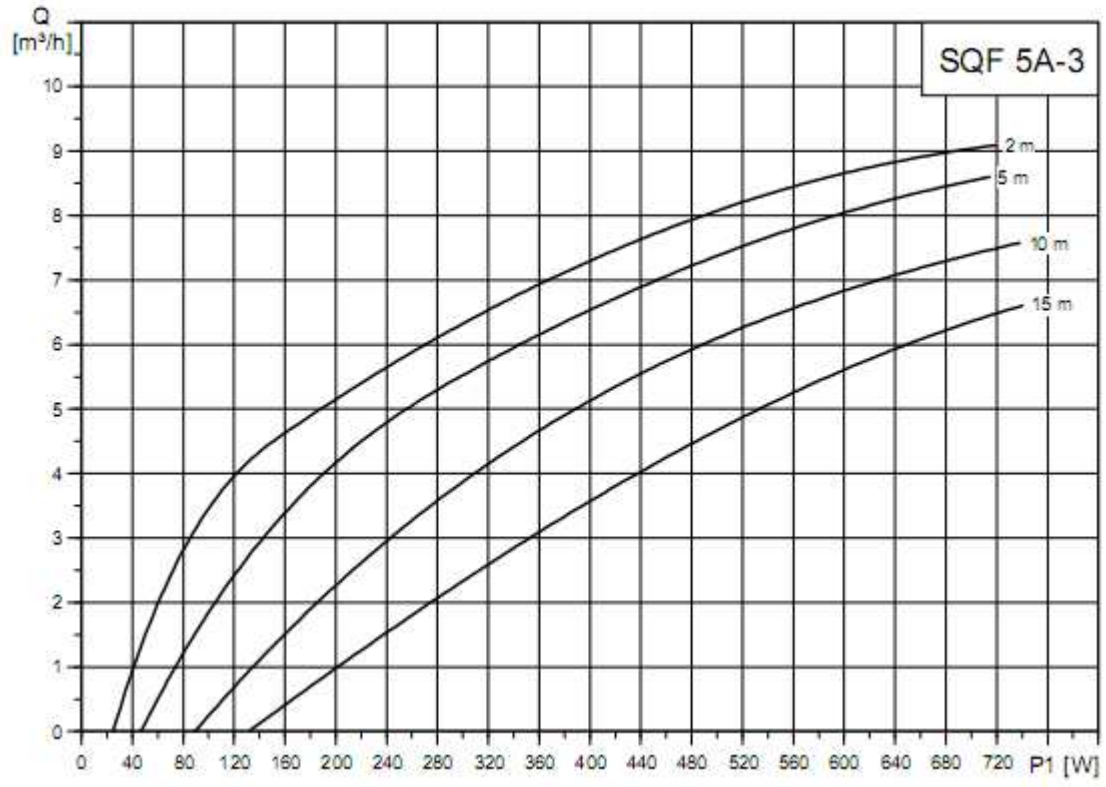

Figure 17 – Grundfos SQF 5A-3 data [Source: Grundfos renewable energy pumps catalogue]

2.10 Matching system components

The overall system efficiency is sensitive to the match between the pump and the PV system. Achieving better system efficiency could mean a reduction in the initial costs. To match the system components some data must be known: consumption curve over a period of time, maximum and minimum pumping head, insolation and PV array size. First it is necessary to choose a pump that works almost all the time near BEP and at the same time guaranties the minimum flow at the maximum pumping head. Running to much away from this point means a reduction on system efficiency and also lowering the pump life time. The second step is matching the PV array size with the insolation and the pump. There is also another method that is commonly used by pump manufactures. They develop electronic units that try to maximize the photovoltaic array power and deliver it to the pump. With this unit the amount of water delivered per day is increased by 10 to 15% [Buschermohle,].

2.11 Electronic Unit Control

Solar powered pump manufactures provide power conditioning circuitry to provide the most suitable voltage-current combination to the motor and at the same time ensuring that solar panels operates at their maximum power point (MPP). In effect, it alters the load impedance to match the optimum impedance of the array [Wenham, 2009].

Electrical impedance extends the concept of resistance to AC circuits, describing not only the relative amplitudes of the voltage and current, but also the relative phases. When the circuit is driven with direct current (DC) there is no distinction between impedance and resistance.

As the light intensity falls the current generated by the solar array drops proportionately and the voltage at the MPP remains approximately constant. However, for a motor/pump if the current drops the voltage also falls. In a direct coupled system, without electronic control, the voltage and current from the solar array is progressively further and further away from its maximum power point [Wenham, 2009]

The maximum power point trackers can improve effectiveness by reducing the possibility for the PV output power to transform into heat, with consequent motor damage, rather than mechanical energy.

3. Photovoltaic Panels

3.1 Semiconductors and J-n junctions

Solar cells are manufactured from semiconductor materials that act as insulators at low temperatures, but conductors when energy or heat is available. At present the most mature technology is silicon-based cells. Other materials are under investigation and may supersede silicon in the long term [Wenham, 2009].

A hole-electron pair is formed and an electron is out in the crystal structure. To form a hole-electron pair it is necessary a certain energy level (E_{ph}). Photons with a greater energy than the energy bandgap E_g ($E_{ph} > E_g$) interact with electrons in the covalent bonds using their energy to break the bonds and create electron-hole pairs. These normally disappear spontaneously as electrons recombine with holes. It is possible to shift the balance between electrons and holes by "doping" the silicon crystal with other atoms. Atoms with one more valence electron than the semiconductor are used to form the n-type material (phosphorous). Atoms with one less valence electron are used to form the p-type material (boron).

3.2 The band model

The band model explains the semiconductors behaviour in terms of energy levels between valence and conduction bands. The electrons in covalent bonds have energies corresponding to those in the valence band. In the conduction band the electrons are free. The forbidden gap corresponds to the minimum energy needed to release the electron from the valence band to the conduction band where it can conduct a current.

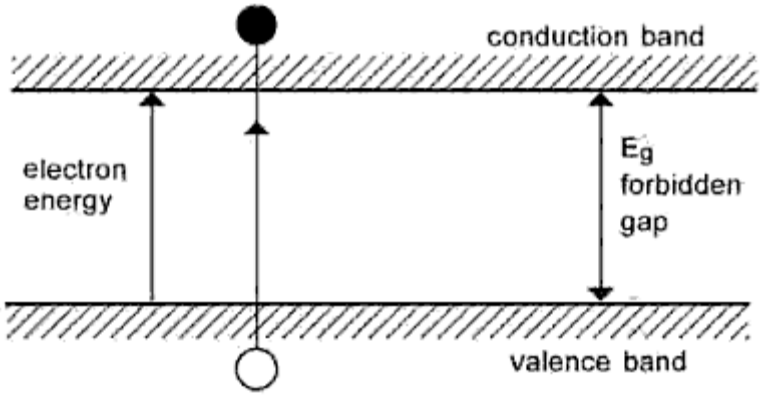

Figure 18 – Schematic of the energy bands for electrons in a solid [Source: Wenham, 2009]

3.3 Semiconductors types

Silicon and other semiconductors used for solar cells can be crystalline, multicrystalline, polycrystalline, microcrystalline or amorphous. Crystals are classified by their grain size. Microcrystalline materials have less than 1 µm, polycrystalline are smaller than 1mm and multicrystalline have less than 10cm.

Crystalline silicon has an ordered crystal structure. It is the most expensive type of silicon, because of the most careful and slow manufacturing processes required. Multicrystalline silicon is widely used for commercial solar cell production. It is cheap and has less critical

production techniques than those required to produce single crystal material. The grain boundary reduces the cell performance by blocking carrier flows, allowing extra energy levels in the forbidden gap, thereby providing effective recombination sites, and providing shunting paths for current flow across the p-n junction. Amorphous silicon can be produced, in principle, even cheaper than poly-silicon. With amorphous silicon, there is no longer range order in the structural arrangements of the atoms, resulting in areas within the material containing unsatisfied or "dangling" bonds. These in turn result in extra energy levels. It is common now to use amorphous silicon with hydrogen that saturates the dangling bonds and improves the material quality.

3.4 ***The p-n junctions***

A p-n junction is formed by joining the n-type and p-type semiconductor materials as shown in Figure 19. The p-junction has many holes and few electrons and the n-junction has many electrons and few holes. When they are joined the excess holes flow by diffusion to the n-type material and the electrons to the p-type material. An electrical field (Ê) is formed to stop the flow. Depending on the materials used, a "built in" potential (V_{bi}) owing to Ê will be formed. If a voltage is applied to the junction, as shown in Figure 19, Ê will be reduced and the built in potential reduces to V and the current flow increases exponentially with the applied voltage. This phenomenon is explained by the *Ideal Diode Law*, expressed as

$$I = I_0 \left[\exp\left(\frac{q_e V}{kT}\right) - 1 \right] \qquad \textbf{Eq. 27}$$

I is the current, I_0 is the dark saturation current (the diode leakage current density in the absence of light), V is the applied voltage, q is the charge on an electron, k is Boltzmann's constant ant T is the absolute temperature. For actual diodes, equation 51 becomes

$$I = I_0 \left[\exp\left(\frac{q_e V}{nkT}\right) - 1 \right] \qquad \textbf{Eq. 28}$$

Where *n* is the ideality factor, a number between 1 and 2 that typically increases as the current decreases. The diode law is illustrated for silicon in Figure 20.

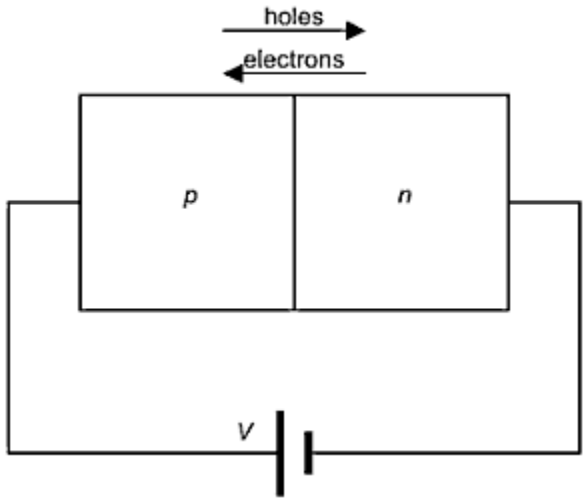

Figure 19 – Application of a voltage to a p-n junction [Source: Wenham, 2009]

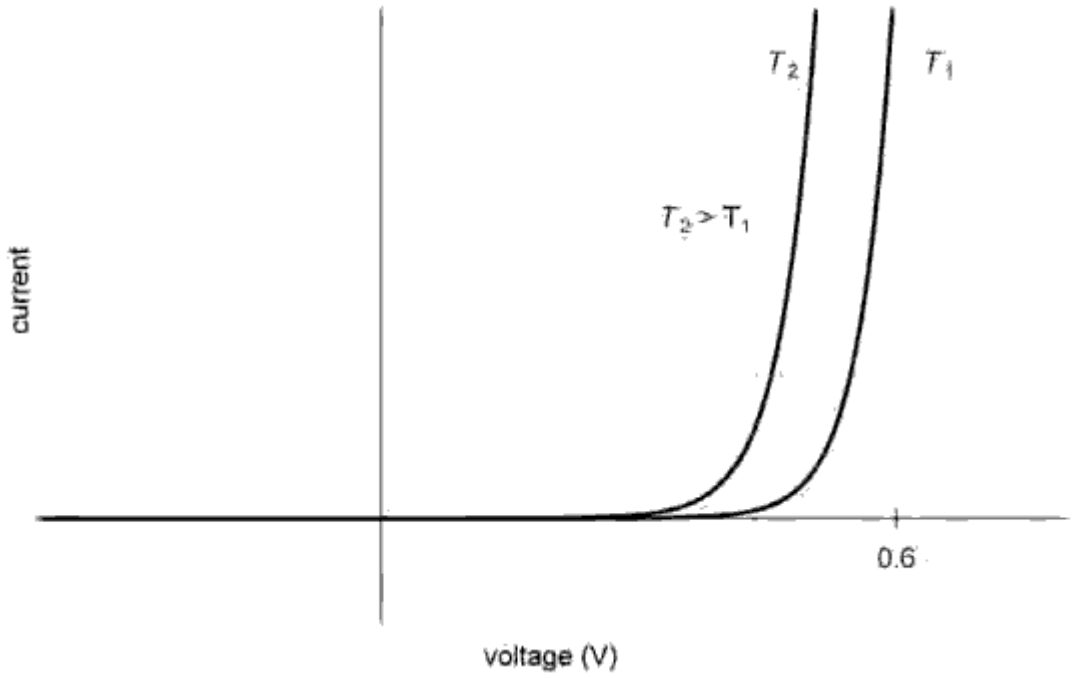

Figure 20 – The diode law for silicon –current as a function of voltage and temperature

3.5 ***The behaviour of solar cells – the I-V curve***

The typical photovoltaic I-V curves are different from Figure 20. Figure 20 was generated by plotting *I* against *V* for a diode with no light falling on the cell. Illumination on the cell merely adds to the normal "dark" currents in the diode so that the equation 52 becomes:

$$I = I_0 \left[\exp\left(\frac{q_e V}{nkT}\right) - 1\right] - I_L \qquad \textbf{Eq. 29}$$

and I_L is the light generated current.

The light has a displacement effect moving the I-V curve to the fourth quadrant. Manipulating the equation 53 it is possible to generate the typical I-V curve for photovoltaic panels-Figure 21.

$$I = I_L - I_0\left[\exp\left(\frac{q_e V}{nkT}\right) - 1\right] \quad \textbf{Eq. 30}$$

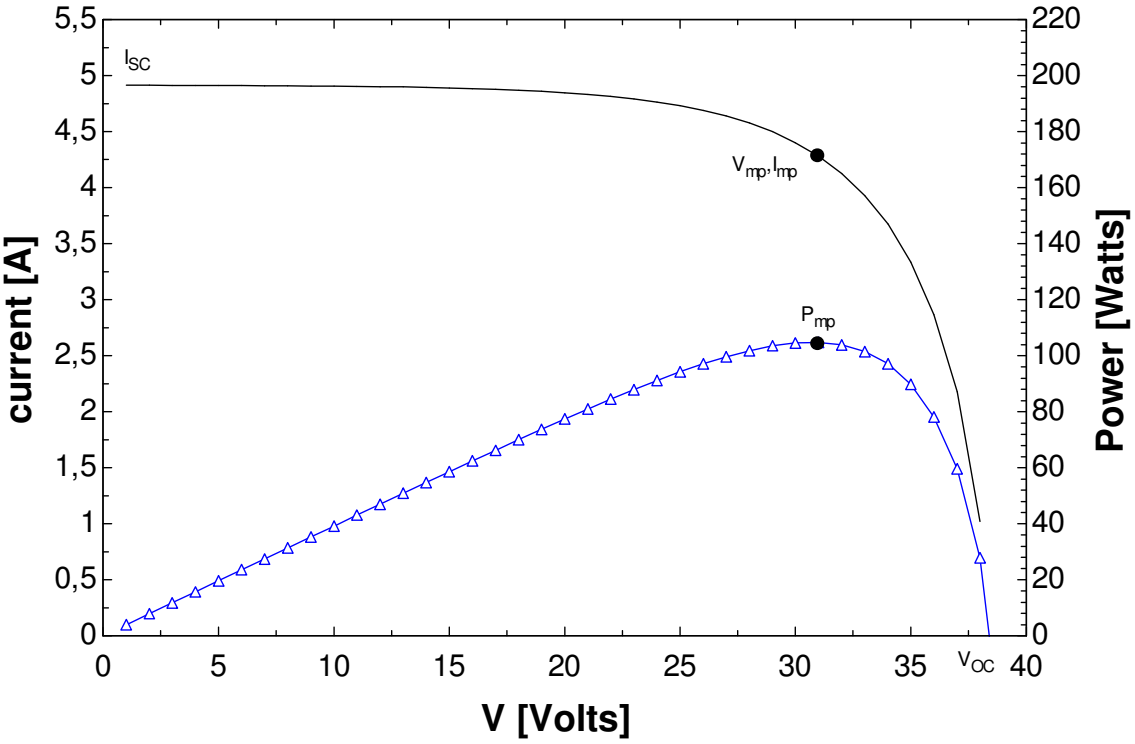

Figure 21 - Typical representation of an I-V curve showing maximum power and corresponding maximum voltage and current and open circuit voltage (V_{OC}) and short circuit current (I_{sc})

Figure 21 shows several important parameters that characterize a photovoltaic panel. V_{OC} is the open circuit voltage – the maximum voltage at zero current and increases logarithmic with the sunlight. I_{sc} is the short circuit current – the maximum current at zero voltage and is proportional to the sunlight. The maximum power point P_{mp} is the product of V_{mp} with I_{mp}. Mathematically is equal to

$$\frac{d(IV)}{dV} = 0 \quad \textbf{Eq. 31}$$

*3.6 **Effect of temperature***

As shown in Figure 20 the temperature affects the cells performance. The short circuit current increases with temperature; however, this is a small effect.

$$\frac{1}{I_{sc}}\frac{dI_{sc}}{dT} \approx 0{,}0006\ ^{o}C^{-1}\ (silicon) \quad \textbf{Eq. 32}$$

V_{oc} decreases with the increase of temperature as shown in Figure 20 and Figure 22 and for silicon as follows:

$$\frac{1}{V_{OC}}\frac{dV_{OC}}{dT} \approx -0{,}003\ ºC^{-1} \qquad \textbf{Eq. 33}$$

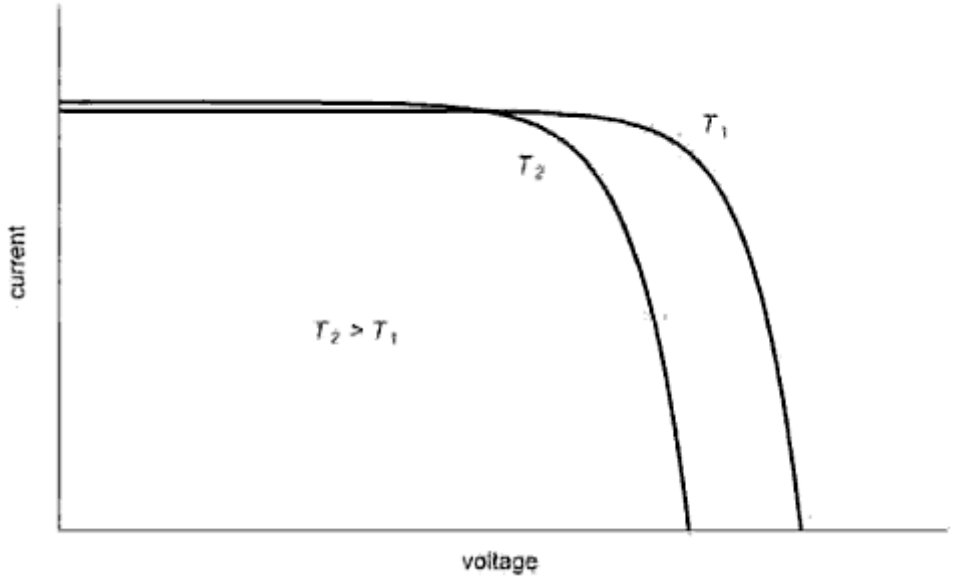

Figure 22 – Effect of temperature on the I-V curve of a solar cell

The maximum power point is also affected by the cell temperature as follows:

$$\frac{1}{P_{mp}}\frac{dP_{mp}}{dT} \approx -(0{,}004 - 0{,}005)\ ºC^{-1}\ (silicon) \qquad \textbf{Eq. 34}$$

Cell temperature depends on air temperature, wind velocity, insolation and NOCT and is calculated by equation 55.

$$T_{cell} = T_{air} + \frac{NOCT - 20}{800} \cdot G_T \qquad \textbf{Eq. 35}$$

The nominal operating cell temperature (NOCT) is defined as the cell temperature reached in open circuited cells in a module with the fallowing conditions:

- Irradiance on cell surface = 800 W/m^2
- Air temperature = 20ºC
- Wind velocity = 1 m/s
- Mounting = open rear surface

3.7 Effect of parasitic resistance

Figure 23 shows the series and shunt resistances. These resistances affect the semiconductor performance. Series resistance (R_s) are bulk resistance of the semiconductor material, the metallic contacts and interconnections and contact resistance between the metallic contacts and the semiconductor. Shunt resistance (R_{sh}) is due to p-n junction defects and impurities near the junction.

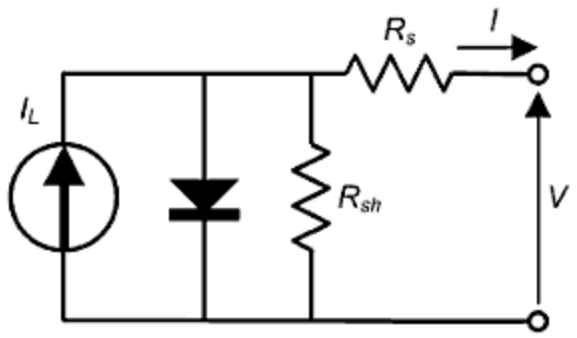

Figure 23 – Parasitic shunt and serie resistances in a solar cell circuit

3.8 ***Photovoltaic modules in series and parallels***

Photovoltaic modules connected in series and/or parallel permit to have different combination (higher current or voltage). As shown in Figure 24 two photovoltaic modules connected in various arrangements produce different currents or voltages. Series connections provide higher voltages and parallel connections provide higher currents. Figure 26 and in Figure 27 shows the series connection that permits to have a higher voltage. If the two panels are connected in parallel the voltage is the same but the current is the double.

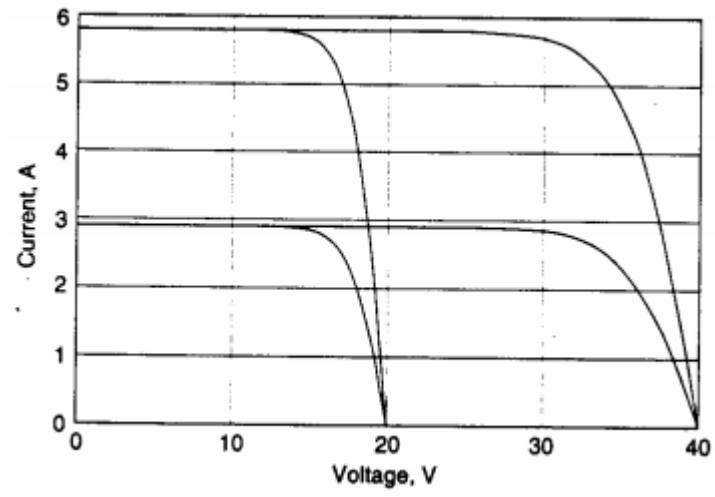

Figure 24 – I-V curve for photovoltaic modules connected in various series and parallel arrangements

4. EES equations and results

The following pages will list the equations that were used to:

- Predict the radiation on a sloped photovoltaic panel
- Generate the photovoltaic I-V curve using manufactures catalogue data
- Pump controller and pump modulation
- Pumping system results

4.1 Solar radiation on a sloped photovoltaic array

To predict the radiation on a sloped photovoltaic array it is necessary to know the power that comes from the sun. To characterize the radiation that comes from the sun there are two important factors: 1) a geometric factor, because of the relative movement of earth around the sun and the rotation of the earth around itself; 2) the solar extraterrestrial radiation that reach the atmosphere, which varies over a year, but is modelled by a constant that is equal to 1367 W/m^2. The extraterrestrial radiation incident on a horizontal surface is given by

$$H_0 = \frac{24 \cdot 3600 \cdot \mathrm{G_{sc}}}{\pi}\left(1 + 0{,}033 \cdot \cos\frac{360 \cdot n}{365}\right) \cdot \left(\cos(\phi)\cdot\cos(\delta)\cdot\sin\omega_s + \frac{\pi\omega_s}{180}\sin\phi\sin\delta\right) \quad \textbf{Eq. 36}$$

And the hourly extraterrestrial radiation on a horizontal surface is equal to

$$I_0 = \frac{12 \cdot 3600 \cdot \mathrm{G_{sc}}}{\pi}\left(1 + 0{,}033 \cdot \cos\frac{360 \cdot n}{365}\right) \cdot \left(\cos(\phi)\cdot\cos(\delta)\cdot\sin(\omega_2-\omega_1) + \frac{\pi(\omega_2-\omega_1)}{180}\sin\phi\sin\delta\right) \quad \textbf{Eq. 37}$$

The monthly average hourly radiation incident on a tilted surface is given by

$$\overline{I_T} = \overline{K_T}\,\overline{H_0}\left[\left(r_t - \frac{\overline{H_d}}{\overline{H}}r_d\right)R_b + \frac{\overline{H_d}}{\overline{H}}r_d\left(\frac{1+\cos(\beta)}{2}\right) + \rho_g\, r_t\left(\frac{(1-\cos(\beta))}{2}\right)\right] \quad \textbf{Eq. 38}$$

To know $\overline{I_T}$ it is necessary to calculate the monthly average clearness index $\overline{K_T} = \overline{H}/\overline{H_0}$ where $\overline{H}$ is the global average monthly radiation given by meteorological data and is listed for each month in Table 3. The meteorological data was taken by an average of 30 years measured in *Maniquenique* station with latitude and longitude equal to 24º44' and 33º32, respectively. G_T that appears after this chapter is in W/m^2 and is calculated by multiplying $\overline{I_T}$, which is in MJ/m^2, by 277,778. To better understand this equations see appendix A.

Table 3 – Global average monthly radiation taken over a period of 30 years in the Maniquenique station [Cuamba, 2006] and average day of the year [Duffie, 1991]

month	$\overline{H}$ [kWh/m^2/day]	n	month	$\overline{H}$ [kWh/m^2/day]	n
1	7,4	17	7	4,3	198
2	7	47	8	5	228
3	6,3	75	9	5,7	258
4	5,4	105	10	6,5	288
5	4,5	135	11	6,8	318
6	4,1	162	12	7,5	344

4.2 Photovoltaic I-V curve equations and results

This chapter summarise the equations that were used to model the photovoltaic array behaviour. Table 4 list some general constants that are needed to plot the typical I-V curve. The PV panels can be connected in various arrangements in series and/or in parallel. The total generator area is equal do the area of a single photovoltaic panel times the number of panels linked in series that formed a string and by multiplying the number of strings linked in parallel. Figure 25 exemplifies one example to better understand. Taking this into account the maximum power current and voltage will be affected by the respective number of panels connect in parallel and series. The same is done to the open circuit voltage and the short circuit current. The number of cells connected in series is also affected.

Table 4 - General constant values for photovoltaic I-V curve equations

T_{air}	25ºC
$T_{cel;ref}$	25ºC
$G_{T;ref}$	1000 W/m^2
Silicon bandgap (ε)	1,12 eV
r_{sh}	1000 Ω

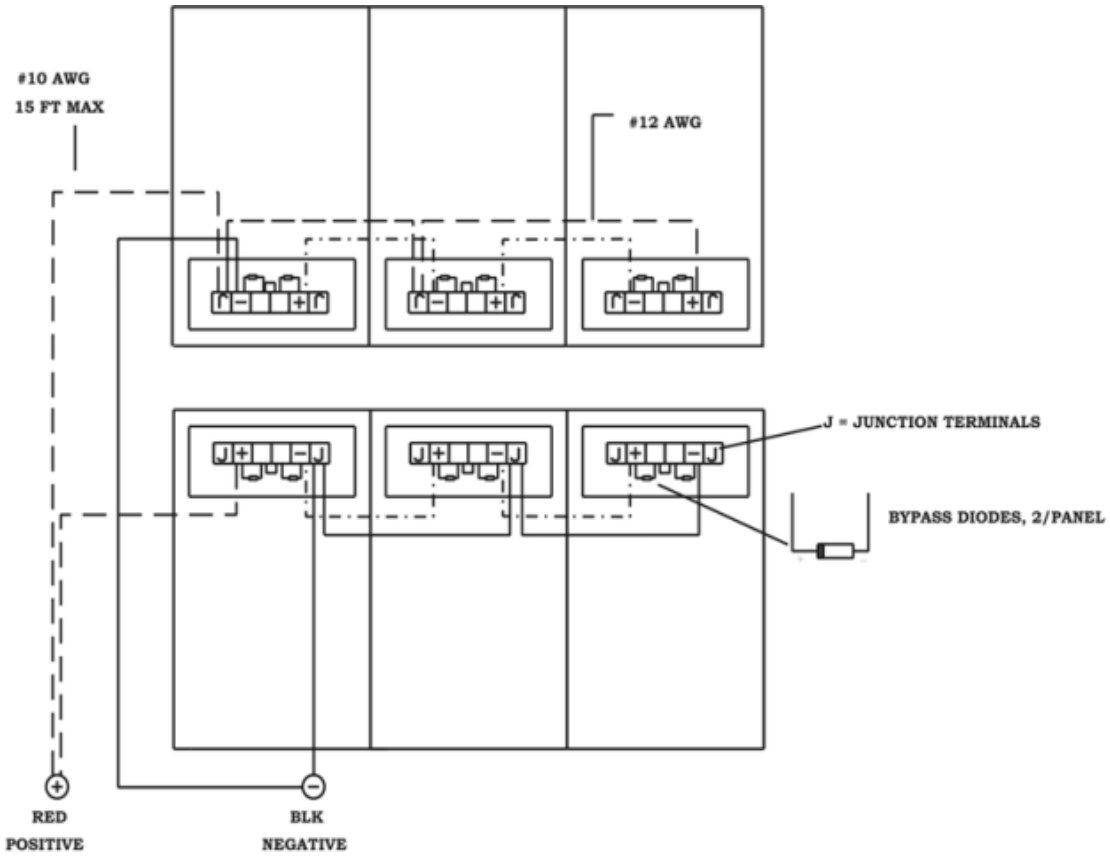

Figure 25 – Example of photovoltaic array with two parallel strings of three in series connection [Source: Sunpumps catalogue]

To plot the photovoltaic I-V curve it is used the equation 48 and the other equations are used to calculate necessary parameters in equation 48. The subscript *ref* means that the quantities are measurements at reference conditions. The reference conditions are radiation of 1000 W/m^2 and an ambient temperature of 25ºC. The result is plotted in Figure 26 and Figure 27. In the modern cells the shunt resistance is very large and the last term of equation 48 can be neglected [Duffie, 1991]. If the I-V curve in manufacture catalogue, at low voltage, exhibits a pronounced negative slope instead of a nearly horizontal line as shown in Figure 24 then it is necessary to consider the shunt resistance. Considering that the shunt resistance R_{sh} is infinite there are 4 parameters to be determined in equation 48.

$$A_{col} = A_{col;single} \cdot nr_{PV\ serie} \cdot nr_{PV\ parallel} \quad \textbf{Eq. 39}$$

$$V_{oc} = V_{oc\ single} \cdot nr_{PV\ serie} \quad \textbf{Eq. 40}$$

$$I_{sc} = I_{sc\ single} \cdot nr_{PV\ parallel} \quad \textbf{Eq. 41}$$

$$V_{mp} = V_{mp\ single} \cdot nr_{PV\ serie} \quad \textbf{Eq. 42}$$

$$I_{mp} = I_{mp\ single} \cdot nr_{PV\ parallel} \quad \textbf{Eq. 43}$$

The temperature coefficient of the open circuit voltage can be obtained from manufacturers catalogue and is defined as

$$\mu_{V;oc} = \frac{dV_{OC}}{dT} = CCT_{V;oc} \cdot V_{oc} \quad \textbf{Eq. 44}$$

Similarly the temperature coefficient of the short circuit current is equal to

$$\mu_{I;sc} = \frac{dI_{sc}}{dT} = CCT_{I;sc} \cdot I_{sc} \quad \textbf{Eq. 45}$$

$$nr_{cel;s} = nr_{cel;single} \cdot nr_{PV\ serie} \quad \textbf{Eq. 46}$$

Another simplification is considering that the reference light current is equal to the short circuit current [Duffie, 1991]:

$$I_{L;ref} = I_{sc} \quad \textbf{Eq. 47}$$

$$I_e = I_L - I_0 \cdot \left[\exp\left(\frac{V_e + I_e \cdot r_s}{a_{cur}}\right) - 1\right] - \left[\frac{V_e + I_e \cdot r_s}{r_{sh}}\right] \quad \textbf{Eq. 48}$$

Solving equation 48 in order to I_0 for I_e=0, I_L=$I_{L;ref}$ and V_e=V_{OC} the result is

$$I_{0;\,ref} = I_{L;ref} \cdot exp\left(\frac{-V_{oc}}{a_{cur;ref}}\right) \quad \textbf{Eq. 49}$$

The light current is obtained by

$$I_L = \frac{G_T}{G_{T;ref}} \cdot \left[I_{L;ref} + \mu_{I;sc} \cdot \left(T_{cel} - T_{cel;ref}\right)\right] \quad \textbf{Eq. 50}$$

And knowing $I_{0;ref}$, I_o is given by

$$\frac{I_0}{I_{0;ref}} = \left[\frac{T_{cel} + 273{,}15}{T_{cel;ref} + 273{,}15}\right]^3 \cdot exp\left[\varepsilon \cdot \frac{nr_{cel;s}}{a_{cur;ref}} \cdot \left(1 - \left[\frac{T_{cel} + 273{,}15}{T_{cel;ref} + 273{,}15}\right]\right)\right] \quad \textbf{Eq. 51}$$

The other variables are determined by the fallowing equations

$$a_{cur;ref} = \frac{\mu_{V;oc} \cdot \left(T_{cel;ref} + 273{,}15\right) - V_{oc} + \varepsilon \cdot nr_{cel;s}}{\frac{\mu_{I;sc} \cdot \left(T_{cel;ref} + 273{,}15\right)}{I_{L;ref}} - 3} \quad \textbf{Eq. 52}$$

$$\frac{a_{cur}}{a_{cur;ref}} = \frac{T_{cel} + 273{,}15}{T_{cel;ref} + 273{,}15} \quad \textbf{Eq. 53}$$

$$r_s = r_{s;ref} = \frac{a_{cur;ref} \cdot \ln\left(1 - \frac{I_{mp}}{I_{L;ref}}\right) - V_{mp} + V_{oc}}{I_{mp}} \quad \textbf{Eq. 54}$$

$$T_{cell} = T_{air} + \frac{NOCT - 20}{800} \cdot G_T \quad \textbf{Eq. 55}$$

$$PV_{power} = I_e \cdot V_e \quad \textbf{Eq. 56}$$

$$PV_{eff} = \frac{PV_{power}}{A_{col;single} \cdot G_T} \quad \textbf{Eq. 57}$$

$$\eta_{system} = \frac{WHP}{A_{col;single} \cdot G_T} \quad \textbf{Eq. 58}$$

Note that $CCT_{V;oc}$ is equal to $\frac{1}{V_{OC}}\frac{dV_{OC}}{dT}$ and $CCT_{I;sc}$ is equal to $\frac{1}{I_{sc}}\frac{dI_{sc}}{dT}$ and they are temperature coefficients.

Table 5 – ISOfotón ISO160 technical data

T_{NOCT}	47ºC
$nr_{cel;single}$	72
$A_{col;single}$	1,264 m^2
$I_{sc;single}$	4,87 A
$V_{oc;single}$	44,2 V
$I_{mp;single}$	4,5 A
$V_{mp;single}$	35,5 V
$CCT_{I;sc}$	0,000254 1/ºC
$CCT_{V;oc}$	-0,00378 1/ºC

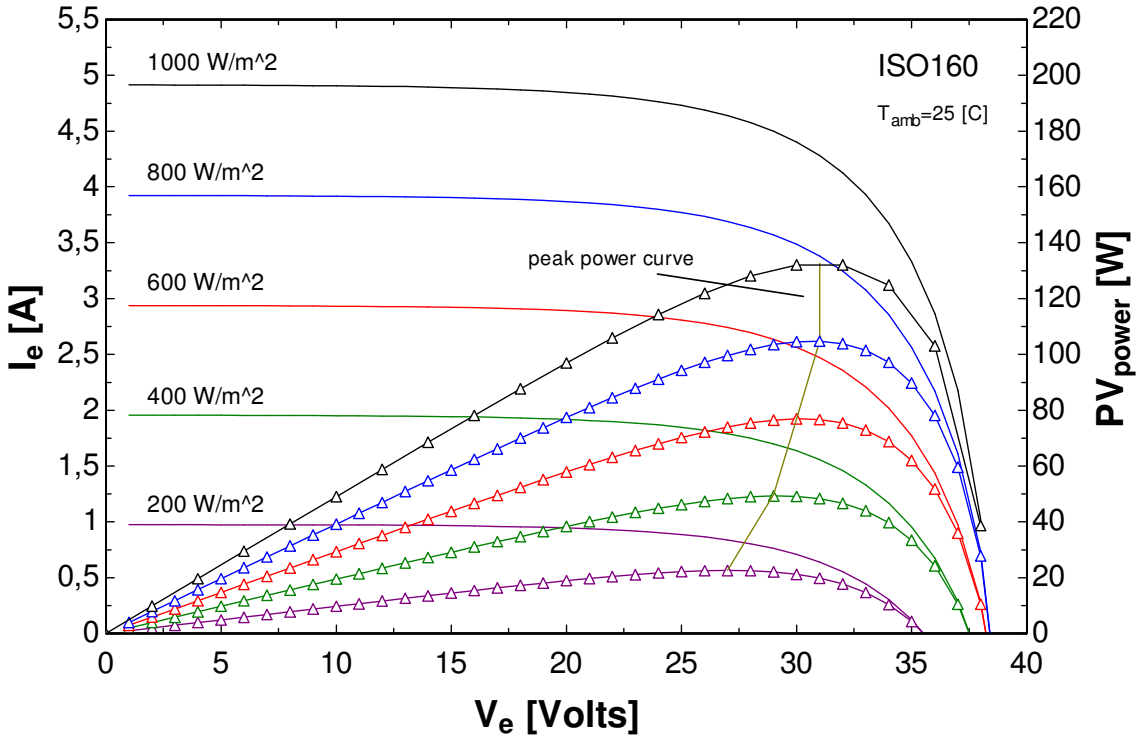

Figure 26 - I-V curve for a single ISO160 PV panel

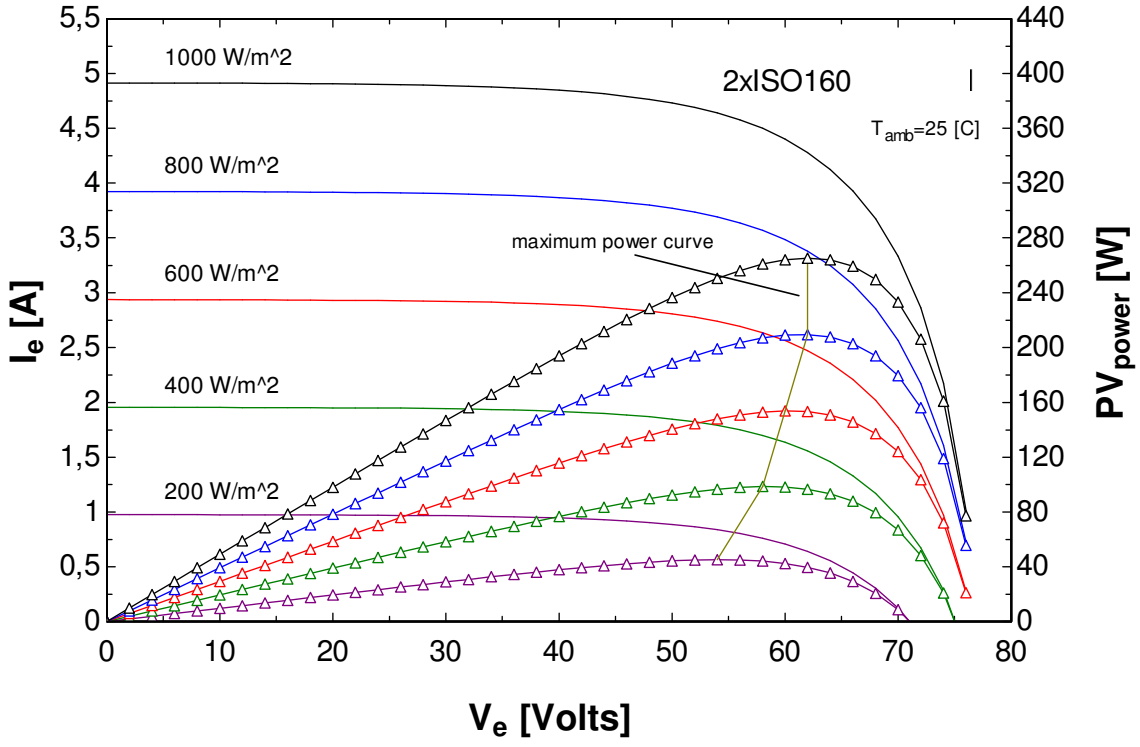

Figure 27 - I-V curve for two ISO160 PV panels connected in series

Table 6 - Cell temperature as a function of radiation considering T_{amb}=25ºC

G_T [W/m^2]	T_{cell} [ºC]
200	31,75
400	38,5
600	45,25
800	52
1000	58,75

4.3 ***Pump controller***

As said before pump manufactures also provide pump controllers and MPP trackers. The pump is operated by solar energy but is controlled by electronics. Pump manufactures don't provide much information about how there controller works and some manufactures call it current boosters. These controllers provide functions as:

- Manual pump on/off
- Automatic pump on/off – tank level switch or dry well
- Limit the current to a maximum value
- Battery over charge/discharge
- Current booster from batteries or PV array to run the pump in the early morning (low insolation
- Prevent battery discharge during zero light (night protection)

In the EES model the controller don't function as an electronic device. Since manufactures don't show detailed information about their electronic units it is assumed that manufactures controls works to extract the maximum power from the PV array.

Another big difficulty is the insufficient data about electric motors that manufactures provide with submersible pumps. There is no information about minimum power or starting current to know if the pump starts early in the morning at low radiations levels. This information was extracted in manufactures graphics but it was not confirmed by the manufacturer.

Manufactures usually provide maximum power, speed, current, minimum and maximum voltage as shown in Table 7 – Grundfos SQFlex pump data provided by the manufacturerTable 7 for Grundfos SQFLEX pumps. Only this information doesn't help to control the pump and predict if the pump is on or off under certain conditions.

Table 7 – Grundfos SQFlex pump data provided by the manufacturer

Motor	Maximum	Minimum
Voltage (VDC)	300	30
Current (A)	8,4	-
Power (W)	1400	-
Angular Speed (RPM)	3600	500

4.4 Maximum power point tracker

Since I-V curves are designed to dimension the photovoltaic system (series and/or parallel connections) it is possible to know the V_{mp} for several solar radiations levels and use a regression line to know the equation that relates V_e with G_T. For ISO160 panel the equation is in Figure 28. Using equation 73 for $V_e=V_{mp}$ the maximum power current I_{mp} is determined.

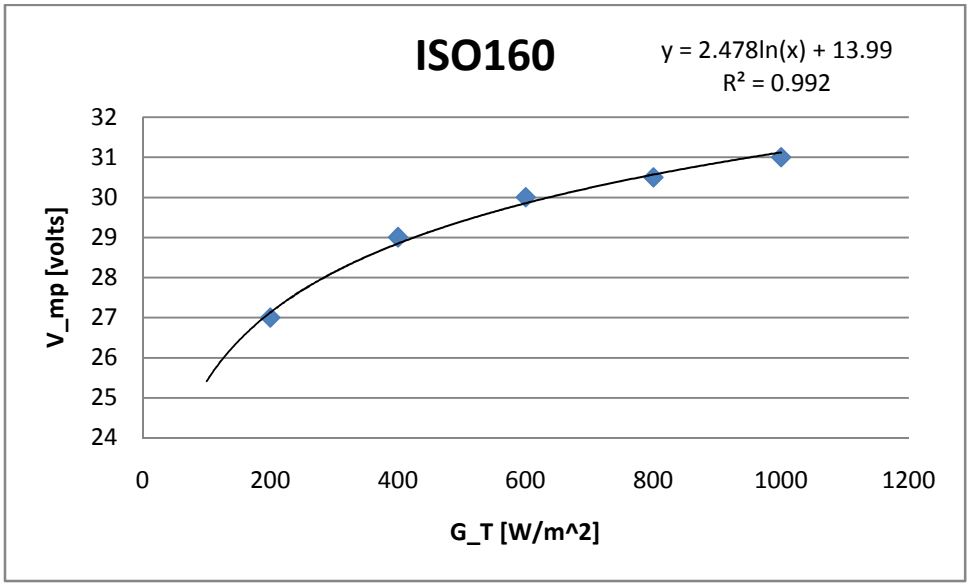

Figure 28 – V_{mp} as function of G_T. Equation and quadratic error

4.5 Pump and water storage modulation – Grundfos SQFlex

Using Grundfos SQFlex catalogue (see Figure 17 for 5A-3 pump) it is possible to know the volume flow as a function of input power and TDH.

Using Excel data analyser (regression) and using Table 10 and
Table 11 data the regression constants results for 5A-3 pump and 2.5-2 (helical rotor pump) are tabled in Table 8 and Table 9, respectively.

Table 8 – Regression results for SQFlex 5A-3 pump

C_0	C_1	C_2	C_3	C_4	C_5	C_6	C_7	C_8
-0,15	547,03	0,06	-25,47	0,00	0,00	0,00	2,91	769,15

Table 9 - Regression results for SQFlex 2.5-2 pump

C_0	C_1	C_2	C_3	C_4	C_5	C_6	C_7	C_8
-0,01	741,31	-0,01	65,32	0,00	0,00	0,00	-5,72	5370,20

Table 10 – Grundfos SQFlex 5A-3 submersible pump data from Figure 17

H	Q	Motor Power
[m]	[m^3/h]	[W]
5,00	0,50	50,00
5,00	1,00	75,00
5,00	2,00	105,00
5,00	2,50	125,00
5,00	3,00	155,00
10,00	0,50	115,00
10,00	1,00	135,00
10,00	2,00	185,00
10,00	2,50	215,00
10,00	3,00	240,00
15,00	0,50	165,00
15,00	1,00	200,00
15,00	2,00	275,00
15,00	2,50	315,00
15,00	3,00	355,00

Table 11 – Grundfos SQFlex 2.5-2 (helical rotor) submersible pump data

H	Q m^3/h	Motor Power
[m]	[m^3/h]	[W]
5	0,5	30
5	1	60
5	2	140
5	2,5	190
10	0,5	40
10	1	75
10	2	165
10	2,5	240
15	0,5	52
15	1	95
15	2	205
15	2,5	275

Using the coefficients in Table 8 and Table 9 and the equation84 it is possible to know the motor power. Using EES it is also possible to know the flow for a given power and TDH.

$$VI = C_0 + C_1 \cdot \dot{V} + C_2 \cdot TDH + C_3 \cdot \dot{V} \cdot TDH + C_4 \cdot \dot{V}^2 + C_5 \cdot TDH^2 + C_6 \cdot \dot{V}^2 \cdot TDH + C_7 \cdot TDH^2 \cdot \dot{V} + C_8 \cdot \dot{V}^2 \cdot TDH^2 \quad \text{Eq. 59}$$

Where $\dot{V}$ is the flow in m^3/h and TDH is the total dynamic head in meters.

4.5.1 – Water Storage

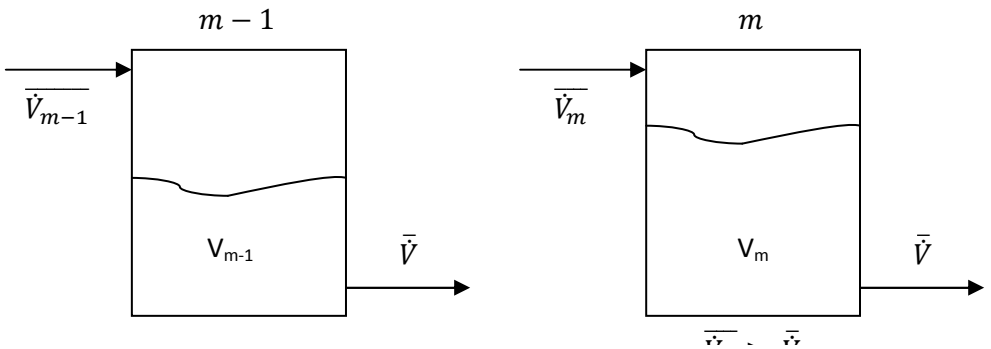

Figure 29 – Water level change between two different months

The volume balance in the storage system based in Figure 31 results in

$$V_m = V_{m-1} + \left(\overline{\dot{V}_m} - \bar{\dot{V}}\right) \cdot n_{month} \quad \text{Eq. 60}$$

The subscript *m* means the month in question; n_{month} is the number of days for the month *m* and $\bar{\dot{V}}$ is the mean consumption daily flow.

4.6 *Water pumping system results*

Two different pumps were analysed, and both of them are from the same manufacturer and have the same cost. Table 12 summarizes the system configurations that were analysed.

Table 12 – Solar water system configuration that were analysed

	System configuration	
Number of PV	2; 3;4 or 5 ISO160 photovoltaic panels interconnected in series	
Selected pump	1 Grundfos SQFlex HR 2.5-2	1 Grundfos SQFlex C 5A-3
Controller	Grundfos C200	Grundfos C200

Table 13 and 14 shows the storage volume as a function of array tilted angle, initial storage volume and using the 320 W_p system with the SQF helical rotor 2.5-2 pump and centrifugal 5A-3 pump, respectively. For the first system the selected $\bar{\dot{V}}$ was 16 m^3/h and for the second system (5A-3 pump) $\bar{\dot{V}}$ = 15 m^3/h. It was considered that the initial volume is equal to the total storage volume.

Table 13 – Water volume in storage tank as a function of tilted array angle, initial storage volume and month for 320W_p with SQF HR 2.5-2 pump system

Beta	Initial Volume	months						
[º]	[m^3]	Jun	Jul	Ago	Set	Out	Nov	Dez
0	45	0	0	0	0	45	45	45
10	45	0	0	0	0	45	45	45
20	45	1	0	0	1	41	45	45
30	45	26	15	8	5	23	45	45
40	45	39	40	32	13	0	0	20
50	45	41	41	21	0	0	0	0

Table 14 - Water volume in storage tank as a function of tilted array angle, initial storage volume and month for 320W$_p$ with SQF C 5A-3 pump system

Beta	Initial Vol.	months						
[º]	[m^3]	Jun	Jul	Ago	Set	Out	Nov	Dez
0	700	396	109	0	0	0	139	434
10	700	477	269	68	0	0	127	401
20	700	532	377	207	63	13	107	337
30	700	565	440	283	131	38	74	237
40	700	579	465	302	125	0	0	66
50	700	576	453	267	44	0	0	0

Figure 30 – Mean monthly daily flow as a function of the year months for the 320W$_p$ system with SQF HR 2.5-2 pump (tilted array angle = 30º)

Table 15 – Mean monthly daily flow [m^3/day] for the system with SQF HR 2.5-2 pump and 320W_p

Jan	Fev	Mar	Abr	Mai	Jun	Jul	Ago	Set	Out	Nov	Dez
18,6	19,0	17,7	17,2	16,1	15,4	15,7	15,8	15,9	16,6	17,1	18,5

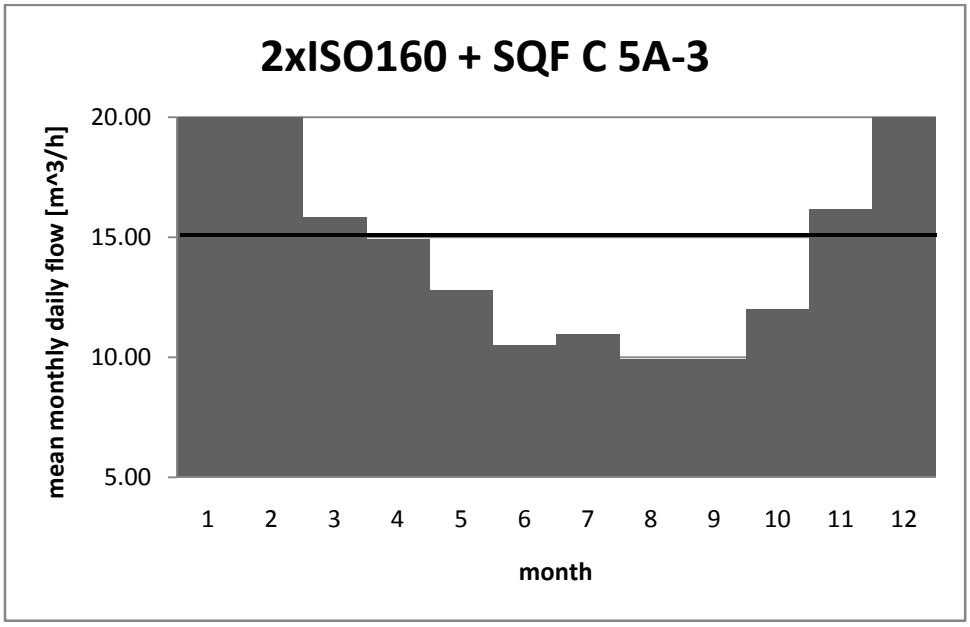

Figure 31 - Mean monthly daily flow as a function of the year months for the 320W_p system with SQF C 5A-3 pump (tilted array angle = 30º)

Table 16 - Mean monthly daily flow [m^3/day] for the system with SQF C 5A-3 pump and 320W_p

Jan	Fev	Mar	Abr	Mai	Jun	Jul	Ago	Set	Out	Nov	Dez
20,5	21,1	15,8	14,9	12,8	10,5	11,0	9,9	9,9	12,0	16,2	20,3

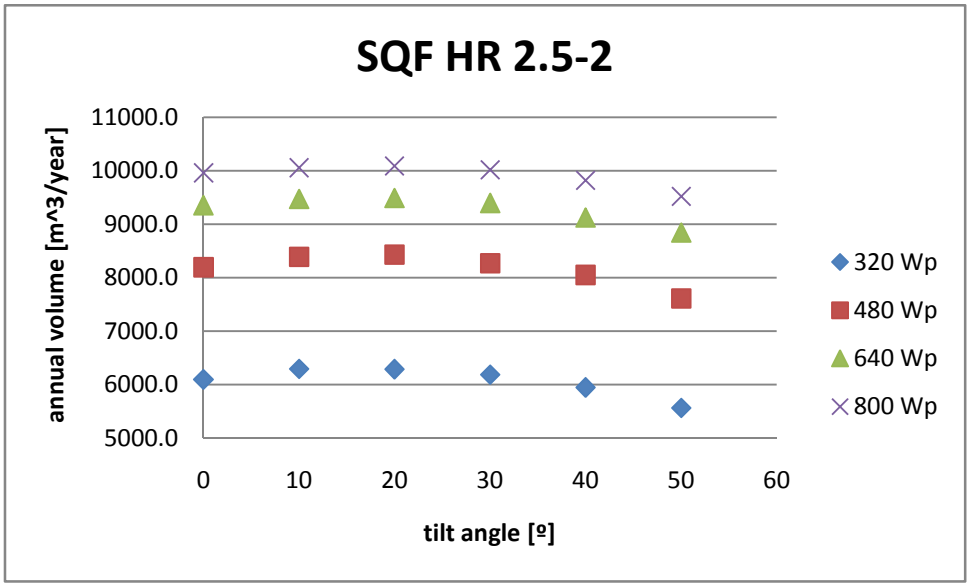

Figure 32 - Annual predicted water volume as a function of array tilted angle and peak power using SQF helical rotor (HR) 2.5-2 pump

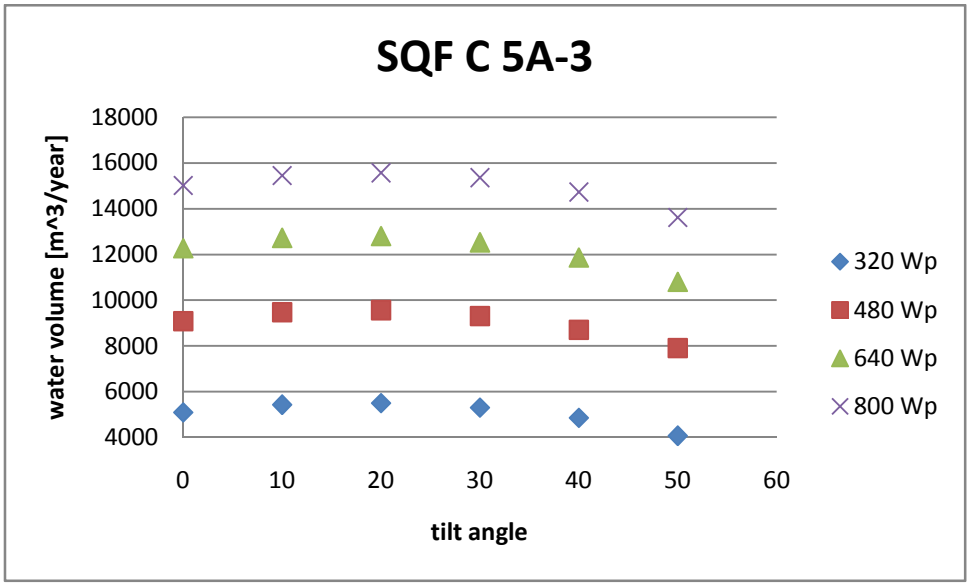

Figure 33 - Annual predicted water volume as a function of array tilted angle and peak power using SQF helical rotor (HR) 5A-3 pump

Table 17 - Annual predicted water volume as a function of array tilted angle using SQF helical rotor (HR) 2.5-2 pump and a 320 W_p array

Beta [º]	0	10	20	30	40	50
V_{anual} [m^3/year]	6092	6293	6284	6184	5942	5560

Table 18 - Annual predicted water volume as a function of array tilted angle using SQF centrifugal (C) 5A-3 pump and a 320 W_p array

Beta [º]	0	10	20	30	40	50
V_{anual} [m^3/year]	5095	5427	5501	5307	4861	4070

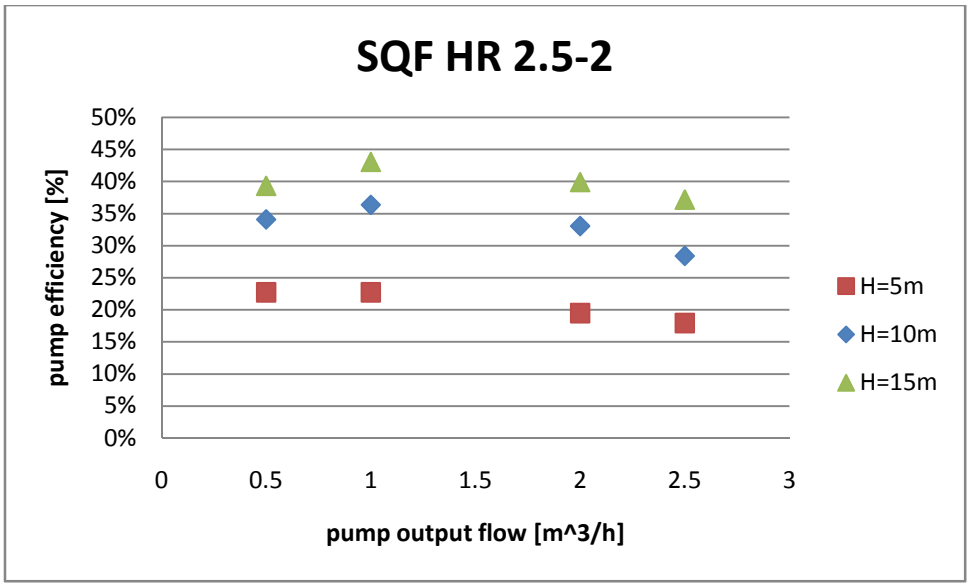

Figure 34 – SQF HR 2.5-2 pump efficiency as a function of pump output flow (discharge) and total dynamic head

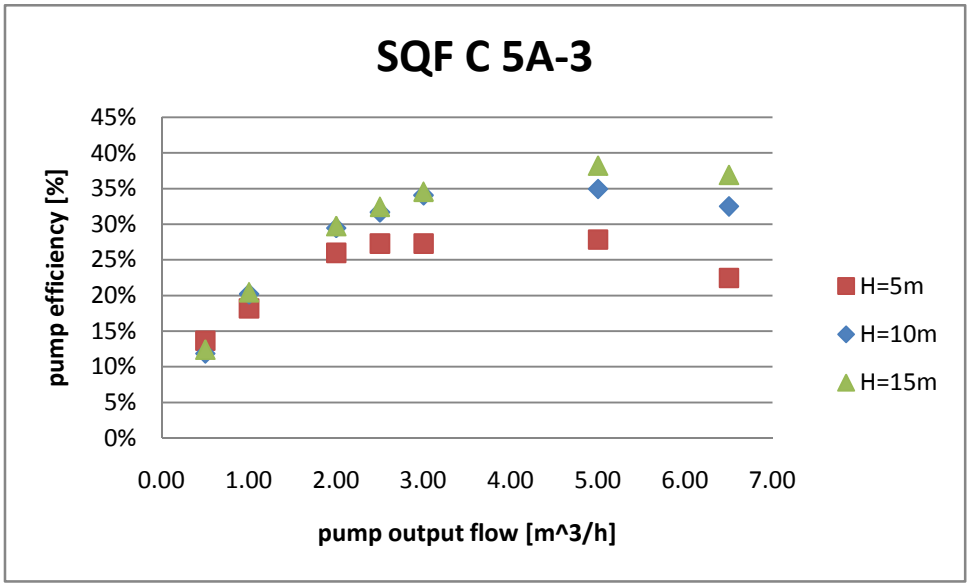

Figure 35- SQF C 5A-3 pump efficiency as a function of pump output flow (discharge) and total dynamic head

Table 19 – SQF HR 2.5-2 pump efficiency as a function of TDH and discharge

TDH	$\dot{V}$	WHP	Motor Power	Pump efficiency
[m]	[m^3/h]	[W]	[W]	
5	0,5	6,8125	30	23%
5	1	13,625	60	23%
5	2	27,25	140	19%
5	2,5	34,063	190	18%
10	0,5	13,625	40	34%
10	1	27,25	75	36%
10	2	54,5	165	33%
10	2,5	68,125	240	28%
15	0,5	20,438	52	39%
15	1	40,875	95	43%
15	2	81,75	205	40%
15	2,5	102,188	275	37%

Table 20 - SQF C 5A-3 pump efficiency as a function of TDH and discharge

H	Q	WHP	Motor Power	Pump efficiency
[m]	[m^3/h]	[W]	[W]	
5,00	0,50	6,81	50,00	14%
5,00	1,00	13,63	75,00	18%
5,00	2,00	27,25	105,00	26%
5,00	2,50	34,06	125,00	27%
5,00	3,00	40,88	150,00	27%
5,00	5,00	68,13	245,00	28%
5,00	6,50	88,56	395,00	22%
10,00	0,50	13,63	115,00	12%
10,00	1,00	27,25	135,00	20%
10,00	2,00	54,50	185,00	29%
10,00	2,50	68,13	215,00	32%
10,00	3,00	81,75	240,00	34%
10,00	5,00	136,25	390,00	35%
10,00	6,50	177,13	545,00	33%
15,00	0,50	20,44	165,00	12%
15,00	1,00	40,88	200,00	20%
15,00	2,00	81,75	275,00	30%
15,00	2,50	102,19	315,00	32%
15,00	3,00	122,63	355,00	35%
15,00	5,00	204,38	535,00	38%
15,00	6,50	265,69	720,00	37%

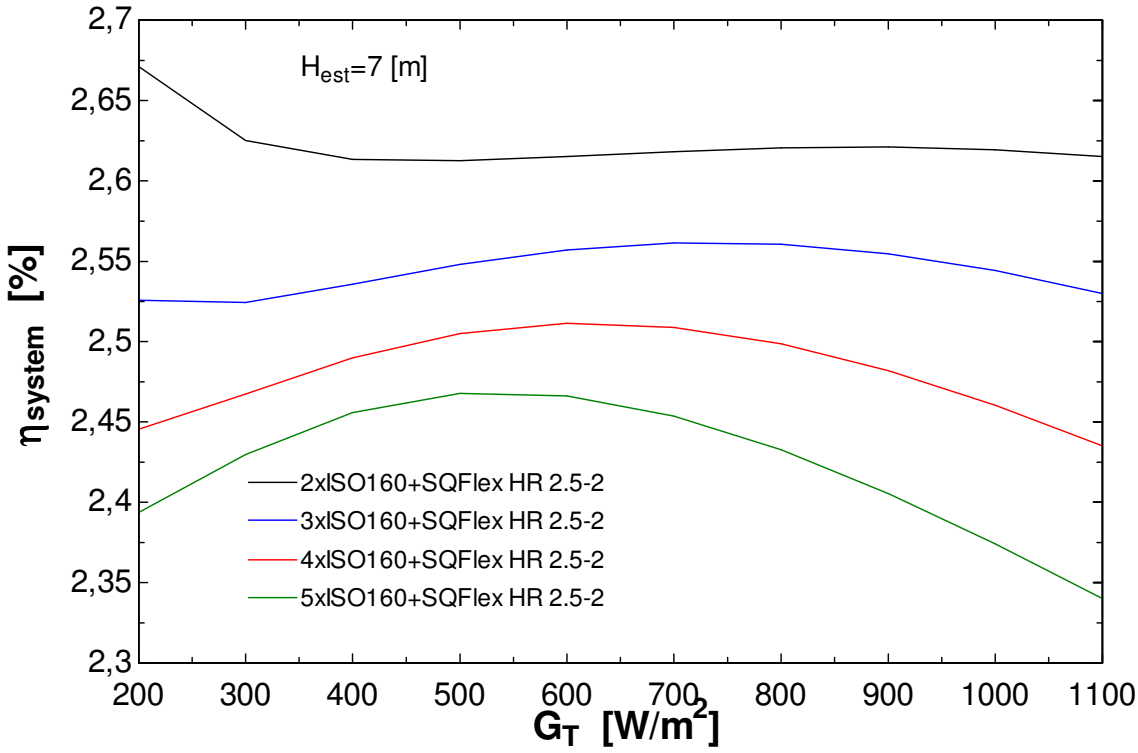

Figure 36 – System efficiency (ISO160 + SQF HR 2.5-2) as a function of radiation incident in the tilted array and array peak power for H_sta=7m

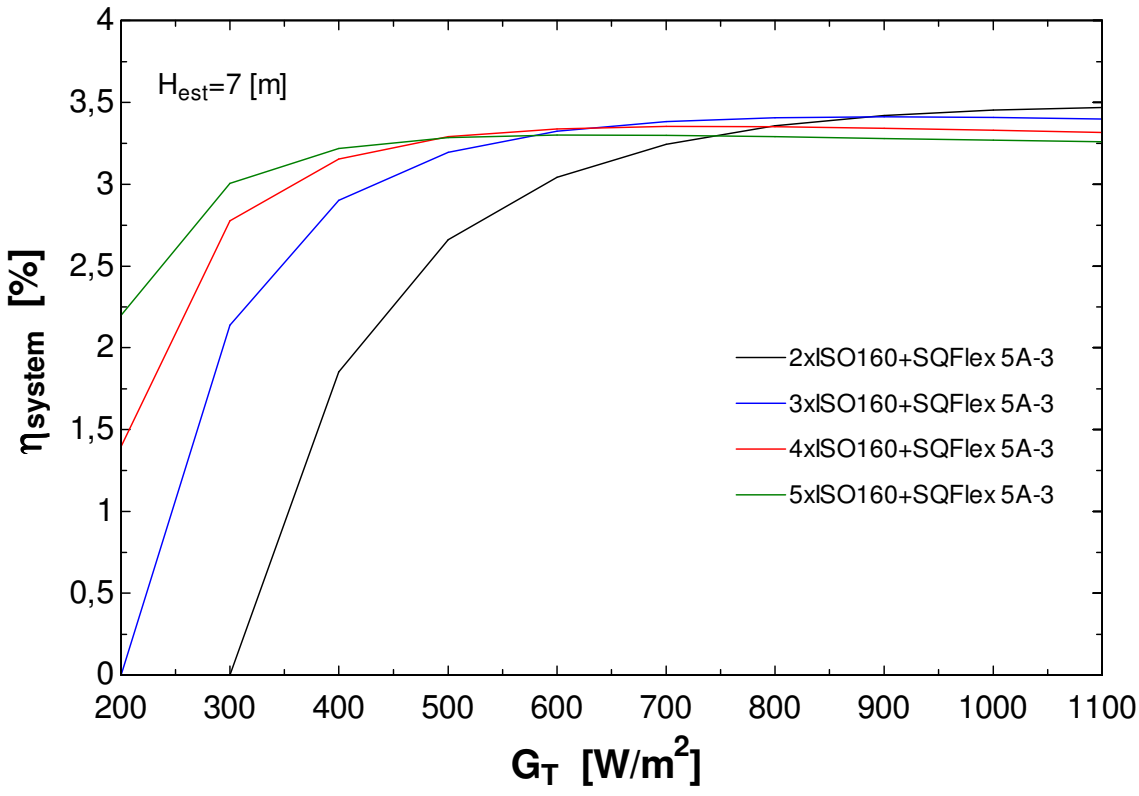

Figure 37 - System efficiency (ISO160 + SQF C 5A-3) as a function of radiation incident in the tilted array and array peak power for H_sta=7m

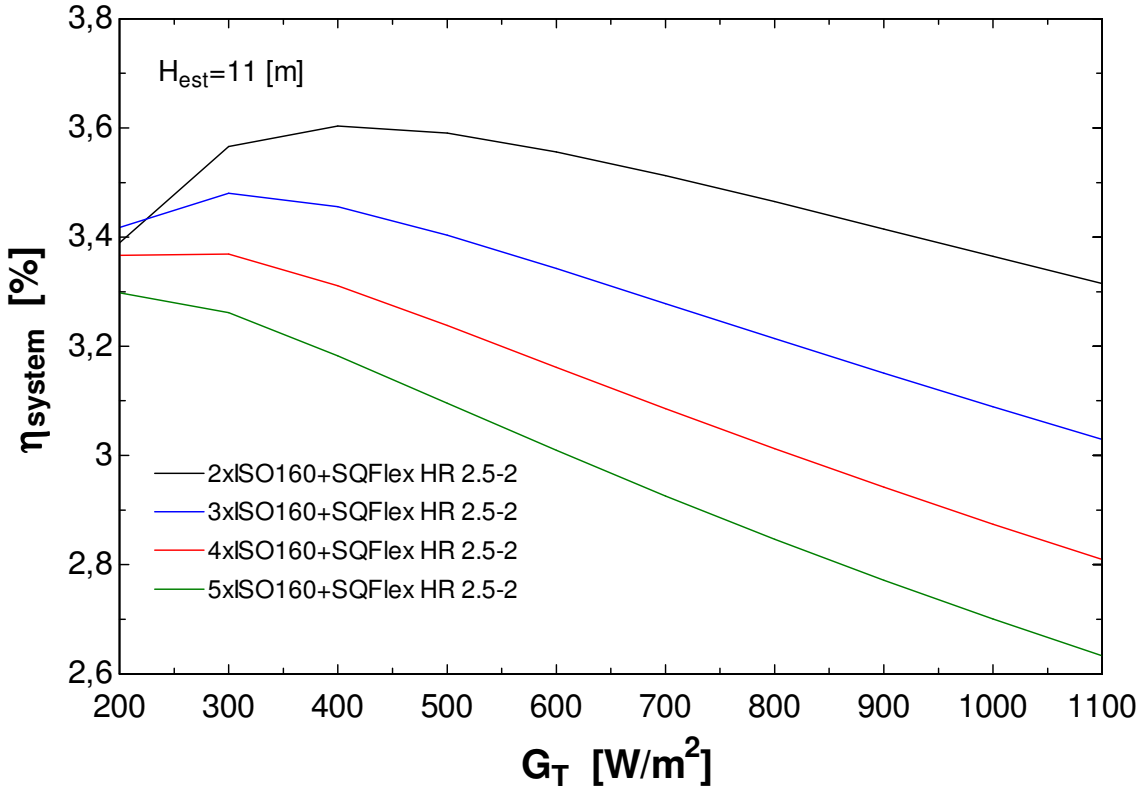

Figure 38 - System efficiency (ISO160 + SQF HR 2.5-2) as a function of radiation incident in the tilted array and array peak power for H_sta=11m

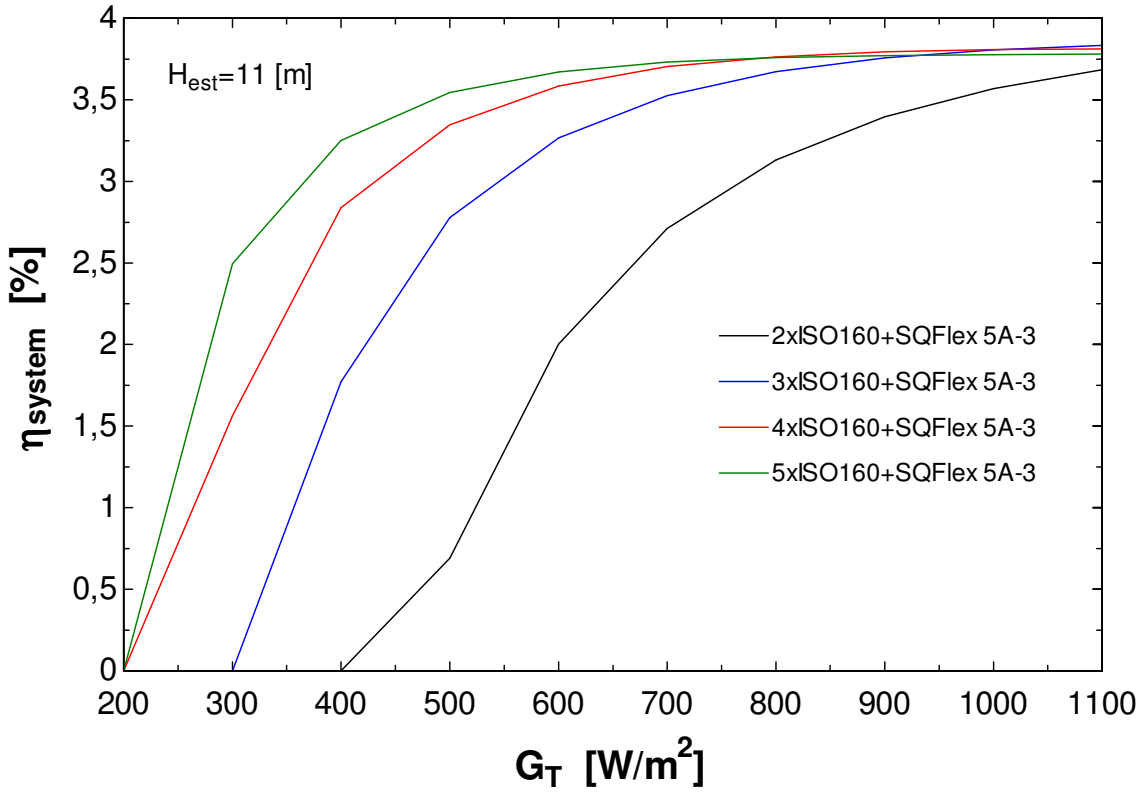

Figure 39 - System efficiency (ISO160 + SQF C 5A-3) as a function of radiation incident in the tilted array and array peak power for H_sta=11m

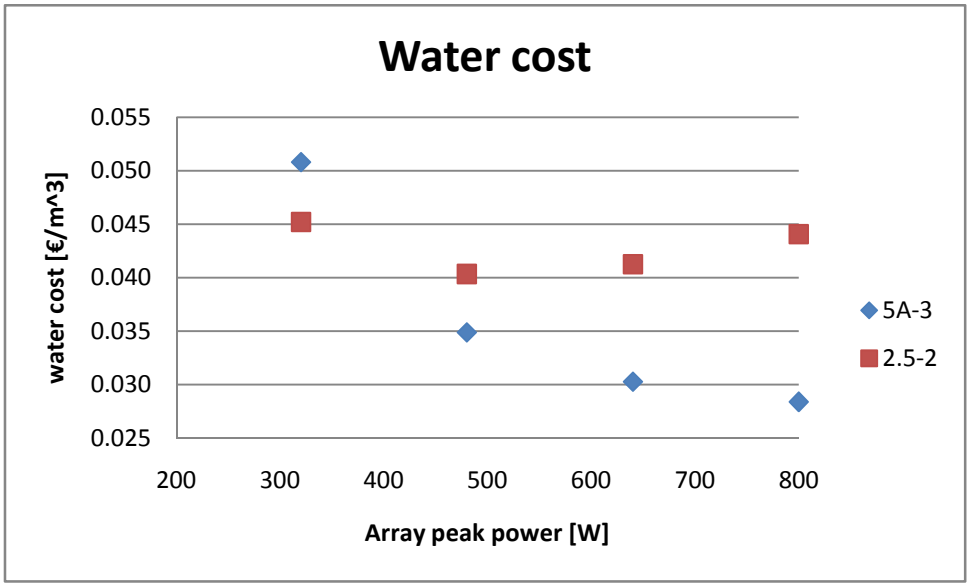

Figure 40 – Water discharged cost as a function of array peak power and pump type, based in a system lifetime equal to 10 years

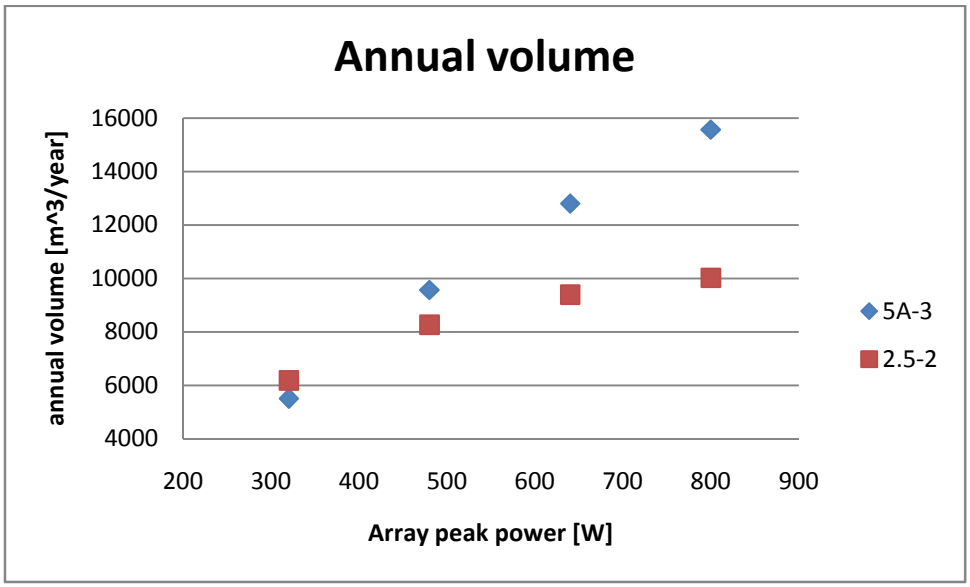

Figure 41 – Annual predicted discharged water volume as a function of array peak power and pump type

Table 21 - Annual predicted water volume and water cost as a function of array peak power and pump type for a system lifetime equal to 10 years

		SQF C 5A-3		SQF HR 2.5-2	
nr_{PV}	Wp	Flow	Cost	Flow	Cost
	[W]	[m3/year]	[€/m3]	[m3/year]	[€/m3]
2	320	5501	0,051	6184	0,045
3	480	9565	0,035	8268	0,040
4	640	12803	0,030	9392	0,041
5	800	15568	0,028	10018	0,044

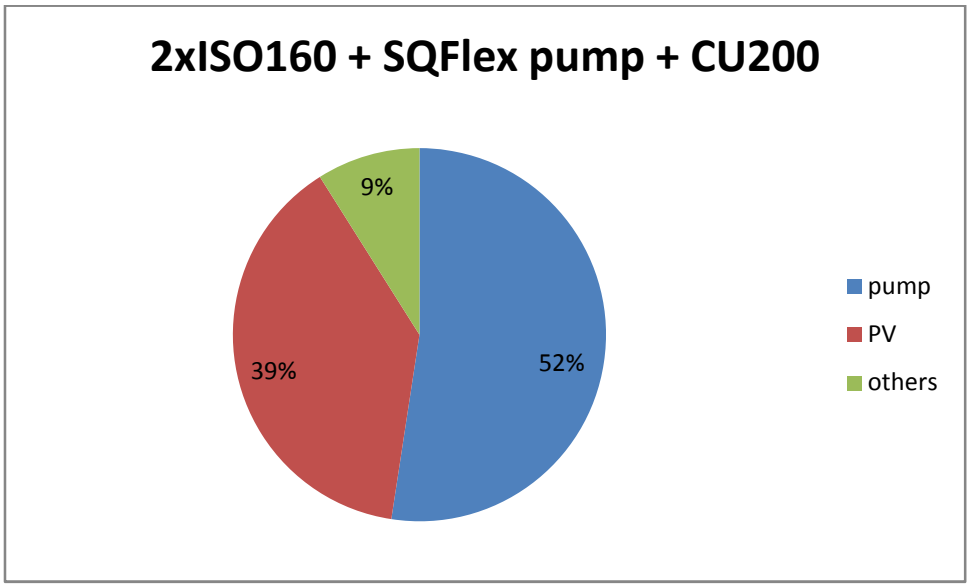

Figure 42 – System relative components cost using a 320 W_p array

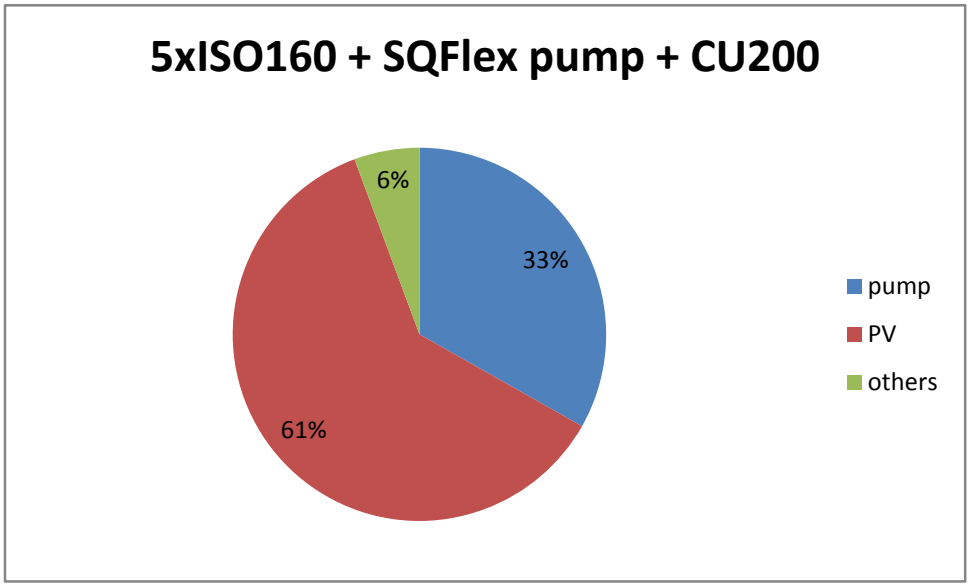

Figure 43 - System relative components cost using a 800 W_p array

Table 22 – Total system cost, peak power cost and system relative components cost as a function of array peak power (ISOfotón 160 peak power panels + Grundofos SQF pump + Grundfos CU200 controller)

Array peak power	Total system cost	System cost	pump	PV	others
[W_p]	[€]	[€/Wp]			
160	2255	14,09	65,0%	23,9%	11,1%
320	2795	8,73	52,4%	38,6%	8,9%
480	3335	6,95	43,9%	48,6%	7,5%
640	3875	6,05	37,8%	55,7%	6,5%
800	4415	5,52	33,2%	61,2%	5,7%

Table 23 –System components unit price

Pump cost	1465	[€][1]
CU 200	250	[€][1]
PV_{cost}	540	[€]
PV_{area}	1,264	[m^2]
Cycle lifetime	10	[years]

Cycle life time is the period after witch costs of maintenance become higher than system costs. It was considered 10 years as a measure of precaution.

[1] 1€=1,297 USD

5. Pumping system results discussion

Figure 30 shows the system match between the consumed flow and the mean predicted flow that is clearly matched resulting in low volume reservoirs as shown in Table 13. As can be seen in Table 14 and in Figure 31 the SQF 5A-3 pump is clearly unmatched with the consumption resulting in too high water tank volumes.

Figure 32 and Figure 33 shows, respectively, the annual volume for the systems SQF HR 2.5-2 and SQF 5A-3 as a function of array tilt angle. For both systems the optimum tilt angle is 20º but for minimum storage volume is 30º as shown in Table 13 and Table 14.

Figure 34 and Figure 35 shows that pump efficiency depends on the flow and the H produced by the pump. For the helical rotor pump the BEP (43%) is for a head of 15m and a flow of 1 m^3/h as seen in Table 19. The centrifugal pump BEP (38%) is for a head of 15m and a flow of 5 m^3/h as showed in Table 20.

Figure 36 and Figure 37 (H_{est}=7m) shows that the system efficiency is higher for the SQF 5A-3 pump, especially for high radiation levels and higher photovoltaic array peak power. The helical rotor pump system as a different behaviour for H_{est}=11m showing a better performance for low radiation levels and low array peak power as illustrated in Figure 38. The centrifugal pump also shows some differences for H_{est}=11m especially low performance in low radiation levels and low peak powers. Figure 39 indicates that the pump only starts with a radiation level higher than 400 W/m^2 for the 320W_p array.

Based in a system lifetime of 10 years the water cost is lower increasing the array peak power for the 5A-3 pump system as shown in Figure 40. With the same considerations the water cost for the 2.5-2 pump is lower than the 5A-3 pump system for the array peak power of 320W_p. The increase of array peak power in the centrifugal pump system decreases the water cost and increases the mean annual volume as shown in Figure 41. Due to low performance of 2.5-2 pump at high flows the annual volume is lower compared to the 5A-3 pump for array peak power of 480W_p. This is also the reason for the increase of water cost shown in Figure 40 for the 2.5-2 pump.

Both pumps have the same initial cost and use the same pump controller as listed in Table 23. Figure 42 and Figure 43 shows the relative components cost for different array peak power. The objective of these charts is to show that using an expensive pump could justify and increase in the number of photovoltaic panels. The total system cost are higher with the increase of photovoltaic panels in the array but the system cost in €/W_p decreases as seen in Table 22.

6. Pumping system components selection

6.1 *Village Water needs*

People in the village rationalises the water because they don't have water in abundance near them. They use dry latrine and wash the cloths in the river if possible. The system will try to satisfy the water needs for 400 villagers. Considering that one person consumes about 40 liters per day the system must produce about 16000 liters/day. To satisfy some needs of water to a communitarian crop or cattle drinking it is possible to use the excess water production during the summer.

6.2 *Components selection*

As said before the system must satisfy the village water needs with the lowest initial cost for the association and at the same time with the lowest operating and maintenance costs. Selecting a solar powered water system make the operation and maintenance costs very low in comparison to diesel engines. The population is interested in the higher volume of water possible per day and the association is interested in the lowest initial costs. Both are interested in the highest reliable system.

It was assumed that the consumption is constant along the year and equal to 16 m^3/day. It is also possible that the volume of water needed by the population increases along the year and through the years.

The system annual mean volume is equal to

$$\bar{V}_{annual} = mean\ daily\ flow \cdot 365 \qquad \textbf{Eq. 61}$$

If the mean daily flow is equal to 16 m^3/h, the annual mean volume is equal to 5840 m^3.

For the initial 16 m^3/day the best pump is the SQF HR 2.5-2 with an array power of 320 W_p and the reasons are:

- Up to 320 W_p this system has the lowest water cost
- Needs 45 m^3 storage tanks to operate over a year without water shortage as predicted by Table 13 considering a constant consumption daily volume
- As shown by Figure 30 the system always has 8 months with a mean daily flow equal or higher than 16 m^3/h
- Comparing Figure 30 and Figure 31 is easy to understand that the SQF C 5A-3 pump is unmatched with the load and the result is a high storage volume as proved in Table 14
- For a tilted angle of 30º the system predicted annual volume is above the system annual mean volume (5840 m^3) as seen in Figure 32

This system is unsuited

- If the mean daily flow is too much higher than 16 m^3/h
- If is predictable that the mean water volume consumption will rise above 27 m^3/h before the 10 years lifetime cycle

The SQF 5A-3 pump should be used if the daily flow is higher than 16 m^3/h, and with the possibility to increase the number of photovoltaic modules the pump will operate even better as shown in Figure 37 and Figure 39 and the water discharged cost will be lower compared to the water cost for the SQF 2.5-2 pump as shown in Figure 40. SQF 5A-3 is a centrifugal pump and the rated flow is 5 m^3/h against the 2.5-2 pump that is a helical rotor pump with a rated flow equal to 2,5 m^3/h. The TDH over a year is low and helical rotor pumps are used in high pumping heads with low flow, so if the daily flow is increased the installed pump should be SQF 5A-3 with a higher array peak power. The system will me more flexible using the centrifugal pump, because increasing the peak power in the array means that the system water output will be much higher compared to the SQF 2.5-2 pump system. The proof is the difference shown in Figure 41. In Figure 36 the system efficiency gets lower when the peak power is increased. This is because the system efficiency is highly influenced by the pump efficiency and the helical rotor pump efficiency is low at high flows.

The SQF 5A-3 pump system should be used with the possibility to adjust the consumption of water over a year to avoid that the system is stopped for long periods in the summer. The excess water produced during summer could be used to agriculture applications.

7. Refrigeration system

7.1 Working fluids

The performance of real machines is determined by the properties of the working fluid. Some working fluids were developed for determinate applications. Others were developed to work in general conditions with some limitations. There is no working fluid that satisfies all the requirements at the same time. For the vapour compression cycle the ideal properties for a refrigerant are:

- High latent heat of vaporization
- High thermal conductivity
- High suction gas density
- Positive but not excessive pressures at evaporating and condensing conditions to avoid air leakage in the system
- Critical temperature and triple point outside the working range
- Chemically stable, compatible with construction materials and miscible with lubricants
- Non-corrosive, non-toxic and non-flammable
- Environmentally friend
- Low cost production

The refrigerant is used to absorb heat at low temperature and low pressure and release heat at a higher temperature and pressure. Most refrigerants undergo phase changes in the cycle. This is why the refrigerant thermodynamic and physic properties are important.

7.1.1 Refrigerant designations

To uniform the nomenclature utilized for refrigerant fluids specific norms were developed, for example the ASHRAE nomenclature. In a general way they are designated by the letter R (refrigerant) plus a number that is related with chemical composition.

Refrigerants are classified in two great groups: synthetic and natural. Synthetic refrigerants are produced with methane or ethane synthesizing with one or more hydrogen atoms replaced for Chloride atoms, Fluor or Bromine. Syntactic refrigerants are divided into three groups:

CFC's – As examples, R11, R12, R113, R114, R115, R500 and R502

HCFC's – As examples, R22, R123, R141b and R142b

HFC's – without chloride in there molecular structure – As examples, R32, R134a, R143a and R152a

7.1.2 Absorption working fluids

Absorption cycles work with two fluids and there are two typical pairs: ammonia (refrigerant)/water (absorber) and water (refrigerant)/lithium bromide (absorber). Other working fluids exist but this two are widely used. Table 24 to Table 26 shows ammonia/water and water/lithium bromide characteristics.

Table 24 – Refrigerant properties [Source: Herold, 1996]

Property	Ammonia/Water	Water/Lithium bromide
High latent heat	Good	Excellent
Moderate vapour pressure	Too high	Too low
Low freezing temperature	Excellent	Limited application
Low viscosity	Good	Good

Table 25 – Absorbent properties [Source: Herold, 1996]

Property	Ammonia/Water	Water/Lithium bromide
Low vapour pressure	Poor	Excellent
Low viscosity	Good	Good

Table 26 – Mixture properties [Source: Herold, 1996]

Property	Ammonia/Water	Water/Lithium bromide
No solid phase	Excellent	Limited application
Low toxicity	Poor	Good
High affinity between refrigerant and absorbent	Good	Good

7.2 Differences between compression and absorption Ammonia/Water and Water/Lithium Bromide cycles

Absorption cycle that operates with ammonia/water have an additional equipment relative to the absorption cycle that operates with water/lithium bromide. It is called rectifier. This is because water is also volatile and when the solution is heated in the generator the formed vapour is also a solution of ammonia and water. It is impossible to use a solution in the condenser/evaporator because in this components heat is transferred at a constant temperature. This situation is only possible in phase changes with pure substances. It is necessary to rectify the vapour phase to increase the ammonia concentration (almost 100%) before it is reached at the condenser. This system is more complex and has higher initial and operating costs to the system. There are cases that only an ammonia/water system is used due to water/lithium bromide limitations, i. e., lithium bromide crystallization or water freezing (evaporator temperature less than 0ºC).

Compression cycles were developed after absorption cycles. Due to electricity expansion it was more practical and with lower costs to use a vapour compression cycle. They have a higher COP, but the comparison between COP's for the two system types is not direct, due to different energy sources. Absorption cycles use heat directly, but the compressor is generally operated by an electric motor as shown in Figure 44. The electric energy used is transformed in a thermal central which burns fuel to transform in electricity, for example.

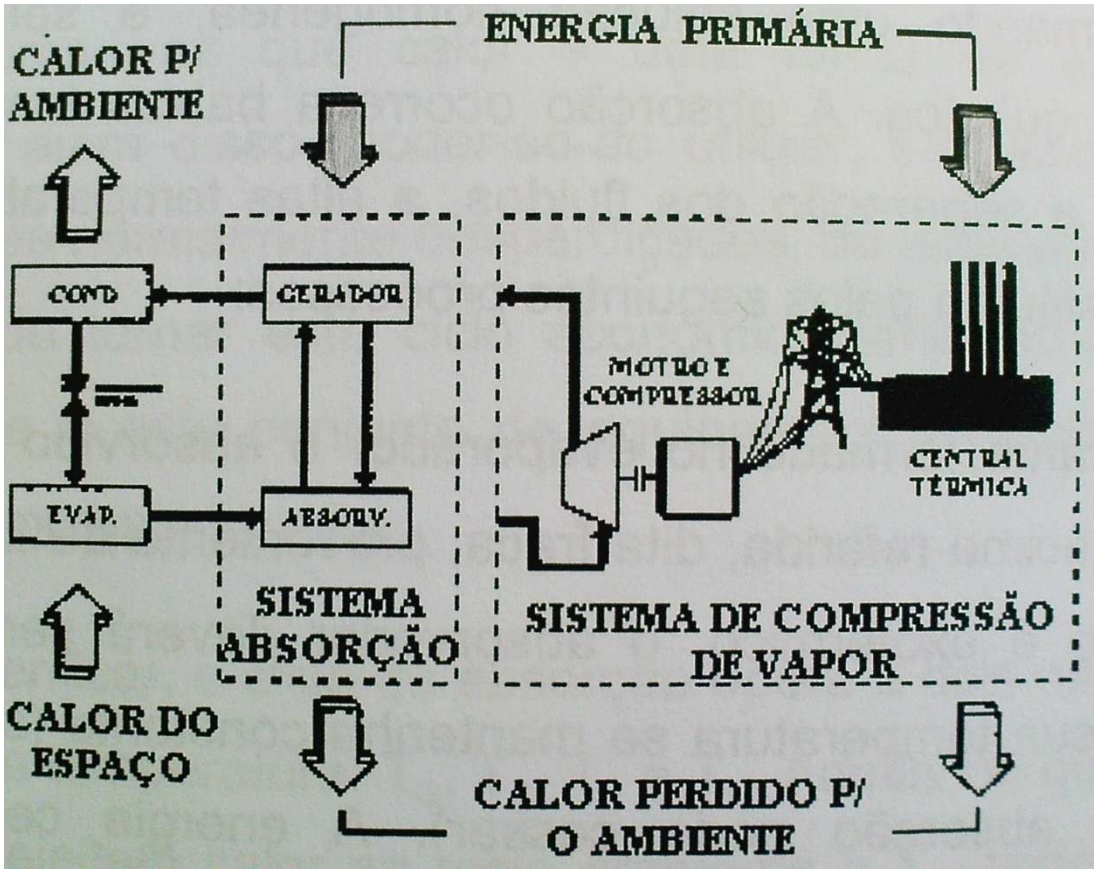

Figure 44 – Absorption and vapor compression cycle differences [Source: Clito, 2007]

8. Thermodynamic properties of absorption working fluids

Pure substances are thermodynamically characterized by two independent properties. In mixtures it is necessary an additional property that quantifies its composition. This property is called mass fraction and for binary mixture is equal to

$$x = \frac{mass\ of\ one\ component}{total\ mass\ of\ both\ components} = \frac{m_2}{m_1 + m_2} \qquad \textbf{Eq. 62}$$

The mass fraction of the other component is equal to (1-x). So component 1 is in its pure state if x=0 and for the component 2 is for x=1.

8.1 Mixtures diagrams

When designing an absorption cycle the most important thermodynamic properties to be considered are: pressure, temperature, mass fraction, enthalpy, entropy and specific volume.

8.1.1 Temperature-mass fraction diagram

Figure 45 shows a typical temperature-mass fraction diagram. To understand this diagram let´s consider a subcooled mixture, point 1', in equilibrium and heat is added to the system at constant pressure. At certain point the point 2' is reached and the first vapour bubble is formed. The vapour is enriched in component B compared to the liquid. Its mass fraction is $x_{2''}$. This is the consequence of higher vapour pressure of component B compared to component A. Point 3 is reached by additional heat where the mass fraction of the vapour (point 3") is in equilibrium with the remaining liquid. The mass fraction of the liquid is now indicated as 3'. At this point, the amount of component B in the liquid phase has been reduced compared to point 2' while the vapour is enriched in component B. However, the vapour contains a lower mass fraction of component B and more of component A. As the evaporation process continues the point 4" is reached and the evaporation process is completed. The vapour at point 4" has the same mass fraction as the initial subcooled liquid. The mass fraction of the last liquid droplet is indicated by point 4'. Further heating produces superheated vapour at point 5".

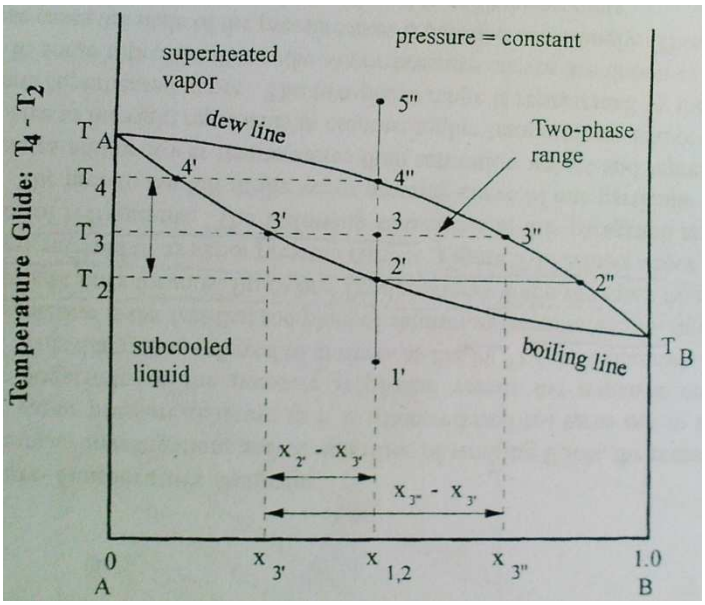

Figure 45 – Temperature mass fraction diagram – subcooled to superheated evolution

8.1.2 Pressure-temperature diagram

Usually this diagram is referred as the ln(P), -1/T diagram, Figure 46. The advantage of this representation is the fact that the plots of saturation temperature versus saturation pressure are almost straight lines for the most fluids mixtures when the mass fraction is constant.

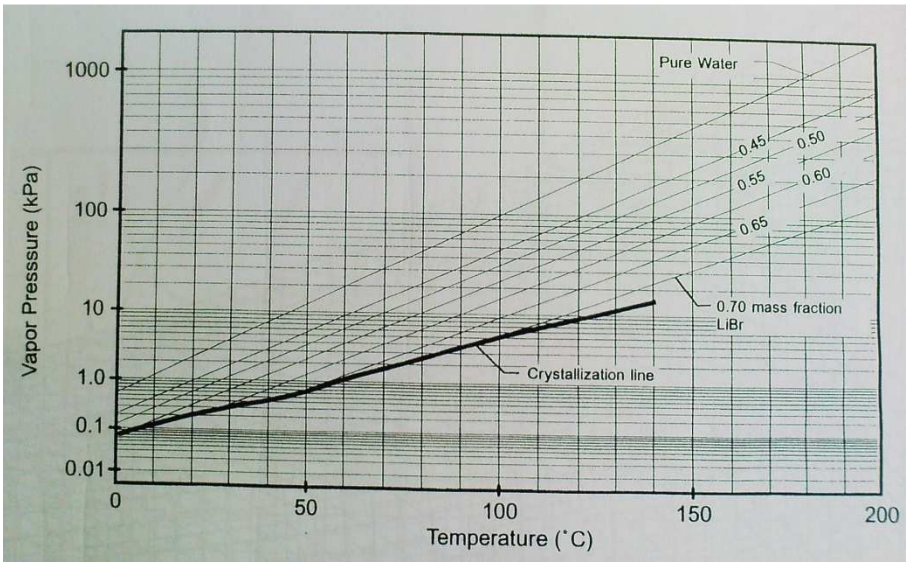

Figure 46 – Water/LiBr vapour pressure temperature diagram

8.1.3 Enthalpy-mass fraction diagram

The enthalpy mass fraction diagram for water/lithium bromide is given by Figure 47. It found wide applications for the design of absorption heat pumps. All lines on this diagram represent saturation properties. The lower region represents the liquid phase, the middle region represents the two-phase region and is bordered by the boiling and dew line and are isobar lines. The enthalpy difference between the boiling and dew lines for x=0 and x=1 represents the latent heat evaporation for each of the pure fluids. Within the two-phase region, the

equilibrium between the vapour and liquid states can be connected by a tie line (isotherm and isobar lines). For last the upper region is the superheated vapour area.

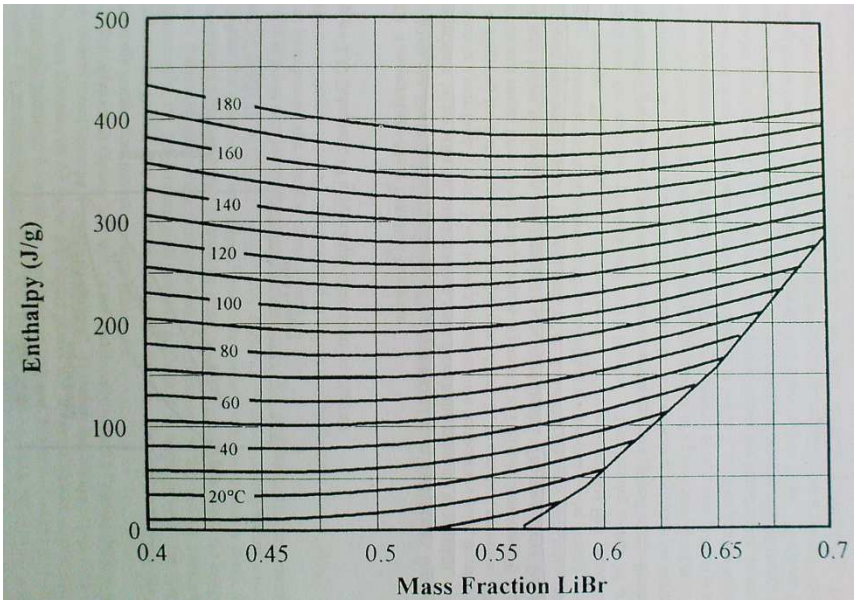

Figure 47 – Enthalpy mass fraction diagram for water/LiBr

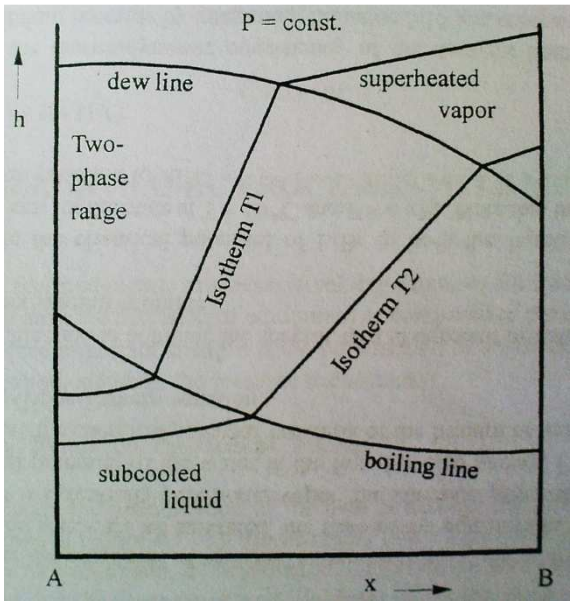

Figure 48 - Enthalpy mass fraction diagram regions

9. Thermodynamic processes with mixtures

Considering the volume control in Figure 49 were (1-x) kg of substance 1 and x kg of substance 2, both at the same temperature, are introduced in the mixing chamber and the results is 1 kg of mixture with a mass fraction x. If the mixture temperature is to remain constant (at substance 1 and 2 temperature), for each kg of mixture it is necessary to give or extract heat from the mixture chamber.

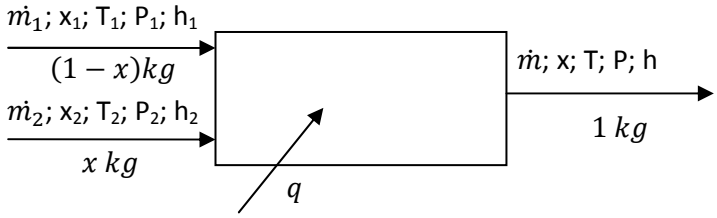

Figure 49 – Two substance mixture with heat addition

Sometimes the mixture heat is relative to the mass of substance 1 (q_1) or 2 (q_2) and not relative to the mixture mass (q). Appling the first thermodynamic law to the volume control we have

$$q = h - h_1 - h_2 \quad \textbf{Eq. 63}$$

$$h_1 = (1-x)h_{pure\,1} \quad \textbf{Eq. 64}$$

$$h_2 = x\,h_{pure\,2} \quad \textbf{Eq. 65}$$

h_{pure1} and h_{pure2} are the substances 1 and 2 enthalpy, respectively, in their pure state and equation 63 can be written as

$$q = h - \left((1-x)h_{pure\,1} + x\,h_{pure\,2}\right) \quad \textbf{Eq. 66}$$

Knowing q, the mass fraction and the enthalpies of pure substances it is possible to calculate from the anterior equation the mixture enthalpy. EES provides a library with procedures that calculates several parameters for the water/lithium bromide mixture. In the literature the water/lithium bromide enthalpy is given by

$$h = \sum_{n=0}^{4} A_n\,x^n + T\sum_{n=0}^{4} B_n\,x^n + T^2\sum_{n=0}^{4} C_n\,x^n \quad \textbf{Eq. 67}$$

And the coefficients A_n,B_n,C_n and the equation domain are listed in Table 27.

Table 27 – Coefficients and equation 67 application domain [Source: Clito, 2007]

A_0=-2024,33	B_0=18,2829	C_0=-3,7008214E-2
A_1=163,309	B_1=-1,1391757	C_1=2,8877666E-3
A_2=-4,88161	B_2=3,248041E-2	C_2=-8,1313015E-5
A_3=6,302948E-2	B_3=-4,034184E-4	C_3=9,9116628E-7
A_4=-2,913705E-4	B_4=1,8520569E-6	C_4=-4,4441207E-9
15<T<165 (ºC)	40<x<70% (LiBr)	

9.1 ***Desorption***

Desorption is the generation of vapour from the condensed phase (liquid or solid) of a mixture of two or more components. The term implies that the vapour contains predominantly one component in contrast to the evaporation process were all the components are assumed to vaporize. Figure 50 exemplify the desorption process in a steady state and steady flow.

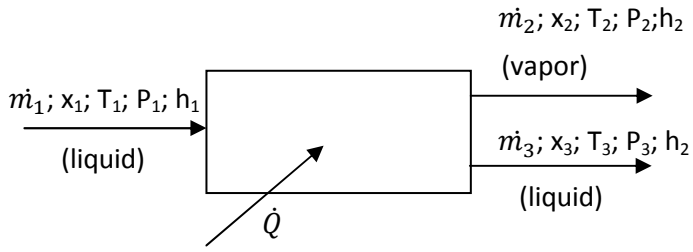

Figure 50 – Desorption process scheme

A vapor stream (2) is formed because heat is added to the initial liquid stream 1 and the remaining liquid leaves the desorber from stream (3). The mass balance to the system results in

$$\dot{m}_1 = \dot{m}_2 + \dot{m}_3 \qquad \textbf{Eq. 68}$$

and for one component

$$\dot{m}_1 x_1 = \dot{m}_2 x_2 + \dot{m}_3 x_3 \qquad \textbf{Eq. 69}$$

and dividing by the vapour mass flow $\dot{m}_2$ the solution circulating ratio, f, can be introduced

$$f = \frac{\dot{m}_1}{\dot{m}_2} \qquad \textbf{Eq. 70}$$

Using the mass balance, equation 68,

$$f = \frac{x_2 - x_3}{x_1 - x_3} \qquad \textbf{Eq. 71}$$

From the energy balance in the desorber results

$$\dot{Q} + \dot{m}_1 h_1 = \dot{m}_2 h_2 + \dot{m}_3 h_3 \quad \textbf{Eq. 72}$$

Or dividing equation 72 by $\dot{m}_2$

$$q + f h_1 = h_2 + (f-1) h_3 \quad \textbf{Eq. 73}$$

The above equation can be rearranged by solving for q,

$$q = h_2 - h_3 + f(h_3 - h_1) \quad \textbf{Eq. 74}$$

From this equation it is possible to conclude that in a desorption process exists two heat components. The first component is an enthalpy difference between a liquid and vapour phase. This term can be seen as accounting for the actual phase change process. The second term describes the heating of the remaining liquid (liquid streams).

9.2 ***Absorption***

The absorption process occurs when vapour is absorbed by a liquid (or solid). It is similar to condensation in the sense that a phase change occurs from a vapour state to a liquid state. However, absorption implies that there is already a condensed phase present at the absorber inlet. Figure 51 exemplify the absorption process. As done for desorption process, mass and energy balances can be applied to determine the absorber heat.

$$q = h_2 - h_1 + f(h_1 - h_3) \quad \textbf{Eq. 75}$$

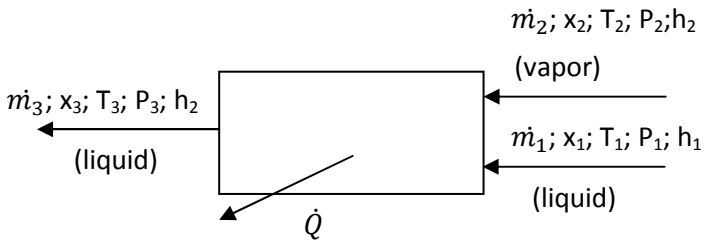

Figure 51 – Absorption process scheme

With q representing the amount of heat released per unit mass of vapor absorbed and f the solution circulation ratio as defined as $f = \dot{m}_1/\dot{m}_2$. Again there is two terms one for the phase change and the other for the solution cooling.

9.3 ***Condensation and evaporation***

The terms condensation and evaporation refer to the phase change of a pure fluid or a mixture where the process is complete. This means that there is only vapour (evaporation) or liquid (condensation) when the process ends. The amount of energy released or gained in the phase change is

$$\dot{Q}_l = \sum \dot{m}_l (h_{out;i} - h_{in;i}) \quad \textbf{Eq. 76}$$

and h_{out} and h_{in} are the enthalpies of the living and entering fluid streams.

9.4 Compression

The compression of vapour is often assumed to be isentropic to simplify the analysis and in most instances the process occurs entirely in the vapour phase. Compressed vapour has a higher pressure compared to the vapour pressure entering in the compressor. The compression work is equal to

$$\dot{W} = \sum \dot{m}_l (h_{out;i} - h_{in;i}) \quad \textbf{Eq. 77}$$

9.5 Pumping

In absorption systems liquid pumps are used to circulate the liquid streams through the piping system and to convey the liquid from the low pressure side to the high pressure side of the system. Assuming that the process is isentropic and the fluid is incompressible the pumping work is equal to

$$\dot{W} = \left(p_{high} - p_{low}\right) \frac{v\dot{m}}{\eta_p} \quad \textbf{Eq. 78}$$

p_{high} - p_{low} represents the pressure difference across the pump, v is the specific volume of the liquid, m the mass flow rate and η_p the pump efficiency.

9.6 Throttling

In absorption cycles throttling devices are used to pass the liquid from the high pressure side to the low pressure side by decreasing the liquid pressure. This process is assumed to be adiabatic, resulting in a constant enthalpy process. The liquid temperature also varies. When a liquid is throttled the outlet state can be a subcooled or a portion of the liquid can flash (vaporize).

9.7 Water/Lithium bromide cycle

Figure 52 shows a single effect water/lithium bromide cycle. The energy source in the generator (or desorber) could be any heat source, for example:

- Burning fossil fuels
- Using heat provided by renewable energies sources
- Heat rejected from electric centrals
- Other processes that rejects heat

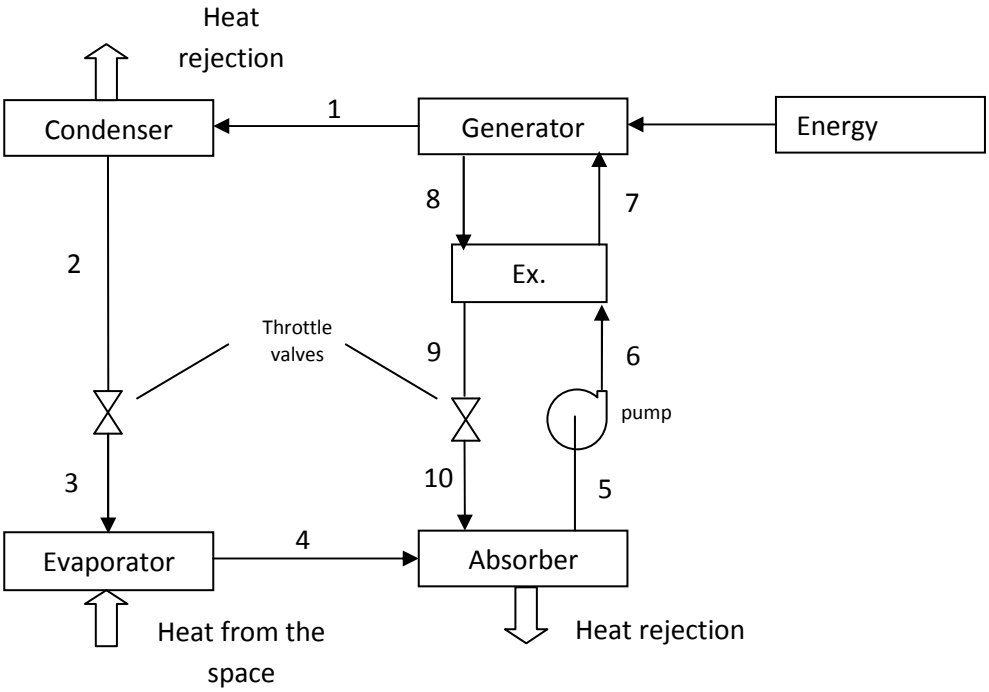

Figure 52 - Water/lithium bromide cycle scheme

The left part of the scheme has the same components used in a vapour compression cycle. The solution circuit (right part) is replacing the vapour compressor. Lithium bromide is a salt and at the generator only water vapour is formed. So from point 1 to point 4 there is only water vapour. This is possible because the normal boiling point for lithium bromide is 1282ºC. Although, from the molecule point of view, exists the possible that some salt molecules may escape from the liquid surface and be present in the steam [Herold, 1996]. To simplify the thermodynamic analysis only steam circulates in the condenser and evaporator.

The steam at point 4 enters in the absorber and it is absorbed by the high concentrated salt solution that enters in the absorber (point 10). Heat is rejected in the absorber due to the mixture as explained above. The mixture (point 5) is pumped by the pump to the heat exchanger were heat is exchanged between the liquid exiting from the desorber and the mixture that exits the pump. Normally in the heat exchanger there is only sensible heat because there is no phase change. This is done to reduce the heat rejection in the absorber and reduce the external heat input to improve system efficiency. In the desorber there is an external heat source that gives energy to the solution entering the desorber (point 7). The formed steam enters in the condenser (point 1) and the high concentrated salt mixture exits the desorber (point 8). To simplify it is considered that the machine operates between two pressure levels. This is possible if it is neglected the changes in elevation and pressure losses in the pipe system. The throttle valves and pumps are devices that work as pressure changers between the two pressure sides.

9.8 Water/Lithium Bromide cycle limitations

The refrigerant is water so the temperature at the evaporator should be higher than 0ºC to avoid refrigerant freezing. The refrigeration temperature for vaccines ranges from 2ºC to 8ºC so using water as refrigerant is not a problem. If the temperature between the fluid circulating in the evaporator and the refrigeration chamber is small then for the same heat transfer the mass flow must be higher.

Another limitation is the lithium bromide mass fraction. When the mass fraction of LiBr exceeds a limit the salt component precipitates. The solubility limit is a strong function of mass fraction and temperature and weak function of pressure. In the cycle the mass fraction of LiBr should not be higher than 70%. This could be avoided by lowering the sink temperature for absorber cooling. Based on the properties of aqueous lithium bromide, low temperatures in the absorber require lower absorption solution and thus avoiding the formation of precipitates.

9.9 Vacuum requirements

Typical pressures in a LiBr absorption machine are subatmospheric. The pressure is determined by the vapor pressure characteristics of the vapor fluid. In the condenser and evaporator circulate essentially water and the pressure of these components is determined by the operating temperature. These low pressures could result in system air leakage. LiBr in the presence of oxygen is very aggressive to many metals. The presence of oxygen in the system accelerates the corrosion process.

9.10 Pressure drops

As said before LiBr absorption machine operates under low pressures. Typical pressures are in the order of 1 to 10 kPa. At this pressure the specific volume of saturated vapour is 129.2 kg/m^3 which results in high velocities. The pressure drop in the pipe system depends on the fluid velocity and the higher the velocity the higher is the pressure drop. At these lower pressures the slope of the vapour pressure curve of water is 14ºC/kPa indicating that small pressure changes have a large influence on temperature.

9.11 Condenser and evaporator as heat exchangers

Thermodynamic cycles always perform between two sources, one with a high temperature (hot source) and one with a lower temperature (cold source). During the entire cycle there are heat exchanges between the refrigeration fluid and other medium fluids. Heat exchangers are mechanical components that are responsible for heat transfer in the cycle. For the absorption cycle there are 5 heat exchangers (condenser, evaporator, absorber, desorber and HX) as shown in Figure 52 that works in different fluid phases.

Condensers are and indirect-contact heat exchanger in which the total heat rejected from the refrigerant is removed by a cooling medium, usually air or water. Condensers are classified based in the fluid that is used to promote the condenser cooling:

- Air-cooled condensers
- Water-cooled condensers
- Evaporative condensers

In air condensers the refrigerant condenses inside the tubes and air circulates in the outside of the tubes. Because air as a low heat transfer coefficient the tubes are finned (higher heat transfer area). There are two types of air condensers the ones that works with free convection and the others work with forced convection. The first type is used in domestic application and the air circulation is done by natural means (no machine). The second type uses a ventilator to promote a higher heat transfer coefficient. Due to low specific heat capacity and high specific volume of air implies a large volume to remove the condenser heat. The fans used to force the volume of air makes noise and uses considerable amounts of power and this limits the applications of forced air-cooled condensers.

Water condensers use cooled water to condensate the refrigerant. The higher heat capacity and density of water makes it an ideal medium for condenser cooling requiring less volume of water per second. The cooled water could be water from a lake, river or well near the plant or from a cooling tower. Two types of water-cooled condensers are widely used for refrigeration purposes: shell and tube and double tube condensers. A double tube condenser consists of two tubes, one inside the other and water is pumped through the inner tube while refrigerant flows in the space between the inner and outer tubes in a counterflow arrangement. Shell and tube condensers are used when larger sizes of water-cooled condenser are necessary and this arrangement is very compact for the same heat transfer capacity.

An evaporative condenser uses the evaporation of water spray to remove the latent heat of condensation of the refrigerant during condensation. It is a simplified combination of a water-cooled condenser and a cooling tower and is very efficient.

The last two types of condenser are generally used in industrial applications. For this project the devices used for domestic applications are more suited, like the air-cooled condenser.

The purpose of the evaporator is to receive low-pressure, low temperature fluid from the expansion valve and to bring it in close thermal contact with the load. The evaporator is also an indirect contact heat exchanger and can be classified mainly into the following three types:

Dry expansion or direct-expansion (DX). The subcooled liquid that is throttled in the throttle valve is sent to the evaporator and is totally vaporized and superheated to a certain degree in the evaporator in its total length. These evaporators are a simple tube that is bended to the desired form to fit in the refrigerator compartment and are commonly used in home refrigerators.

Flooded refrigerant feed. In evaporators with flooded refrigerants feeds, liquid refrigerant is fed through a throttling device and vaporizes outside the tubes within a shell. The refrigerant-side surface area is always wetted by the liquid refrigerant, which results in a higher surface heat-transfer coefficient.

Liquid overfeed. Liquid refrigerant is fed by a mechanical or gas pump and is then overfed to each evaporator. The inner surface in overfeed evaporator is also wetted by liquid refrigerant.

9.12 *Lithium bromide absorption system analysis*

9.12.1 Mass flow balances

There are two important mass balances in the system. One is in the desorber as fallows

$$\dot{m}_7 = \dot{m}_8 + \dot{m}_1 \quad \textbf{Eq. 79}$$

The other is in the absorber

$$\dot{m}_5 = \dot{m}_{10} + \dot{m}_4 \quad \textbf{Eq. 80}$$

The other mass balances are equal to $\dot{m}_5$, $\dot{m}_8$ or $\dot{m}_1$,

$$\dot{m}_5 = \dot{m}_6 = \dot{m}_7 \quad \textbf{Eq. 81}$$

$$\dot{m}_8 = \dot{m}_9 = \dot{m}_{10} \quad \textbf{Eq. 82}$$

$$\dot{m}_1 = \dot{m}_2 = \dot{m}_3 = \dot{m}_4 \quad \textbf{Eq. 83}$$

The mass of lithium bromide that enters and exits from the desorber are the same, considering that the water vapour (point 1) as zero salt content

$$\dot{m}_7 x_7 = \dot{m}_8 x_8 \quad \textbf{Eq. 84}$$

Subtracting equation 84 to 79 results

$$\dot{m}_7(1 - x_7) = \dot{m}_8(1 - x_8) + \dot{m}_1 \quad \textbf{Eq. 85}$$

Another important mass flow parameter is the solution circulation ratio, f,

$$f = \frac{\dot{m}_7}{\dot{m}_1} \quad \textbf{Eq. 86}$$

Dividing equation 85 by $\dot{m}_1$ and solving the equation in order to f

$$f = \frac{\dot{m}_7}{\dot{m}_1} = \frac{x_8}{x_8 - x_7} \quad \textbf{Eq. 87}$$

9.12.2 Energy balances

Using equation 76 and for i=1 (only one inlet and one exit) for the condenser and evaporator the energy balance is

$$\dot{Q_c} = \dot{m_1}(h_2 - h_1) \quad \textbf{Eq. 88}$$

$$\dot{Q_e} = \dot{m_1}(h_4 - h_3) \quad \textbf{Eq. 89}$$

The energy balance in the generator and the absorber results

$$\dot{Q_g} = \dot{m_1}h_1 + \dot{m_8}h_8 - \dot{m_7}h_7 \quad \textbf{Eq. 90}$$

$$\dot{Q_a} = \dot{m_5}h_5 - \dot{m_4}h_4 - \dot{m_{10}}h_{10} \quad \textbf{Eq. 91}$$

Applying equation 78 in the pump volume control the pump power consumption is equal to

$$\dot{W_{pump}} = (p_6 - p_5)\frac{\nu\,\dot{m_5}}{\eta_{pump}} \quad \textbf{Eq. 92}$$

Considering that the heat exchanger is adiabatic (doesn't exchange heat with the exterior), the heat that the hot fluid lost is equal to the heat received by the cold fluid. This assumption results in

$$\dot{Q_{cold}} = \dot{Q_{hot}} = \dot{m_5}(h_7 - h_6) = \dot{m_8}(h_8 - h_9) \quad \textbf{Eq. 93}$$

The heat exchanger efficiency is equal to

$$EX\varepsilon = \frac{(h_7 - h_6)}{(h_8 - h_6)} \quad \textbf{Eq. 94}$$

Assuming that throttling is considered adiabatically, resulting in a isenthalpic process

$$h_3 = h_2 \quad \textbf{Eq. 95}$$

$$h_{10} = h_9 \quad \textbf{Eq. 96}$$

9.13 Refrigeration capacity - Q_e

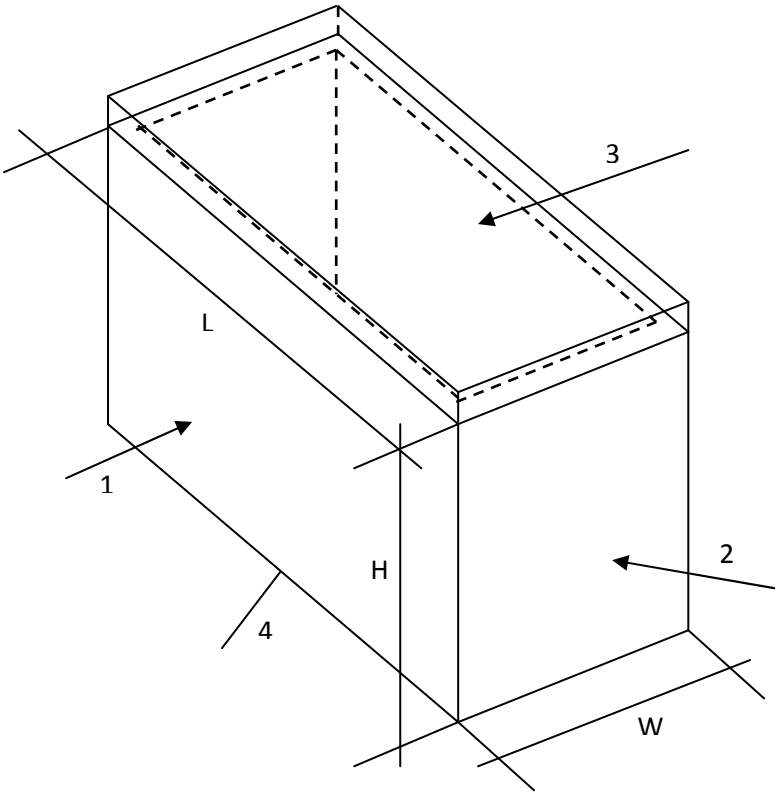

Figure 53 – Refrigerator physical measures and surfaces

The evaporator should extract an amount of energy in the refrigerator that balances the heat losses by air leaks, heat transfers in the walls and the energy that is required to refrigerate a determinate mass M from a higher temperature to a lower temperature. To simplify the calculations air leaks are treated as a percentage of the evaporator capacity (50% higher), based in the percentage calculated in [Clito,]. The refrigeration capacity Q_e is calculated by

$$\dot{Q}_e = \left[\left(\sum_{i=1}^{4} U_{r;i}\right) \cdot (T_{ext} - T_{int}) + \frac{Mc_p(T_{enter} - T_{int})}{refrig.\ time}\right] \cdot 1{,}5 \qquad \textbf{Eq. 97}$$

$$\sum_{i=1}^{4} U_{r;i} = \sum_{i=1}^{4} \frac{1}{R_{total\ i}} \qquad \textbf{Eq. 98}$$

Based in Figures 54 and 55 $R_{total\ i}$ and $R_{total\ 4}$ are equal to

$$R_{total\ i} = \frac{R_{cv,ext\ i} \cdot R_{rad,ext\ i}}{R_{cv,ext\ i} + R_{rad,ext\ i}} + \sum_{j=1}^{3} R_{cond\ j} + \frac{R_{cv,int\ i} \cdot R_{rad,int\ i}}{R_{cv,int\ i} + R_{rad,int\ i}} \qquad \textbf{Eq. 99}$$

$$R_{total\ 4} = \frac{R_{cv,ext\ i} \cdot R_{rad,ext\ i}}{R_{cv,ext\ i} + R_{rad,ext\ i}} + \sum_{j=1}^{3} R_{cond\ j} \qquad \textbf{Eq. 100}$$

The index "i" is used for different surfaces as illustrated in Figure 59 and the index j is linked to the different wall layers. Equation 99 is different from equation 100 because the radiation in the bottom is neglected due to possible surface bottom contact.

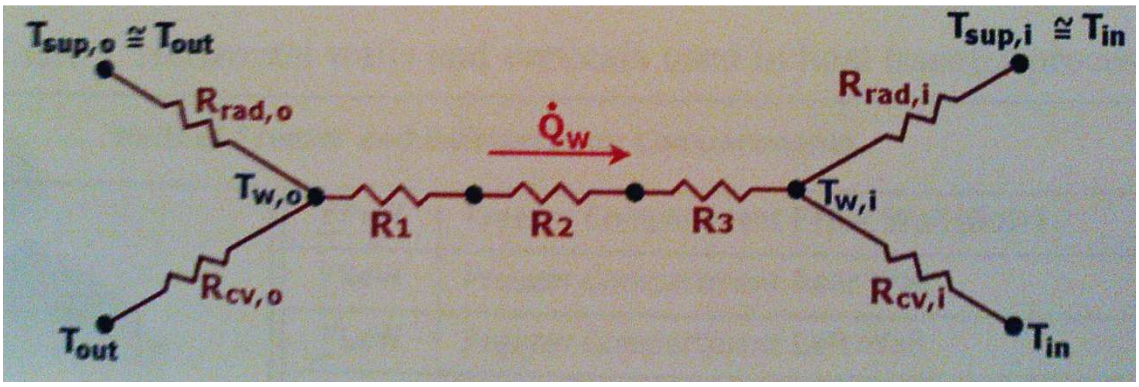

Figure 54 – Heat transfer resistance scheme for general refrigerator walls

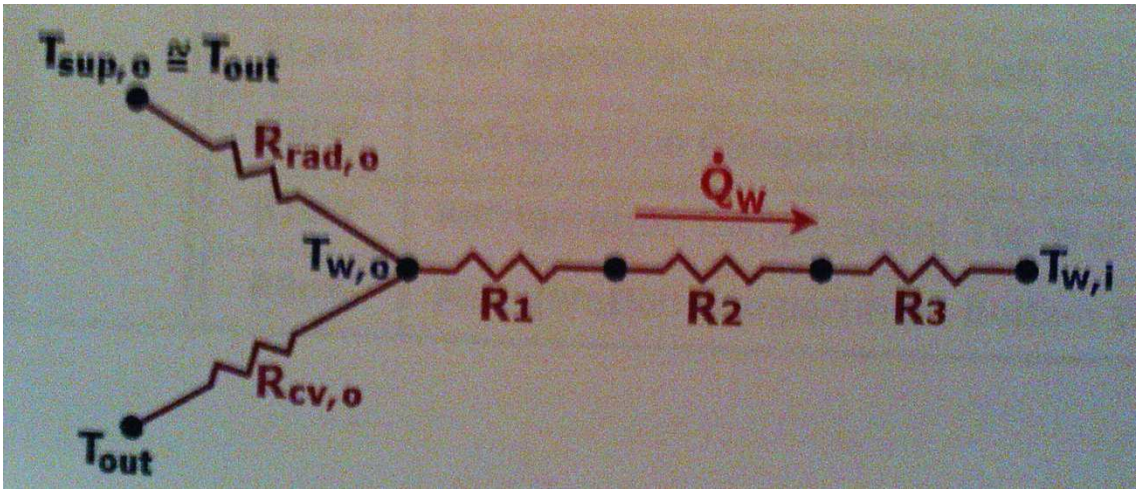

Figure 55 - Heat transfer resistance scheme - bottom refrigerator wall

9.13.1 Heat transfer by conduction through the walls

$$\dot{Q_{cond}} = \lambda \cdot A \frac{\Delta T}{e} \quad \textbf{Eq. 101}$$

$$\dot{Q_{cond}} = \frac{\Delta T}{R_{cond}} \quad \textbf{Eq. 102}$$

$$R_{cond;i} = \frac{e_i}{\lambda_i \, A} \quad \textbf{Eq. 103}$$

R_{cond} is the thermal resistance of the layer against heat conduction. The walls are composed by three layers so there is three R_{cond}. The material properties are listed in Table 28.

Table 28 – Material properties that are possible to be used in the refrigerated

Thickness [m]	Thermal conductivity [W/mK]	Emissivity
0,001	45	0,4
0,055	0,027	0,7
0,001	0,52	0,5

9.13.2 Heat transfer by convection through the walls

$$\dot{Q}_{conv} = \alpha \cdot A_s(T_s - T_\infty) \quad \textbf{Eq. 104}$$

$$\dot{Q}_{conv} = \frac{\Delta T}{R_{conv}} \quad \textbf{Eq. 105}$$

$$R_{conv} = \frac{1}{\alpha \cdot A_s} \quad \textbf{Eq. 106}$$

The convection (natural convection) coefficient depends from surface geometry, the nature of fluid motion, the properties of fluid and the bulk velocity. It can be calculated by the fallowing expression

$$\alpha_{conv} = \frac{Nu \cdot \lambda_f}{L_{ref}} \quad \textbf{Eq. 107}$$

$$Nu = C \cdot Ra^n \quad \textbf{Eq. 108}$$

The constants *C* and *n* depends on the geometry of the surface and the flow regime which is characterized by the range of the Raleigh number (Ra) (seeFigure 56). The Raleigh number is equal to

$$Ra = \frac{g\beta(T_s - T_\infty){L_{ref}}^3}{\vartheta^2} P_r \quad \textbf{Eq. 109}$$

The corresponding thermal resistances between the outside air and external wall surfaces, $R_{cv,o}$ as well as between the internal wall and inside air, $R_{cv,\,i}$ were calculated, considering different wall geometry (or orientation) and temperatures.

GEOMETRY:	L_{ref}	Nusselt	C	n	Range of Ra
HORIZONTAL PLATE — Upper surface of a hot plate, $T_p > T_\infty$ or Lower surface of a cold plate, $T_p < T_\infty$	$L_{ref} = \frac{A}{P}$	$Nu = C \cdot (Ra)^n$	0,54 0,15	1/4 1/3	$10^4 < Ra_{Lref} < 10^7$ $10^7 < Ra_{Lref} < 10^{11}$
HORIZONTAL PLATE — Upper surface of a cold plate, $T_p < T_\infty$ or Lower surface of a hot plate, $T_p > T_\infty$	$L_{ref} = \frac{A}{P}$	$Nu = C \cdot (Ra)^n$	0,27	1/4	$10^5 < Ra_{Lref} < 10^{10}$
VERTICAL PLATE — L, T_p > or < than T_∞	$L_{ref} = L$	$Nu = C \cdot (Ra)^n$	0,59 0,10	1/4 1/3	$10^4 < Ra_{Lref} < 10^9$ $10^9 < Ra_{Lref} < 10^{13}$

Figure 56 – Nusselt number for horizontal and vertical plates as a function of Raleigh number

9.13.3 Heat transfer by radiation through the walls

When a surface of emissivity ε and surface area A_s at an absolute temperature T_p is completely enclosed by a much larger surface at absolute temperature, T_{sup}, separated by a gaseous medium (air) that not intervene with radiation, the net radiation heat transfer between these two surfaces is calculated by

$$\dot{Q}_{rad} = \varepsilon \cdot \sigma \cdot A_s \left(T_s^4 - T_\infty^4\right) \quad \textbf{Eq. 110}$$

Where σ = 5,729x10^{-8} W/m^{2}K^4 is the Stefan-Boltzmann constant.

$$\dot{Q}_{rad} = \frac{T_p - T_{sup}}{R_{rad}} \quad \textbf{Eq. 111}$$

$$R_{rad} = \frac{1}{\alpha_{rad} \cdot A_s} \quad \textbf{Eq. 112}$$

$$\alpha_{rad} = \varepsilon \cdot \sigma \cdot A_s \cdot (T_s + T_\infty) \cdot \left(T_s^2 + T_\infty^2\right) \quad \textbf{Eq. 113}$$

The same done for the convection coefficient was done for the radiation coefficient. It was calculated the outside and inside thermal resistances due to radiation designated by $R_{rad,\,o}$ and $R_{rad,\,i}$.

The surfaces areas are calculate as follows

$$A_{ext;1} = L \cdot H \quad \textbf{Eq. 114}$$

$$A_{ext;2} = W \cdot H \quad \textbf{Eq. 115}$$

$$A_{ext;3} = L \cdot W \quad \textbf{Eq. 116}$$

$$A_{int;1} = (L - 2 \cdot wall_{thicness}) \cdot (H - 2 \cdot wall_{thicness}) \quad \textbf{Eq. 117}$$

$$A_{int;2} = (W - 2 \cdot wall_{thicness}) \cdot (H - 2 \cdot wall_{thicness}) \quad \textbf{Eq. 118}$$

$$A_{ein;3} = (L - 2 \cdot wall_{thicness}) \cdot (W - 2 \cdot wall_{thicness}) \quad \textbf{Eq. 119}$$

9.14 Cycle thermodynamic states

Assuming that only steam circulates in points 1, 2, 3 and 4 the respective enthalpies are calculate by knowing the pressure, temperature and/or vapour quality (at least two properties). As considered before there is two pressure levels. Points 1, 2, 6, 7, 8, 9 are at the higher pressure and points 3, 4, 5 and 10 are at the lower pressure. From here several assumptions could result in very different results with different system COP. For example, point 4 could be superheated water vapour or saturated water vapour (vapour quality = 1). The difference between the lower and higher pressure sides could be large or very small depending on the system operating temperatures. The mass flow circulating in the pump could vary between several values resulting in different, higher or lower, mass flow rate at point 1. The heat exchanger efficiency affects the system efficiency and operation points.

Table 29 – Base system operating points

Point	State	Notes
1	Superheated water vapour	Assuming zero salt content
2	Saturated liquid	Vapour quality = 0
3	Vapour liquid water state	Due to water flash during throttling
4	Saturated water vapour	Vapour quality = 1
5	Saturated liquid solution	Vapour quality = 0
6	Subcooled liquid solution	Higher pressure, constant temperature
7	Subcooled liquid solution	State calculated from heat exchanger model
8	Saturated liquid solution	Vapor quality = 0
9	Subcooled liquid solution	State calculated from heat exchanger mode
10	Vapour liquid solution state	Due to water flash during throttling

10. Absorption System EES results

Table 30 – Refrigerator surfaces global heat transfer coefficient and respective resistances

Surface number	$R_{cond,i}$	$R_{cv\_e,i}$	$R_{cv\_i,i}$	$R_{rad\_e,i}$	$R_{rad\_i,i}$	R_{total}	$U_{r;i}$
	[K/W]	[K/W]	[K/W]	[K/W]	[K/W]	[K/W]	[W/K]
1	1,359	0,334	0,574	0,277	0,334	1,722	0,581
2	2,039	0,500	0,898	0,416	0,522	2,596	0,385
3	1,359	0,233	1,017	0,277	0,334	1,737	0,576
4	1,359	0,655	0,448			2,462	0,406

Table 31 – Refrigerator exterior dimensions

L [m]	W [m]	H [m]
1,5	1	1

Table 32 – Exterior and interior surfaces areas

Surface number	A_{ext}	A_{int}
	[m^2]	[m^2]
1	1,5	1,228
2	1	0,785
3	1,5	1,228
4	1,5	1,228

Table 33 – Absorption system constants

ΔT_{refrig}	120	s
T_{enter}	8	ºC
$T_{surface}$	25	ºC
$T_{[1]}$	80	ºC
P_{atm}	103	kPa
T_{ext}	35	ºC
$\dot{Q}_g$	180	W
PCI_{Butane}	45E6	J/kg
eff_{pump}	0,45	
eff_{HX}	0,6	
L_{fin}	0,11	m
fin_S	0,015	m
L_c	1	m
eff_{ger}	0,7	
eff_{fin}	0,36	
UA_e	50	W/K
x_{high}	0,62	
x_{low}	0,47	

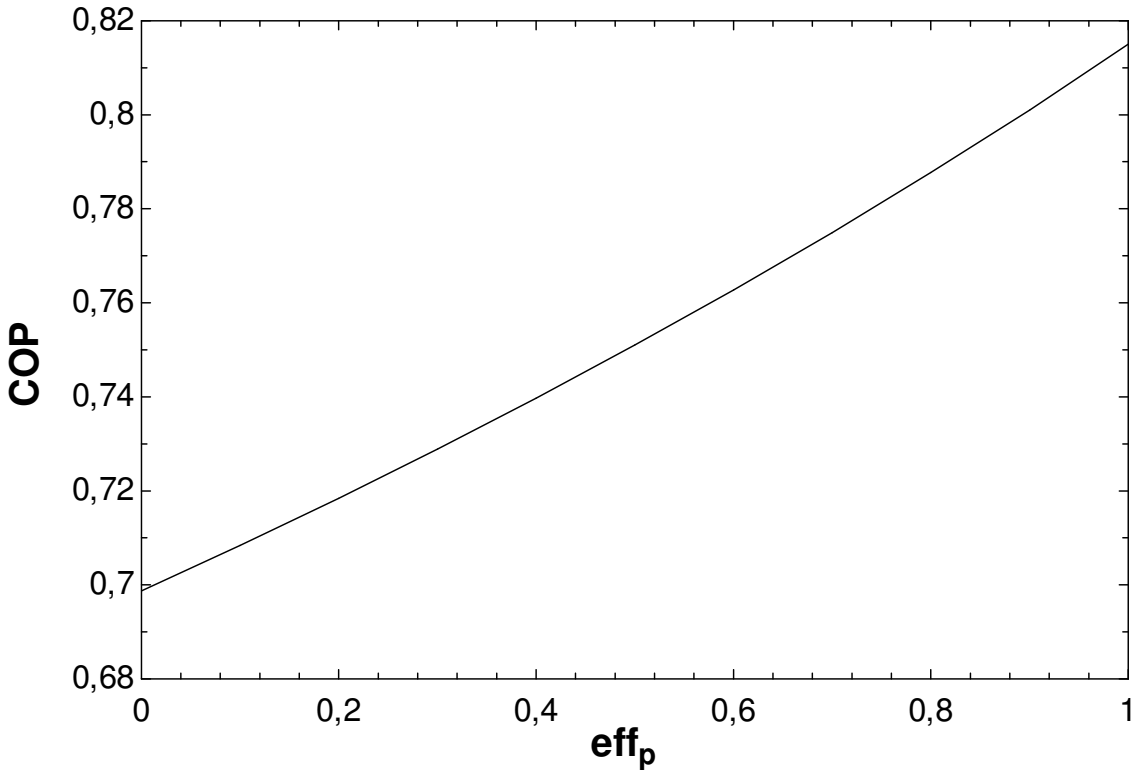

Figure 57 – Effect of solution heat exchanger on COP

Table 34 – Effect of solution heat exchanger on COP and refrigerator mean air temperature

HX_{eff}	COP	$T_{air;i}$
		[C]
0	0,699	6,378
0,1	0,708	6,313
0,2	0,718	6,245
0,3	0,729	6,174
0,4	0,740	6,101
0,5	0,751	6,024
0,6	0,763	5,943
0,7	0,775	5,859
0,8	0,788	5,77
0,9	0,801	5,676
1	0,815	5,577

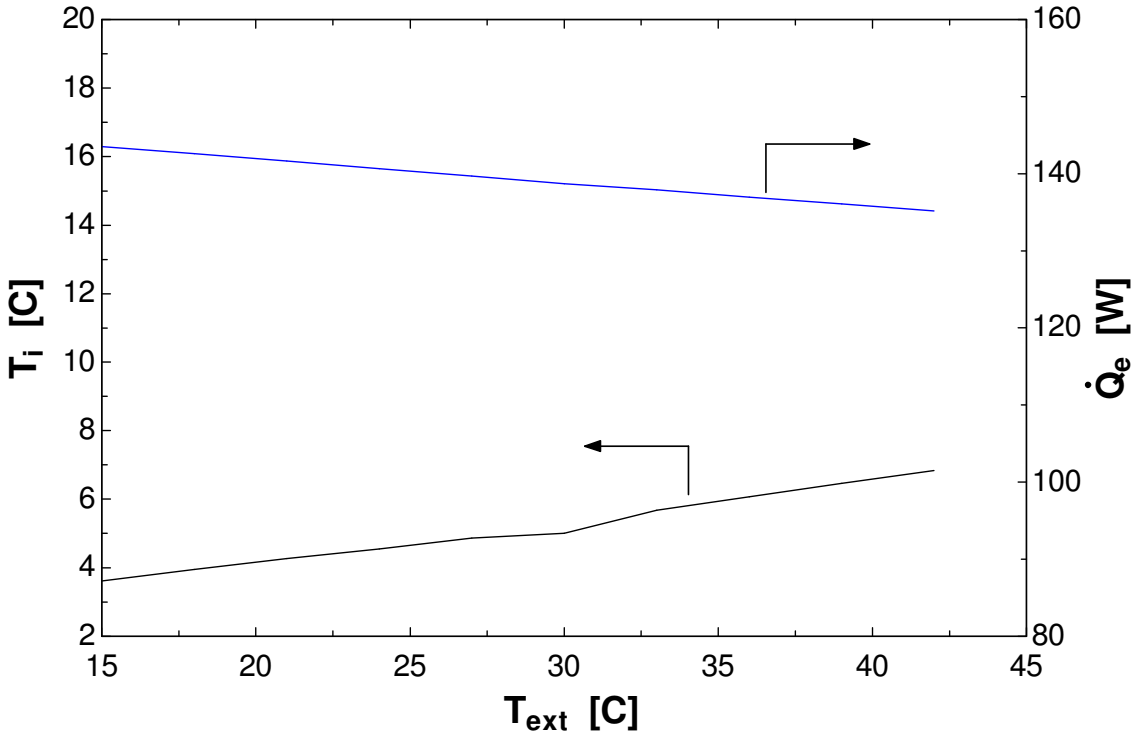

Figure 58 – Refrigerator mean air temperature and evaporator heat rate as a function of external temperature and considering that generator power is equal to 180W

Table 35 – Refrigerator COP, inside air and evaporator outlet temperatures as a function of exterior temperature

T_{ext}	COP	$\dot{Q}_e$	$T_{air;i}$	T_4
[C]		[W]	[C]	[C]
15	0,798	143,6	3,615	0,7435
18	0,792	142,6	3,95	1,099
21	0,787	141,6	4,27	1,438
24	0,782	140,7	4,547	1,734
27	0,776	139,7	4,862	2,068
30	0,771	138,7	4,999	2,225
33	0,766	137,9	5,68	2,923
36	0,761	137	6,074	3,334
39	0,756	136,1	6,46	3,739
42	0,751	135,2	6,844	4,141

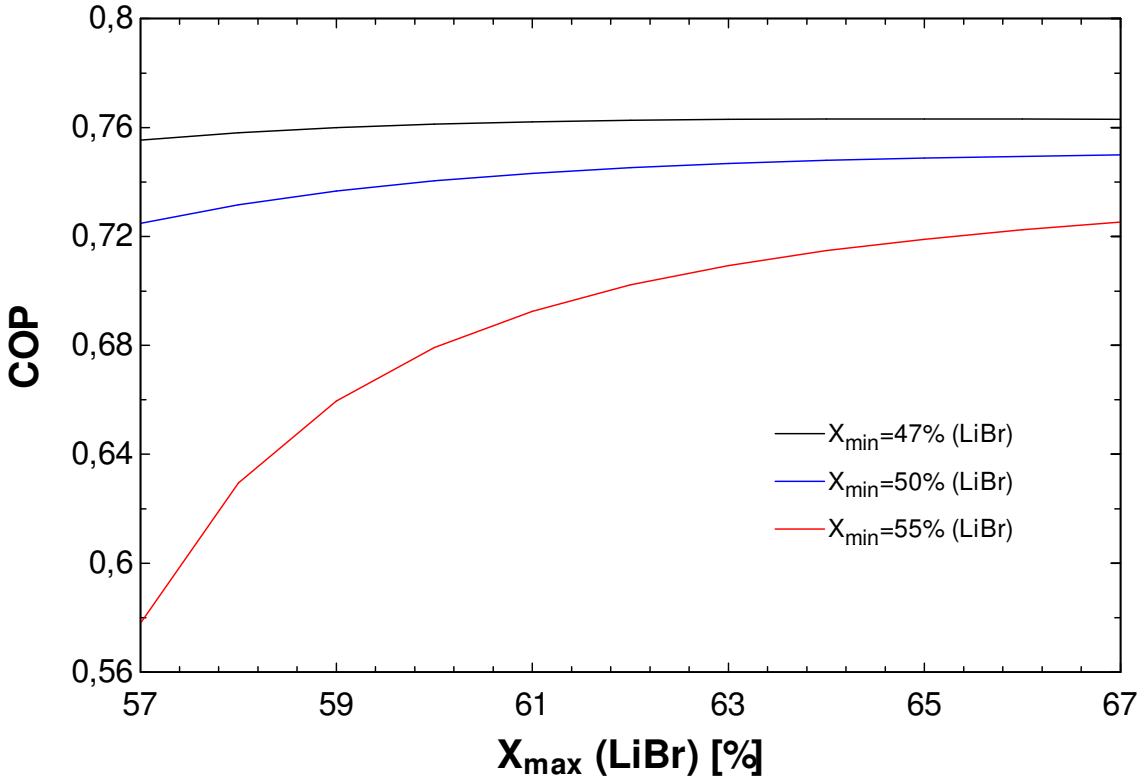

Figure 59 – COP as a function of maximum and minimum LiBr mass fraction

Table 36 – COP, condenser and absorber outlet temperatures and mean refrigerator air temperature as a function of generator heat power

$\dot{Q}_g$	COP	T_2	T_4	$T_{air;i}$
[W]		[C]	[C]	[C]
50	0,803	40	8,696	9,499
70	0,797	43	7,819	8,934
90	0,790	45	6,955	8,378
110	0,784	47	6,105	8
130	0,778	49	5,265	7,287
150	0,772	51	4,435	7
170	0,766	53	4	6,213
190	0,760	55	2,783	6
210	0,754	56,59	1,807	4,973
230	0,748	58	1,193	4,636

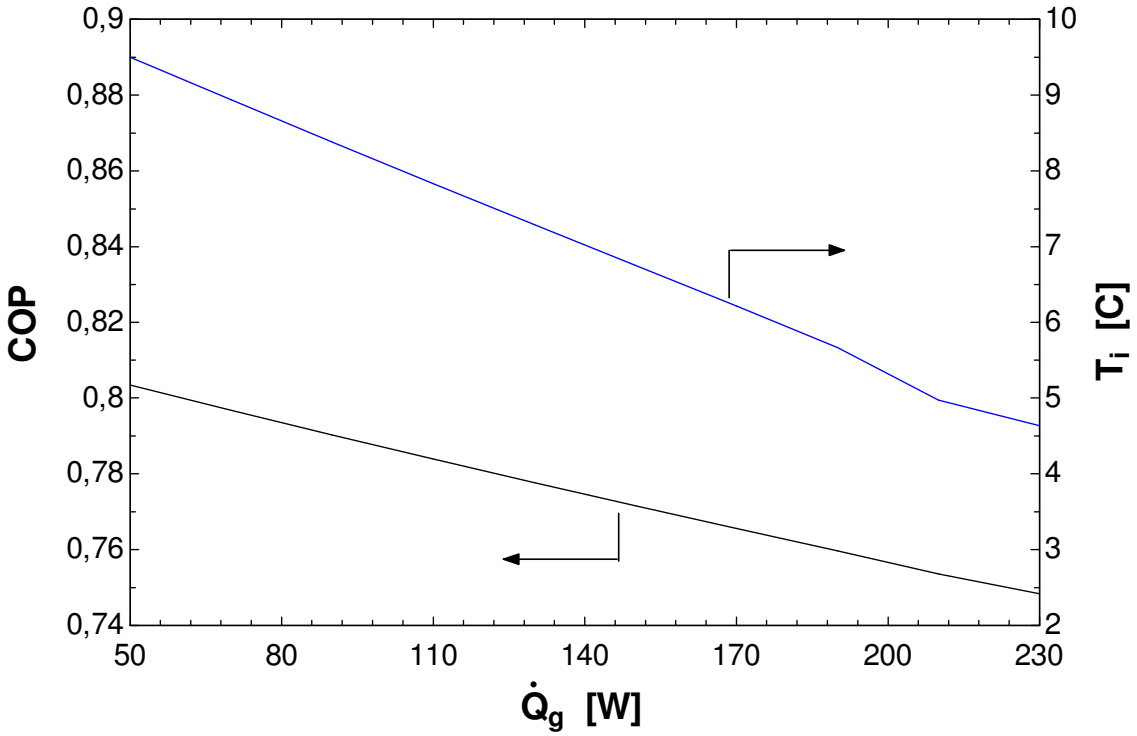

Figure 60 – COP and refrigerator mean air temperature as a function of generator heat rate

Table 37 – Condenser length effect on condenser outlet temperature, COP, evaporator heat rate, refrigerator inside mean air temperature and evaporator outlet temperature

L_c	T_2	COP	$\dot{Q}_e$	$T_{air;i}$	T_4
[m]	[C]		[W]	[C]	[C]
0,5	70,68	0,7273	131	6,185	3,566
0,6	65,22	0,7392	133	6,104	3,442
0,7	61,2	0,7476	135	6,047	3,355
0,8	58,11	0,7538	136	6,005	3,291
0,9	55,67	0,7587	137	5,971	3,239
1	53,7	0,7627	137	5,943	3,198
1,1	52,07	0,766	138	5,921	3,163
1,2	50,71	0,7688	138	5,902	3,134
1,3	49,54	0,7712	139	5,885	3,109

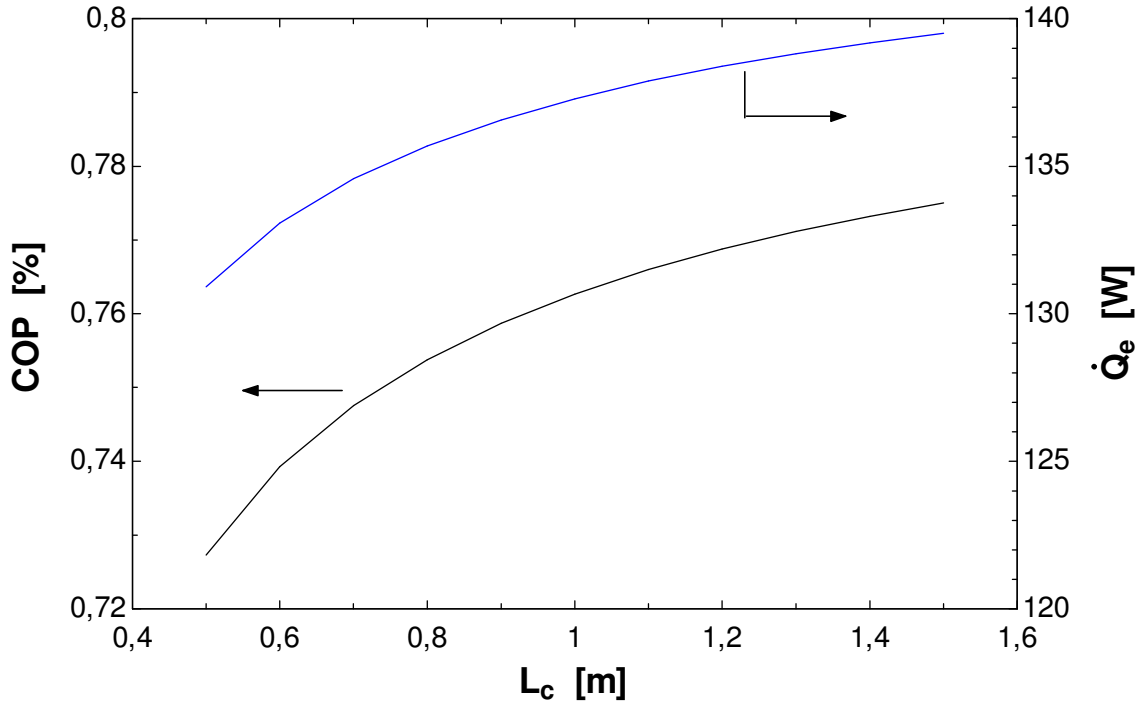

Figure 61 – COP and evaporator heat rate as a function of condenser length

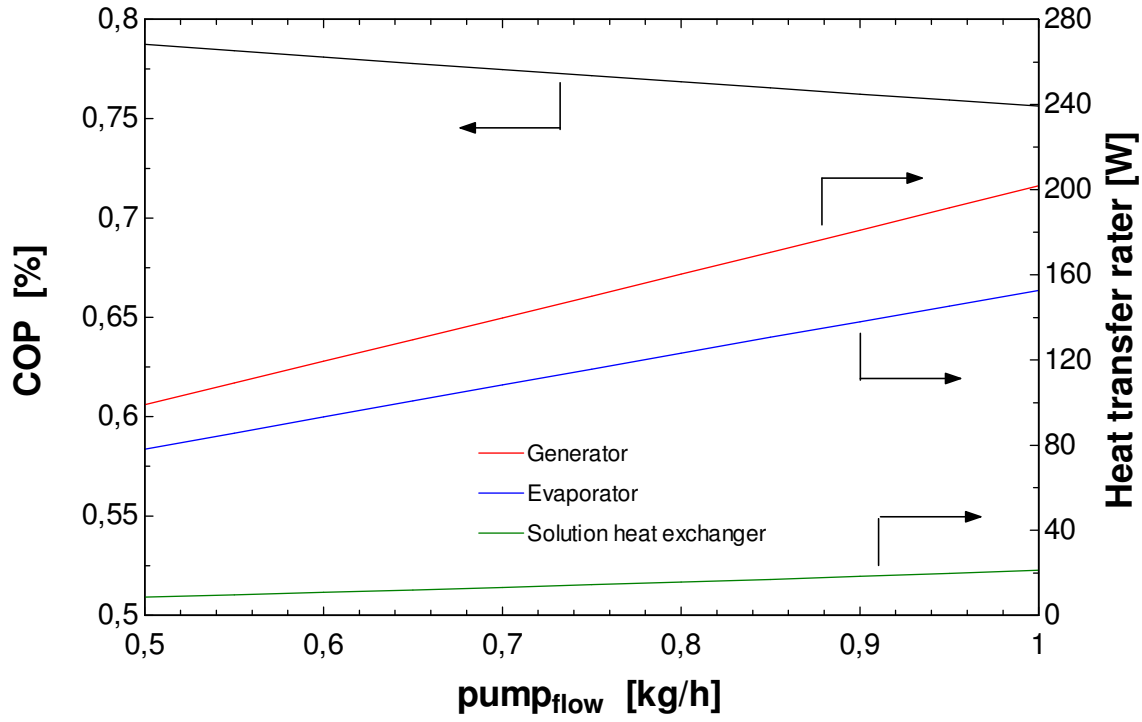

Figure 62 – COP and heat transfer rate for generator, evaporator, and solution heat exchanger as a function of pump flow

Table 38 – COP, evaporator and generator heat transfer rates and evaporator and mean inside refrigerator air temperature as a function of pump flow

$pump_{flow}$	COP	$\dot{Q}_e$	$\dot{Q}_g$	q_ex	T_4	$T_{air;i}$
[kg/h]		[W]	[W]	[W]	[C]	[C]
0,5	0,7874	78	99	8,608	6,568	8,128
0,55	0,7842	86	109	9,689	6,139	7,852
0,6	0,781	93	119	11	5,712	7,576
0,65	0,7779	101	130	12	5,285	7,3
0,7	0,7747	108	140	13	5	7,025
0,75	0,7716	116	150	14	4,435	6,75
0,8	0,7685	123	160	16	4	6,474
0,85	0,7655	131	171	17	3,585	6,197
0,9	0,7624	138	181	18	3,158	5,917
0,95	0,7594	145	191	20	2,725	5,632
1	0,7563	153	202	21	2,276	5,329

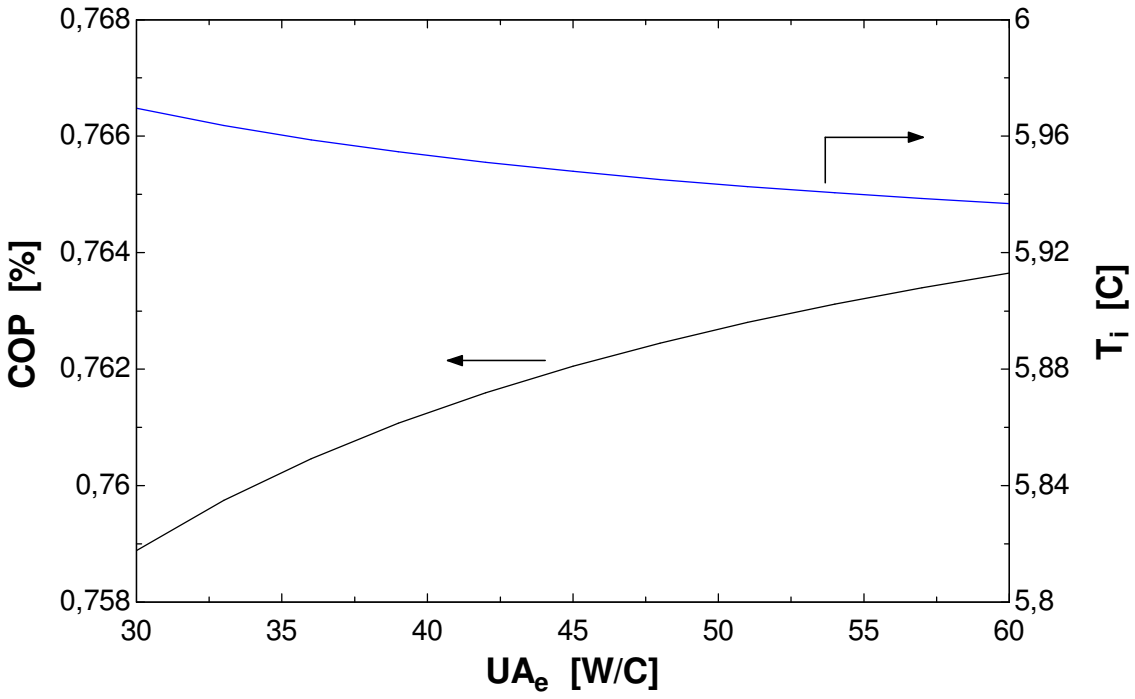

Figure 63 – Absorption refrigerator COP and interior mean air temperature as a function of UA_e

Table 39 - Absorption refrigerator COP, evaporator heat rate, interior mean air temperature and outlet evaporator temperature as a function of UA_e

UA_e	COP	$\dot{Q}_e$	$T_{air;i}$	T_4
[W/C]		[W]	[C]	[C]
30	0,7589	137	6	1,416
33	0,7597	137	5,964	2
36	0,7605	137	5,959	2,156
39	0,7611	137	5,955	2,442
42	0,7616	137	5,951	2,687
45	0,762	137	5,948	3
48	0,7624	137	5,945	3,086
51	0,7628	137	5,943	3
54	0,7631	137,4	5,941	3,397
57	0,7634	137	5,939	3,528
60	0,7636	138	5,937	3,646

11. Absorption system results discussion

The coefficient of performance of absorption system is highly influenced by the solution heat exchanger efficiency as seen in Figure 57 – Effect of solution heat exchanger on COPFigure 57. The difference is almost 10% less performance when compared to 80% heat exchanger efficiency and by not having a solution heat exchanger.

Figure 58 shows the refrigerator mean air temperature as a function of exterior air temperature considering that the generator power is 180W. The heat gained by the refrigerator decreases with the increase of exterior air temperature because the inside temperature increases. The machine input power is constant and the evaporator operating temperature also increases and this influence the evaporator heat rate that decreases with the increase of outside air temperature as shown in Table 35. It is important that the machine has a generator gas flow valve to control the heat input in the generator.

The mass fraction of LiBr circulating between the generator and absorber influences the cycle performance as shown in Figure 59. The max COP occurs when the difference between x_{max} and x_{min} is maximum. The weak solution in LiBr is influenced by the pressure and temperature of absorber and the strong solution that exits the generator is dependent of the pressure and temperature of generator. To avoid LiBr crystallization problems there should be a difference between the x_{max} of cycle and the 70% maximum LiBr concentration by controlling the absorber and desorber temperature.

The power in the generator influences the machine performance. As shown in Figure 60 the higher the generator power is the lowest is the performance of the machine, but the effect in the inside air temperature of refrigerator is higher. Considering the selected configuration for the condenser (L_c=1m) it is clearly unmatched for the generator power (180W) as can be seen in Table 36 where the outlet condenser temperature is higher than 53ºC at outside air temperature of 35ºC. Figure 61 shows the COP is higher with a higher condenser length and an increase in the evaporator heat rate for a generator power of 180W. As can be seen in Table 37 the effect on inside air temperature is less than 0,4ºC compared to have a 0,5m or 1,5m condenser length.

With the outlet water vapour temperature equal to 80ºC, the higher the solution flow circulated by the pump is, the higher is the generator, evaporator and solution heat exchanger heat rates as shown in Figure 62. As commented before the COP is lower because the generator power is higher, but the effect on refrigerator inside temperature is higher as shown again in Table 38.

The global heat transfer coefficient for the evaporator has little effect on COP and on the inside air temperature as shown in Figure 63. However the effect on the outlet evaporator temperature is not negligible because for the same heat transfer the difference between outlet evaporator temperature and refrigerator inside air temperature is higher.

12. Selecting Vaccine refrigerator

World Health Organization (WHO) created a guideline for manufacturers of vaccine refrigerators. A certain product of a manufacture is actually qualified if specific Performance, Quality and Safety (PQS) requirements are satisfied. The anterior performance specifications and verification protocols were the PIS that were replaced by the PQS in 2007. For refrigerators or combined refrigerator-icepack freeze with an absorption cycle the PQS performance requirements are:

- The acceptable temperature range for storing vaccine is +2°C to +8°C
- Holdover time: The time in hours during which all points in the vaccine compartment remain between +2°C and +10°C, at the maximum ambient temperature of the temperature zone for which the appliance is rated, after the fuel supply has been disconnected (minimum of 3 hours)
- Hot zone appliances must operate at a steady +43°C ambient temperature and over a+43°C/+25°C day/night cycling temperature range
- Moderate zone: Moderate zone appliances must operate at a steady +27°C ambient temperature and over a+27°C/+10°C day/night cycling temperature range
- Temperate zone: Temperate zone appliances must operate at a steady +32°C ambient temperature and over a+32°C/+15°C day/night cycling temperature range
- Fuel supply is natural gas, propane or kerosene
- Externally readable cabinet-mounted gas or vapour pressure dial thermometer
- The product is to be designed to achieve a maintenance-free life of not less than 10 years apart from re-fueling, wick replacement and trimming (kerosene units) flue cleaning, routine de-frosting and cleaning and replacement of batteries (if any)

12.1 *Product datasheet*

Table 40 – Zero Appliances GR265 G/E product performance information

Ice pack Freezer, With Vaccine	+32°C	4.2kg/24hrs
	+43°C	1.8kg/24hrs
Hold Over Time During Power Cut		5.5 hours(+32°C)
		1.5 hours (+43°C)
Power Consumption: Gas		660g/24hrs (+32ºC) (without a gas thermostat)
		770g/24hrs (+43ºC) (without a gas thermostat)

Table 41 – Sibir V110GE product performance information according to EPI/PROC/5

Safe Ice pack freezing	**32 ambient (ºC)**	**1,2kg**
Hold over time	32 ambient (ºC)	4,02h
EPI specification		E3/RF.2

Table 42 - Sibir V110GE product input/consumption information

Gas inlet pressure (Propane)	30 mbar
Max input	170 W
Gas consumption	385 g/24h

Table 43 - Zero Appliances GR265 G/E product specifications

Vaccine Storage Capacity	Refrigerator	57L
Frozen Ice Pack Storage Capacity	Freezer	9.6L
Manufacturers Gross Volume	Refrigerator	180L
	Freezer	32L
External Dimensions (HxWxL) (Not Boxed)		150x60x68cm
Type Of Kerosene Burner/Gas Jet Size		Jet Size 13

Table 44 - Sibir V110GE product specifications

Net capacity	102 l
Net vaccine storage capacity	20 l
Net freezer capacity	15 l

13. Conclusions

The match between the consumed and the outputted water volume by the pump can be evaluated by the total storage volume. The lowest volume is always the best and it is not recommended for this specific case a zero storage volume. Two or three days are the minimum recommended storage volume. Considering a 16 m^3/day the minimum storage volume should range between 32 to 48 m^3.

The optimum angle over a year could be the angle that optimises the water pump output or benefit the months with the lowest water pump output. A fixed angle of 30º benefit the months with the lowest water pump output.

To satisfy the villagers water needs the best studied pump is the SQF centrifugal 5A-3 pump with an array peak power higher than 320W_p. The SQF helical rotor is limited to 10000 m^3/year and is recommended to be installed in places with higher static heads. Possibly the initial system cost will be between 3000€ to 5000€ because it was not considered the storage tanks and support structure costs, labour hand and transportation. The price depends also from photovoltaic support structure and the number of installed panels.

The coefficient of performance of absorption system is highly influenced by the solution heat exchanger efficiency. It's also influenced by the environment air temperature and solution concentration between the absorber and the generator. The condenser length has also an impact in the COP and the global heat transfer in the evaporator also influences the COP but as a higher impact in the evaporator outside temperature.

It's not possible to select the best refrigerator because it depends from the dimension of the future health center. The selected refrigerators in the above chapter are very different from the point of view of vaccine capacity, holdover time, propane consumption and safe ice pack freezing capacity at outside air temperature of 32ºC. Both of them are approved by the PIS but they are not yet approved by the new PQS performance specifications. Only a few models are prequalified to be approved by the new PQS performance specifications. For high vaccine capacity the best one is the Zero Appliances GR265 G/E, but for low vaccine capacity the best one is the Sibir V110GE refrigerator. In the new prequalified list there are only products that work with a compression cycle, using AC or DC electric motors and some models uses photovoltaic panels with batteries. This could mean that the vaccine refrigerators manufactures are excluding the use of LP gas or kerosene as a heat source, because it's not easy to find a PIS certificated product that works with an absorption cycle.

14. References

[1] Afonso, C. Félix, *"Sebenta de refrigeração",* Aefeup Editorial, 2007

[2] Afonso, C., Castro, M., Matos, J. – "Air infiltration on domestic refrigerators: the influence of the magnetic seals"

[3] ASHRAE, "*Refrigeration: 1998 ASHRAE handbook"*, 2nd edition, Am. Soc. Heat., Refrig., [4] Air-Cond. Eng., USA, 1998

[5] Buschermohle, M. J., Burns, R. T., "Solar-Powered Livestock Watering Systems"

[6] Çengel, Yunus A., Boles, Michael A. - "Thermodynamics: an engineering approach" - 5th edition in SI units. - Boston: McGraw-Hill/Higher Education, cop. 2006

[7] Cuamba, B. C., et. al.- "A solar energy resources assessment in Mozambique"- Journal of Energy in Southern Africa, Vol. 17 Number 4, 2006

[8] Dinçer, I., "*Refrigeration Systems and Application"*, Wiley, West Sussex, 2003

[9] Dougherty, Robert L., "Centrifugal pumps" - September 2007, Das Press

[10] Duffie, John A., Beckman, William A., "Solar engineering of thermal processes" - 2nd ed. - New York [etc.]: John Wiley & Sons, cop. 1991

[11] Fiaschi, D., Graniglia, R., Giampaolo M., 2005 – "Improving the effectiveness of solar pumping systems by using modular centrifugal pumps with variable rotational speed", Solar Energy, Vol. 79 – pag. 234-244

[12] Gottlieb, I. - "Practical electrical motor handbook" – Elsevier Science, 1997

[13] Herold, K. E.; Radermacher, Reinhard; Klein, Sanford A., *"Absorption chillers and heat pumps"*, CRC Press, 1996

[14] Herold, Keith E., Radermacher Reinhard, Klein, Sanford A., "Absorption chillers and heat pumps", CRC Press, cop. 1996

[16] Huacuz, J. M., Flores, R., Agredano, J., 1995 – "Field Performance of Lead-Acid Batteries in Photovoltaic Rural Electrification Kits", Solar Energy, Vol.55 – pag. 287-295

[17] Incropera, Frank P., "Fundamentals of heat and mass transfer" - 6th ed. - Danvers: John Wiley & Sons, cop. 2007

[18] Messenger, Roger A., Ventre, Jerry - "Photovoltaic systems engineering" - 2nd ed. - CRC Press, cop. 2004

[19] Odeh I., Yohanis Y.G., Norton B., "Economic viability of photovoltaic water pumping systems", July 2005 [Solar Energy 80 (2006) 850–860]

[20] Odeh, I., 2006 "Influence of pumping head, insolation and PV array size on PV water pumping system performance", Solar Energy, Vol. 80 – pag. 51-64

[21] SELF, "A cost and reliability comparison between solar and diesel powered pumps", Jully 2008

[22] Short, T.D., P. Thompson, 2003 – "Breaking the mould: solar water pumping – the challenges and the reality", Solar Energy ,Vol. 75 – pag. 1-9

[23] Stoecker, W.F., Jones., J. W. "Refrigeration and air conditioning" - 2nd ed. - Auckland: McGraw- Hill Book Company, 1982

[24] Vick, B. D., Clark, R. N., 1996 – "Performance of Wind-Electric and Solar-PV Water Pumping Systems for Watering Livestock", Jornal of Solar Energy Engineering, Vol. 118 - pag. 212-216

[25] Wang, Shan K. – "Handbook of Air Conditioning and Refrigeration", McGraw-Hill, 2nd editon, 2000

[26] Wenham, Stuart R., "Applied Photovoltaics" - 2nd. - London : Earthscan, 2009

[27] White, Frank M. (2003), "*Fluid Mechanics"* - 6th ed. - McGraw-Hill/Higher Education : Boston [etc.], cop. 2008

Websites

[28] E03 Refrigerators and freezers for storing vaccines and freezing icepacks - http://www.who.int/immunization_standards/vaccine_quality/pqs_e03_fridges_freezers/en/index.html

[29] Electrical Impedance - http://en.wikipedia.org/wiki/Electrical_impedance

[30] Grundfos WEBCAPS/SQFlex catalogue– http://net.grundfos.com/Appl/WebCAPS/InitCtrl?mode=13

[31] Millennium Development Goals - http://unstats.un.org/unsd/mdg/Default.aspx

[32] Naps System - http://www.napssystems.com/

[33] Performance, Quality and Safety (PQS) - Prequalified equipment - http://www.who.int/immunization_standards/vaccine_quality/e03_prequalified_equip/en/index.html

[34] Solar Energy for Africa - http://www.solarafrica.org/

[35] Sunpumps products catalogue - http://www.sunpumps.com/ProductsClient.aspx

[36] Vaccine refrigerator - http://en.wikipedia.org/wiki/Vaccine_refrigerator

[37] WHO - http://www.who.int/immunization_standards/vaccine_quality/pqs_e03_rf02_1.pdf

[38] Wikipedia Millennium Development Goals - http://en.wikipedia.org/wiki/Millennium_Development_Goals

Appendix A - Solar radiation

Before analysing the photovoltaic panels it is important to understand the energy source – the sun. Studying solar geometry helps to know the sun position, the direction of beam radiation incident on surfaces of various orientations and shading. To better understand the solar geometry it is necessary to define important definitions.

A.1 - Definitions

Air mass m is the ratio of the mass of atmosphere through which beam radiation passes to the mass it would pass through if the sun were at the zenith (shortest path). For zenith angle between 0º and 70º at sea level m is equal to:

$$m = 1/\cos(\theta_z) \qquad \textbf{Eq. A.1}$$

Beam radiation is the direct solar radiation. In other words is the solar radiation that wasn't scattered by the atmosphere.

Diffuse radiation is the solar radiation received from the sun after its direction has been changed by scattering the atmosphere.

Total solar radiation is the sum of beam and diffuse radiation on a surface.

Irradiance (G) is the rate at which radiant energy is incident on a surface, per unit area of surface.

Irradiation is the incident energy per unit area on a surface found by integrating irradiance over a specified time. The subscript *H* is used for insolation for a day. The symbol *I* is used for insolation for an hour. The symbols *H* and *I* can represent beam, diffuse, or total and can be on surfaces of any orientation. Subscripts on *G, H* and *I* are as follows: 0 refers to extraterrestrial radiation, b and d refer to beam and diffuse radiation; T and n refers to radiation on a tilted plane and normal plane; If the plane is horizontal the symbols doesn't have any subscript.

A.1.1 - Direction of beam radiation

The following definitions refer to angles that describe the geometric relationships between a plane and earth at any time. The angles are as follows:

Latitude (ϕ) site angular location relative to the equator between -90º and 90º (north-positive or south - negative).

Declination (δ), the angular position of the sun at solar noon with respect to the plane of the equator, north positive; -23,45º< δ<23,45º

$$\delta = 23{,}45 \cdot \sin\left(360 \cdot \frac{284+n}{365}\right) \qquad \textbf{Eq. A.2}$$

Slope (β), the angle between the plane of the surface and the horizontal plane; 0º<β<90º.

Surface azimuth angle (γ), the deviation of the projection on a horizontal plane of the normal to the surface from the local meridian, with zero due south, east negative and west positive; -180º< $\delta_{surface}$ <180º

Hour angle (ω)**,** the angular displacement of the sun east or west of the local meridian due to the rotation of the earth on its axis at 15º per hour, morning negative and afternoon positive.

Angle of incidence (θ) the angle between the beam radiation on a surface and the normal to that surface

Zenith angle (θ_z) the angle between the vertical and the line to the sun

Solar altitude angle (α_s), the angle between the horizontal and the line to the sun (complement to the zenith angle)

Solar azimuth angle (γ_s), the angular displacement from south of the projection of the beam radiation on the horizontal plane

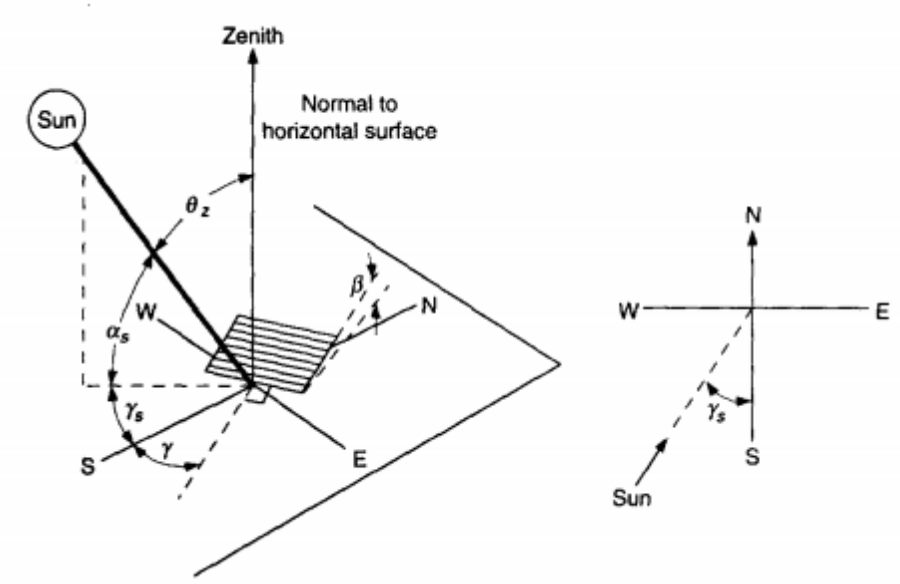

Figure A.1 – Zenith angle (θ_z), slope (β), surface azimuth angle, and solar azimuth angle (γ_s) for a tilted surface [Source: Duffie and Beckman]

A.2 - Ratio of beam radiation on tilted surface to that on horizontal surface

The most common available data are the total radiation for hours or days on a horizontal surface. To know the beam and diffuse radiation on the plane of the collector it is used the geometric factor R_b. This factor is the ratio of beam radiation on the tilted surface to that on a horizontal surface at any time.

$$R_b = \frac{G_{b,T}}{G} = \frac{G_{b,n} \cdot \cos(\theta)}{G_{b,n} \cdot \cos(\theta_z)} = \frac{\cos(\theta)}{\cos(\theta_z)} \qquad \textbf{Eq. 120}$$

To simplify **Erro! A origem da referência não foi encontrada.**it is considerer that the surface is oriented to north (southern hemisphere) or south (northern hemisphere). For δ =0º (northern hemisphere):

$$R_b = \frac{\cos(\phi - \beta) \cdot \cos(\delta) \cdot \cos(\omega) + \sin(\phi - \beta)}{\cos(\phi) \cdot \cos(\delta) \cdot \cos(\omega) + \sin(\phi) \cdot \sin(\delta)} \quad \text{Eq. A.4121}$$

In the southern hemisphere, δ=180º and the R_b is equal to:

$$R_b = \frac{\cos(\phi + \beta) \cdot \cos(\delta) \cdot \cos(\omega) + \sin(\phi + \beta)}{\cos(\phi) \cdot \cos(\delta) \cdot \cos(\omega) + \sin(\phi) \cdot \sin(\delta)} \quad \text{Eq. A.5}$$

Equations A.4 and A.5 are valid if the latitude is between -60º and 60º.

A.3 - Extraterrestrial radiation incident on a horizontal surface

Extraterrestrial daily solar radiation on a horizontal surface is obtained by integrating the solar radiation on a horizontal surface outside the atmosphere. If G_{sc} is in W/m^2 the H_0 is in joules per square meter. G_{sc} is the solar constant and is equal to 1367 W/m^2.

$$H_0 = \frac{24 \cdot 3600 \cdot \mathrm{G_{sc}}}{\pi} \left(1 + 0{,}033 \cdot \cos\frac{360 \cdot n}{365}\right) \cdot \left(\cos(\phi) \cdot \cos(\delta) \cdot \sin\omega_s + \frac{\pi\omega_s}{180}\sin\phi \sin\delta\right) \quad \text{Eq. A.6}$$

Where n is the day of the year and ω_s is the sunset hour angle, in degrees, calculated by eq. A.17.

It is also necessary to calculate the extraterrestrial radiation on a horizontal surface for an hour period. The process is equal to the anterior but the integral is done for an hour between hour angles ω_1 and ω_2 where $\omega_2 > \omega_s$.

$$I_0 = \frac{12 \cdot 3600 \cdot \mathrm{G_{sc}}}{\pi} \left(1 + 0{,}033 \cdot \cos\frac{360 \cdot n}{365}\right) \cdot \left(\cos(\phi) \cdot \cos(\delta) \cdot \sin(\omega_2 - \omega_1) + \frac{\pi(\omega_2 - \omega_1)}{180}\sin\phi \sin\delta\right) \quad \text{Eq. A.7}$$

A.4 - Solar radiation data

Solar energy is measured by pyranometers. The collected information usually is available in two forms. The first is monthly average daily total radiation on a horizontal surface. The second is hourly total radiation on a horizontal surface *I* for each hour for extended periods such as one or more years.

A.5 - Clearness index K_t

It is important to know the frequency of occurrence of periods of various radiation levels, for example, good and bad days. The frequency distribution is the link between two kinds of correlations. The first is the daily fraction of diffuse with daily radiation and the second is the monthly average fraction of diffuse with monthly radiation [Duffie, 1991].

The monthly average clearness index is the ratio of monthly average daily radiation on a horizontal surface to the monthly average daily extraterrestrial radiation.

$$\overline{K_T} = \frac{\overline{H}}{\overline{H_0}} \qquad \textbf{Eq. A.8}$$

Replacing the monthly average daily radiation by daily radiation or hourly radiation it is calculated the daily clearness index and hourly clearness index, respectively:

$$K_T = \frac{H}{H_0} \qquad \textbf{Eq. 122}$$

$$k_T = \frac{I}{I_0} \qquad \textbf{Eq. A.11123}$$

The data $\overline{H}$, H is from measurements of total solar radiation on a horizontal surface and obtained by pyranometers measurements. $\overline{H_0}$, H_0, I_0 can be calculated as described before.

A.6 - Diffuse component of monthly radiation

Figure A.2 shows the distribution of monthly average daily radiation into its beam and diffuse components as a function of $\overline{K_t}$. As can be seen in figure A.2 there is significant differences among the various correlations. Instrumental problems and atmospheric variables (air mass, season, or other) may contribute to the differences. Seasonal dependence is expressed in terms of the sunset hour angle of the mean day of the month (*n*).

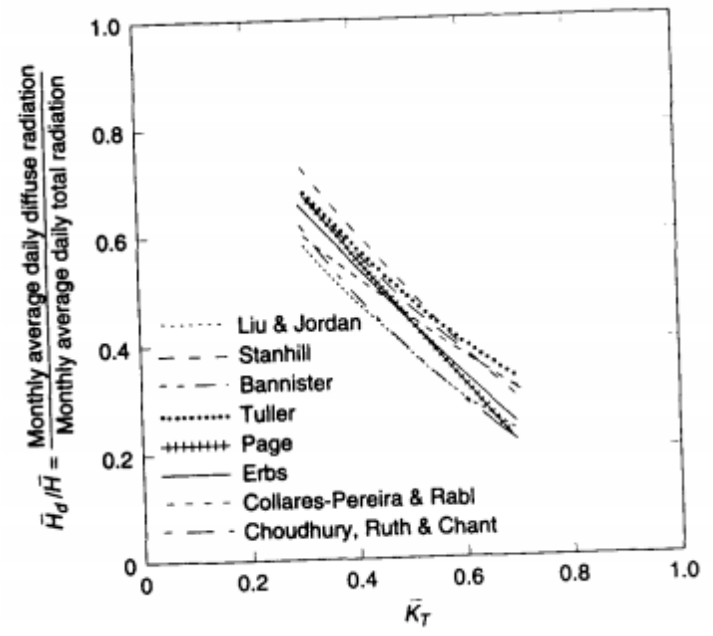

Figure 64 – Correlations of average diffuse fractions with average clearness index [Source: Duffie, 1991]

The dependence $\frac{\overline{H_d}}{\overline{H}}$ on $\overline{K_T}$ is shown by Eq. 33 and 34 (Erbs correlations) as a function of ω_s (season dependence).

For $\omega_s \leq 81{,}4º$ and $0{,}3 \leq \overline{K_T} \leq 0{,}8$

$$\frac{\overline{H_d}}{\overline{H}} = 1{,}391 - 3{,}560\overline{K_T} + 4{,}189\overline{K_T}^2 - 2{,}137\overline{K_T}^3 \quad \textbf{Eq. A.12}$$

And for $\omega_s \geq 81{,}4º$ and $0{,}3 \leq \overline{K_T} \leq 0{,}8$

$$\frac{\overline{H_d}}{\overline{H}} = 1{,}311 - 3{,}022\overline{K_T} + 3{,}427\overline{K_T}^2 - 1{,}821\overline{K_T}^3 \quad \textbf{Eq. A.13}$$

A.7 - Estimation of hourly radiation from daily data

To know the hourly radiation there is two ways. The first is to have hourly radiation from meteorological stations for several years. The second is to estimate the hourly radiation from daily data. As with the estimation of diffuse radiation, this is not an exact process. The method presented here work best for clear days, and those are the days that produce more energy [Duffie, 1991]. This method tends to overestimate.

r_t is the ratio between hourly total and daily total radiation on a horizontal surface, as a function of day length and the hour in question:

$$r_t = \frac{I}{H} = \frac{\pi}{24}(a + b\cos(\omega))\frac{\cos\omega - \cos\omega_s}{\sin\omega_s - \frac{\pi\omega_s}{180}\cos\omega_s} \quad \textbf{Eq. A.14}$$

The coefficients *a* and *b* are calculated by

$$a = 0{,}409 + 0{,}5016\sin(\omega_s - 60) \quad \textbf{Eq. A.15124}$$

$$b = 0{,}6609 + 0{,}4767\sin(\omega_s - 60) \quad \textbf{Eq. A.16}$$

Where ω is the hour angle in degrees for the time in question (midpoint of the hour), and ω_s is the sunset hour angle in degrees.

r_d is the ratio between hourly and daily diffuse radiation on a horizontal surface, as a function of day length and the hour in question:

$$r_d = \frac{I_d}{H_d} = \frac{\pi}{24}\frac{\cos\omega - \cos\omega_s}{\sin\omega_s - \frac{\pi\omega_s}{180}\cos\omega_s} \quad \textbf{Eq. A.17}$$

$$\cos(\omega_s) = -\tan(\phi)\cdot\tan(\delta) \quad \textbf{Eq. 125}$$

A.8 - Radiation incident on a tilted surface – Isotropic and anisotropic sky definition

To calculate the radiation incident on a tilted surface it is necessary to know the directions from which the beam and diffuse components reach the tilted surface. Diffuse radiation

behaviour is a function of conditions of cloudiness and atmospheric clarity, which are high variable. Diffuse radiation is composed by three parts: 1) the isotropic part, received uniformly from the entire sky dome; 2) the circumsolar diffuse, resulting from forward scattering of solar radiation and concentrated in the part of the sky around the sun; 3) the horizon brightening is concentrated near the horizon, and is most pronounced in clear skies.

Many models have been developed to calculate and simulate the diffuse radiation behaviour in the sky. They differ from the way they treat the different parts of diffuse radiation. Isotropic sky treats the diffuse radiation as isotropic the radiation is uniform in all directions. The isotropic diffuse model, considers three components: beam, isotropic diffuse and solar radiation reflected from the ground.

$$I_T = I_b R_b + I_d \left(\frac{1+\cos(\beta)}{2}\right) + I\,\rho_g \left(\frac{(1-\cos(\beta)}{2}\right) \qquad \textbf{Eq. A.19}$$

The isotropic diffuse model is conservative and simple. However models based in anisotropic sky were developed. Some models consider circumsolar and/or brightening components. There complexity tends to be higher if the three diffuse components are considered. Due to isotropic diffuse model simplicity only this model is considered.